BOEING

SEATTLE, WASHINGTON

F. Brdon, 716

Contract No. NAS5-10443
Radiation-induced Nonlinear
Degradation of Transistor Gain

D2-125680-2
Six Month Progress Report
Electron Nonlinear Damage

Prepared for:
NASA Goddard Space Flight Center
Greenbelt, Maryland

Transmitted by Boeing Letter
2-1101-93-3-729-0R

Prepared by: R. R. Brown
L. L. Sivo

THE BOEING COMPANY
Aerospace Group
Seattle, Washington

ABSTRACT

This document constitutes the semi-annual progress report for NASA Contract NAS 5-10443. Included is a description of research conducted during the period of January 4, 1968 to July 4, 1968. Work on the program has been directed toward accomplishing the main objective which is the establishment of correlation and equivalence factors of radiation induced nonlinear degradation of transistor current gain. Research is progressing essentially in full accordance with the program plan as outlined in the Boeing technical proposal document D2-125398-1, "Radiation Induced Nonlinear Degradation of Transistor Gain," April 1967.

A short account of the experimental conditions during the 1 MeV electron test is given, including a description of the different transistor groups, the measurements and the exposure conditions. The bulk of the report deals with the analysis of the extensive amount of data obtained during the 1 MeV test. Certain special measurements carried out on selected groups are analyzed against the theoretical background of nonlinear damage as it is understood today. Differences between NPN and PNP, passive and active (during exposure) devices are illustrated and discussed in detail. Other measurements, common to all the devices, gave us a detailed picture on the dependence of the nonlinear damage upon the emitter current during gain measurements. These measurements also furnished data for a statistical study in which differences in irradiation response among devices within a batch, among batches and between manufacturers were revealed.

Also included in this report are i) a discussion of the experimental results on the analytical forms of the buildup of the nonlinear damage with fluence, and ii) some thoughts on the problem of selecting the proper quantities in terms of which the radiation sensitivities of transistors can be compared.

ACKNOWLEDGEMENTS

In addition to the authors, the following personnel have made significant contributions to the research performed to date under contract NAS 5-10443.

Betty R. Barry Chalmers R. Brittain	Data acquisition, handling, and analysis
Donald Borgholthaus	1 MeV Electron Test Dosimetry
Loren D. Milliman	Modification and Servicing of the Computer Program for Damage Analysis
Daryl E. Swedenburg	Design and Assembly of Test Circuitry and Operation of the Dynamitron Accelerator

KEY WORDS

Dosimetry

Statistical analysis

Electrons

Ionization

Nonlinear damage

Surface Effects

Transistors

TABLE OF CONTENTS

LIST OF FIGURES

LIST OF FIGURES (Continued)

LIST OF FIGURES (Continued)

LIST OF FIGURES (Continued)

LIST OF FIGURES (Continued)

LIST OF TABLES

1.0 INTRODUCTION

1.1 NEEDS

The general needs that relate to space mission vulnerability of electronic systems include the ability to:

1. Extrapolate from laboratory-simulated radiation tests to space radiation performance;

2. Extrapolate from performance on an in-flight test to other space mission conditions;

3. Generalize from radiation effects on a limited number of transistors to the effects on many types; and

4. Develop techniques to allow for standardization in qualification testing of new devices.

1.2 PROGRAM DESCRIPTION

Phase I of this program was completed under NASA Contract NAS 5-9578. The objective of Phase I research was the establishment of valid space radiation equivalences for permanent displacement damage to silicon transistors. The results of that work (specifically the relative effectiveness of electrons and protons of different energies as well as Cobalt-60 gamma rays) were reported in NASA report CR-814, "Space Radiation Equivalences for Effects on Transistors", by R. R. Brown and W. E. Horne, July 1967.

Phase II of this program is being conducted under this contract NAS 5-10443, "Radiation-Induced Nonlinear Degradation of Transistor Gain". The objective of Phase II is the establishment of correlation and equivalence factors of radiation-induced nonlinear degradation of transistor current gain for use in the evaluation of semiconductor devices for spacecraft missions. The integration of efforts and goals of Phase I and Phase II are shown in Figure 1.

The work in Phase II was divided into three tasks.

Task A -- Empirically formulate the dependence of nonlinear damage on radiation, by:

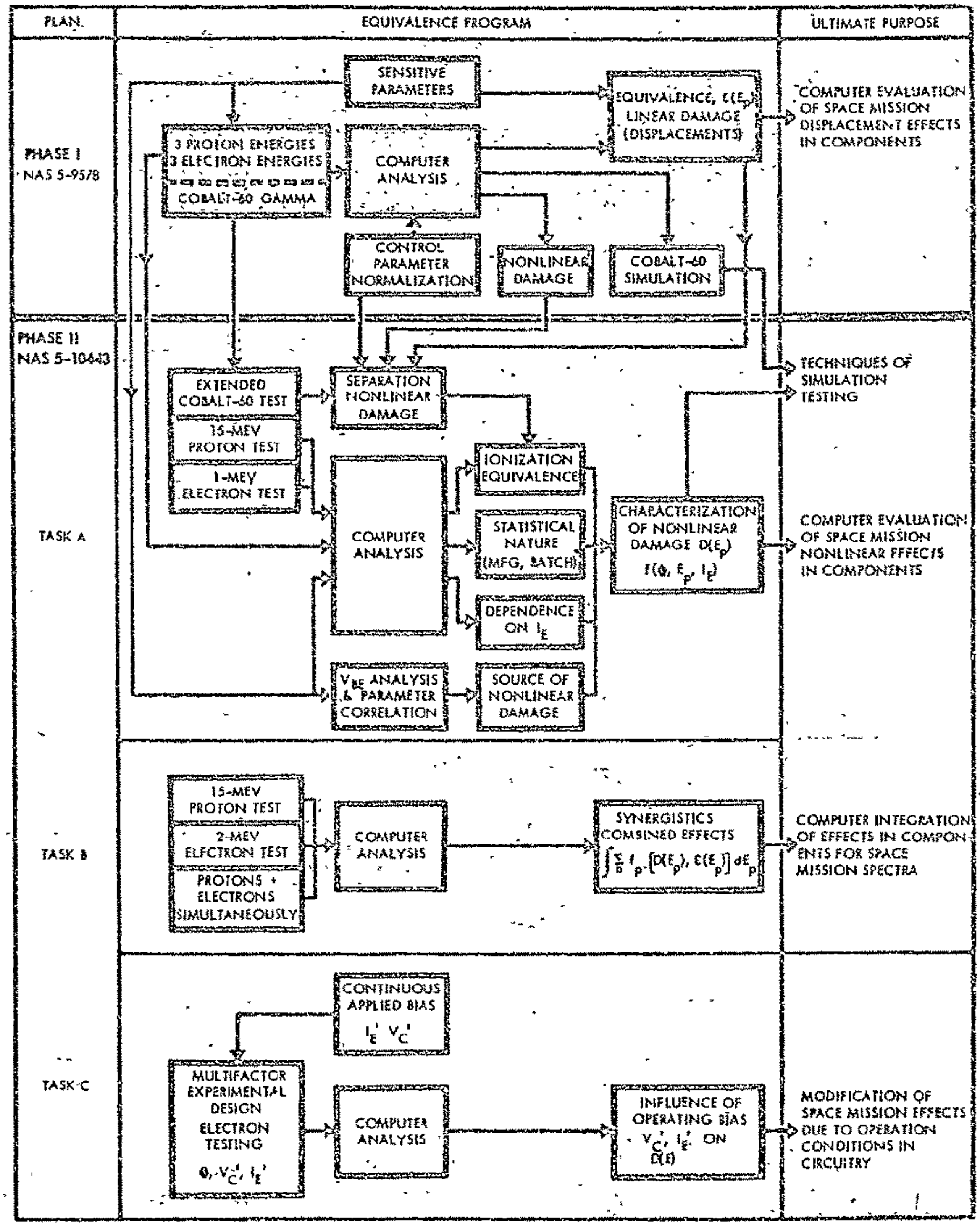

Figure 1. Equivalence Program

1. Establishing the dependence of nonlinear gain degradation on the emitter current at which the gain is specified.

2. Determining the statistical spread in the increase of nonlinear damage with radiation exposure for: (a) one batch type; (b) different batch types; and (c) devices from manufacturers with different processing controls.

3. Establishing ionization equivalences for nonlinear damage.

4. Exploring the source of nonlinear damage by the use of V_{BE} versus I_B analysis and initial parameter correlation.

Task B -- Determine the synergistics of combined effects, by:

1. Testing transistors with simultaneous exposure to electrons and protons.

2. Comparing the results of combined tests with separate exposures to determine the extent of nonadditive damage.

3. Studying the methods required for integrating the ionization and displacement effects on a device for particle energy spectra typical of the space environment.

Task C -- Determine the influence on radiation equivalence for operation of devices under continuous electrical bias during exposure, by:

1. Use of a multifactor experimental design to irradiate transistors under various combinations of: (a) particle exposure; (b) operating current, I_E'; and (c) bias voltage, V_C'.

2. Use of a computer program for a statistical analysis of the functional dependence of gain degradation on particle exposure, I_E', and V_C'.

3. Modification of ionization equivalence values due to electrical operating conditions.

1.3 SUMMARY OF PROGRESS

Degradation of oxide passivated planar transistor parameters, due to surface effects induced by ionizing 1 MeV electron irradiation, was the subject of our study. In particular the gain degradation due to surface effects called the nonlinear damage received our main attention. The behavior of our devices, 2N1613 - NPN and 2N1132 - PNP, was monitored during exposure under both passive and active conditions. Both the NPN and the PNP transistors were procured from two manufacturers, Fairchild and Raytheon, in specified batches in order to study the differences in irradiation response among the devices within a given batch, among batches and between manufacturers.

Beside the measurements of 16 parameters (h_{FE} at various injection levels, I_{EBO}, I_{CBO}, V_{sat}...) on all the devices, special measurements (I_B vs. V_{BE}, I_{EBO} vs. V_R, I_{CBO} vs. V_R, C_{BE}, C_{BC} ...) were also carried out on selected groups of devices in order to help in the interpretation of the data.

The degradation of the transistor parameters are interpreted in terms of the current models of the effects of ionizing irradiation on oxidized Si surfaces; namely in terms of the positive charge accumulation and of the new interface states.

Some of the highlights of our results are given below:

A tremendous difference in radiation sensitivity between the passive and active NPN devices was observed. The active bias during exposure strongly enhanced gain degradation. Charge accumulation on the SiO_2 surface was also enhanced by the active bias; the redistribution of these charges during off-beam and off-bias periods gave rise to slow drifts (recoveries), in the transistor parameters.

No significant differences between the passive and active PNP devices were noted. The gain degradation was approximately of the same order as that of the passive NPN devices.

A considerable interest was focussed recently on the problem of predicting nonlinear damage by finding the proper functional relation between gain degradation, in terms of $\Delta 1/h_{FE}$, and fluence (or dose). A simple power law of the form $\Delta 1/h_{FE}$ = constant Φ^x $(0 < x < 1)$ is advocated by some workers.

Our results indicate that other functional forms of the buildup of damage with fluence also exist. Moreover, if some of the curves for the active NPN devices are to be approximated by a power law then $x > 1$ value should be used.

An interesting and useful relation between gain loss Δh_{FE} and initial gain, β_o, was noted experimentally, resembling somewhat a correlation between those two quantities in a certain fluence range. Consequently, an approximate prediction of gain loss from initial gain is possible subject to some limitations.

The dependence of the nonlinear damage on the measuring collector current is also given, both in mathematical and in parametric representation. The dependence is rather strong, the gain degradation being most drastic at the low current values. Nonetheless, gain loss was significant even at high currents.

A statistical study designed to establish the scatter in gain degradation among presumably "identical" devices during the same exposure conditions revealed the following:

i) Devices within a batch tend to behave similarly,

ii) Devices coming from separate batches are likely to behave dissimilarly if the batch numbers (i.e., the date codes) are very different,

iii) Devices originating from separate manufacturers are likely to be very dissimilar due to differences in surface preparation, geometry, etc.

Comparing devices from different sources as to their radiation sensitivity raised the problem of finding the proper quantity(ies) in terms of which the devices can be compared. Both $\Delta 1/h_{FE}$ and $\Delta h_{FE}/h^{\circ}_{FE}$ were used for such purposes.

The Latin Cube computer calculations have been performed. Data on the dependence of damage on I, V, and Ø (as well as interdependence) are being analyzed and will be summarized in the final report.

2.0 DETAILED DISCUSSION OF PROGRESS

2.1 SHORT SUMMARY OF EXPERIMENTAL CONDITIONS

2.1.1 Transistors Used

Oxide passivated Si planar transistors (2N1613-NPN and 2N1132-PNP) were selected for our study. Each type was purchased from two different manufacturers, Fairchild and Raytheon.

During irradiation the devices were divided into two groups, one group was under active bias, the other was passive.

Unbiased (passive) group: Consisted of 30 Fairchild 2N1613, 30 Raytheon 2N1613, 28 Raytheon 2N1132, and 30 Fairchild 2N1132. These transistors were part of a statistical analysis to indicate differences between manufacturers and among batches. The batch number is simply a date code marked on the device can indicating the year and the week when the device passed its final electrical test during manufacturing. Throughout this report the expressions batch number and date code will be used interchangeably as synonyms.

Biased group: Consisted of 50 Fairchild 2N1613 and 50 Raytheon 2N1132. The devices were used to reveal the influence of the different bias conditions on the nonlinear gain degradation.

2.1.2 Measurements of Transistors

2.1.2.1 Fairchild Series 500 Test Data

The Fairchild Series 500 transistor tester was programmed to automatically perform 16 sequential measurements per transistor. Data from all transistors was automatically logged on IBM cards using a Fairchild Model Option K data logging module, and an IBM 526 Card Punch.

The Fairchild Series 500 test set was programmed to measure the following parameters: d.c. common emitter current gain, h_{FE}, at a collector voltage of 10 volts and at emitter currents of 10, 30, 100, and 300 μa, 1, 3, 10, 20, and 40 ma; V_{CE}(sat) at h_{FE} = 10 for I_C = 150 ma; I_{CBO} at V_{CB} = 5, 20, and 60 volts for 2N1613's and V_{CB} = 5, 20, and 50 volts for 2N1132's;

I_{EBO} at V_{EB} = 1, 3, and 6 volts (except for Fairchild 2N1132's which were tested at 1, 2, and 4 volts). Current gain values for collector currents of 2 ma and above were made using the short pulse mode (350 usec) in order to limit device heating. A Wyle Environmental Chamber Model CN 1060640 was used to control the ambient transistor temperature to 35 ± ½°C during measurement.

To verify instrument repeatability "standard" transistors were measured periodically and values were compared with those obtained earlier.

2.1.2.2 <u>Special Measurements on Selected Devices</u>

Table 1 summarizes the program of special transistor measurements made on selected devices. In any given selected group the transistors represent three different biasing conditions applied during irradiation: passive, 10 V - 0.1 ma and 10 V - 10 ma. The special measurements were useful in furnishing more detailed information on the source of nonlinear damage.

2.1.3 Irradiation Conditions

The electron test setup used in the initial Phase I work (NASA report NAS CR-814) was improved in preparation for the 1-Mev electron test. The beam handling system is essentially the same as that shown in Figure 2. Changes to this system include: 1) a four element slit system (current pickup capability on the slits) used to position and monitor the beam, 2) an automatic remote controlled rotating Faraday cup for dosimetry mapping, 3) an aluminum block mounted beside the rotating Faraday cup. This can be rotated into a position to block and monitor the electron beam at its entrance to the test chamber, and 4) a one-fourth-inch thick aluminum diaphragm mounted so as to baffle electrons scattered at large angles and prevent them from increasing the low energy background at the transistor mounting plate.

After experimenting with many different foil thicknesses a 10 mil aluminum foil was selected in order to obtain a reasonably uniform exposure of transistors positioned on a large diameter ring, cylindrically symmetrical to the beam axis. Scattered beam intensity versus scattering angle is shown in Figure 3. Rings of transistors were located at 22 and 26 degrees scattering angle.

Table 1. Special Measurements on Transistors

MEASUREMENT	TEST CONDITIONS	WHEN MEASURED	NUMBER OF THE TRANSISTORS IN TYPES	
			2N1613	2N1132
I_C and I_B versus V_{BE}	$T = 35°C$ $V_{BE} = (0.1\text{-}0.72)V$	Before and after irradiation ≈After every third Φ_K	20 5	20 5
I_{EBO} and I_{CBO}	$T = 35°C$ $V_{BE} = 2V$ $V_{BC} = 10V$	After each Φ_K	10	10
I_{EBO}, I_{CBO} versus T	$T = 35°C\text{-}200°C$ $V_{BE} = 2V$ $V_{BC} = 10V$	Before irradiation	10	10
I_{EBO}, I_{CBO} versus V	$T = 35°C$ $T = 100°C$	≈After every third Φ_K Before irradiation	5 5	5 5
$C_{BE}(0V)$, $C_{BC}(0V)$	T = room temperature	After each Φ_K	10	10
C_{BE}, C_{BC} versus V	T = room temperature $V_{BE} = (0\text{-}6)V$ $V_{BC} = (0\text{-}24)V$	Before and after irradiation	5	5
t_b from h_{FE}(db) tester	T = room temperature f = 30 MHz $I_E = (0.7\text{-}40)$ ma	Before and after irradiation	60 (All No bias transistors in the 1 MeV electron test)	60

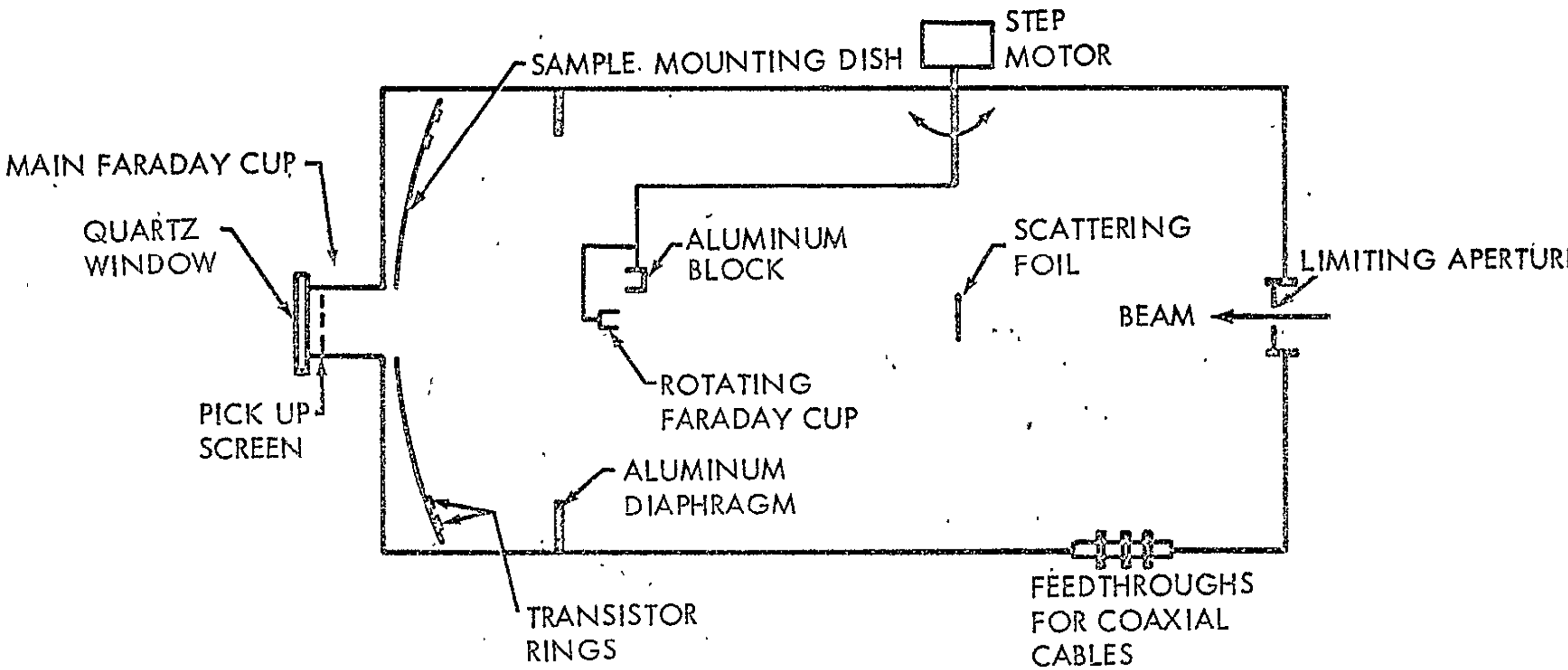

Figure 2. Electron Beam Handling System

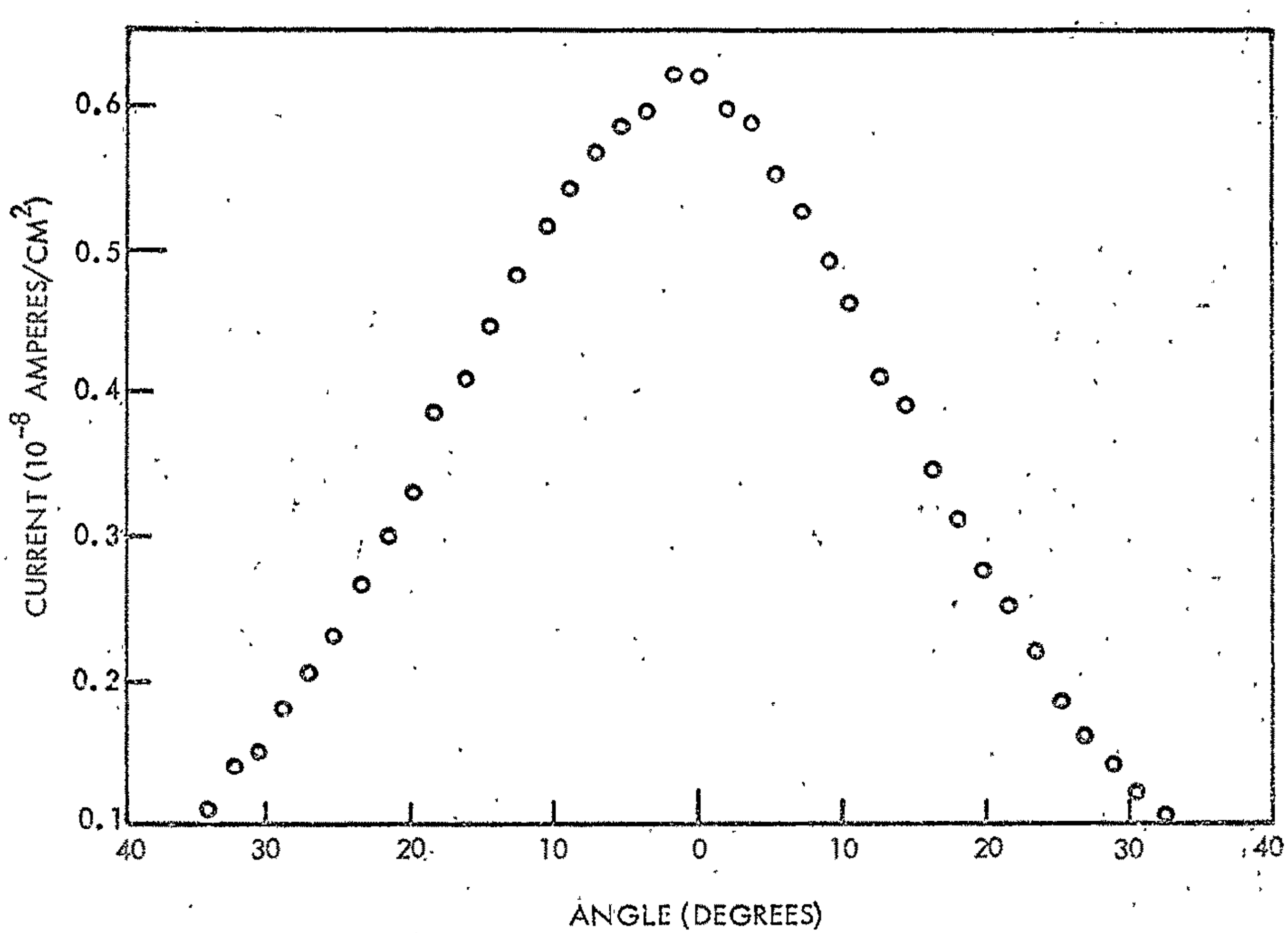

Figure 3. Angular Dependence of the Scattered Beam Intensity. (1 μa current of 1.4-Mev electrons is incident on a 10 mil Al foil. The angle is measured from the beam axis in the horizontal plane, and the distance of the rotating Faraday Cup is 8.3" from the scattering foil.)

TLD powder dosimeters were mounted in the test chamber during the beam mapping tests. Total dose as determined from measurement of the TLD powder, agreed well with fluence values calculated from current reading taken from the rotating Faraday cup.

Other relevant experimental details of the 1 Mev electron test are given below:

Source of electrons: The Dynamitron accelerator providing the DC electron beam. The beam energies were approximately 1.4, 1.3, and 1 Mev when incident on the 10 mil Al scattering foil, on the 8 - 11 mil Kovar transistor can and on the Si chip respectively. Although electrons with 1 Mev energy caused lattice displacements in silicon, the number of such events was relatively small below about 10^{15} electrons/cm^2 fluence. No effects on the transistor parameters due to lattice displacements were observed below the quoted fluence value.

Beam intensities: Exposure rate was increased by a factor of about 50 during the course of the experiment. (Initial stages: 1/2 μa; final stages: 24 μa incident beam on the scattering foil.) Such variation was a practical necessity in order to cover about 4 orders of magnitude in fluence values within reasonable times.

Temperature of irradiation (as monitored by a Copper-Constantan thermocouple, fastened to the transistor cans): Temperature varied between 25 - 32°C for the unbiased transistors and between 35 - 41°C for the biased transistors. T_{irr} increased gradually as higher and higher beam intensities were used. Note that most of the biased transistors were heatsinked in orde to avoid excessive temperatures due to internal heating.

Fluence values: 17 fluence points were chosen in the range of about 3×10^{11} - 3×10^{15} electrons/cm^2. In the calculation of the actual fluence values the transmission losses suffered by the electrons, when traversing the transistor cans, were taken into account.

Measurement conditions after irradiation: The bias supply was turned off within two minutes after completion of a given irradiation. Generally, the pulse measurements of gain and other parameters were started on the Fairchil

Series 500 within less than an hour and were completed within an additional 2-1/2 hours. Forward biasing of certain selected devices also took place from time to time during the I_B and I_C vs. V_{BE} measurements. The reason for stressing these conditions now is that in certain cases a recovery of surface damage was observed in-between irradiations, even at room temperature. This recovery might have been a simple function of time and/or it might have been initiated or accelerated by the measurement itself (due to the injection). Consequently, it was desirable to monitor the conditions.

2.2 SOURCE OF NONLINEAR DAMAGE (TASK A4)

2.2.1 Theoretical Background

In the following we will give a brief review of the effects of ionizing irradiation on oxide passivated Si surfaces and on the subsequent physical events leading to planar transistor degradation. This step is necessary because our experimental results will be discussed and analyzed against this background.

2.2.1.1 Effects of Ionizing Irradiation on Oxide Passivated Si Surfaces

According to numerous investigators an oxidized Si surface when exposed to ionizing irradiation undergoes the following changes:[1]

i) Positive charge is accumulated within and sometimes on the SiO_2.

ii) New energy levels are introduced into the forbidden band of Si at the Si-SiO_2 interface. Shortly, new "interface states" are created.

Let us discuss the physics of these two events briefly in turn:

i) Physical origin of the accumulated charges and their buildup with dose:

The accumulation of positive charge within the SiO_2 in the presence of a uniform electric field across the oxide (during irradiation), is quite satisfactorily explained by Mitchell[2]. His model assumes that hole-electron pairs are created in the SiO_2 by the radiation and that some of the electrons thus created drift out of the SiO_2 layer under the action of an applied potential across the oxide, V_G, while the corresponding holes become trapped. The analysis predicts 1) a dependence of charge buildup on radiation dose D, approximately of the form $1 - \exp(-\beta D)$ where β is a material dependent constant; 2) a linear dependence of the charge buildup at saturation on V_G, for both polarities of V_G; and 3) the dependence of the charge buildup on the total dose absorbed and not on the rate at which the dose was received.

Experiments by Mitchell himself as well as by others on MOS structures (NOT on bipolar transistors) support the type of charge buildup process predicted by the equation $1 - \exp(-\beta D)$. We will also make an attempt to correlate our gain degradation vs. dose curves with the predicted charge buildup vs. dose relation.

Another important case we should try to understand is the experimentally observed positive charge accumulation within the SiO_2 when there is no electric field across the oxide layer during irradiation ($V_G = 0$). Unfortunately there is no satisfactory treatment accounting for the charge accumulation under zero bias conditions. Only some tentative ideas have been proposed so far.(2)

The understanding of charge collection on the SiO_2 surface of a planar transistor is relatively easy. It occurs only when the collector base junction is reverse biased during irradiation. It is due to the irradiation induced ionization of the gas within the transistor can and the subsequent collection of the positive ions over the base or the collector by the electric field existing between the can and the base (the can is connected to the collector).

ii) Physical Origin of the Interface States and Their Buildup with Dose:

At the present time there is no theoretical treatment predicting the functional form of buildup of new interface states with dose, like the one worked out for charge accumulation. The primary reason is probably that even the identity or the physical origin of the defects responsible for the interface states, both original and new, is in question. Some workers claim that the new states are due to the breakup of Hydrogen-Si bonds at the interface by the irradiation.(3) Hence, the states are independent of the accumulated charges within the oxide. Other researchers(4) propose that the interface states are due to some positive and negative charges located in the oxide within a certain distance from the $Si-SiO_2$ interface. There are quite a few valid arguments for or against either proposition. It is very likely that there are several sources of the original and the new interface states, including the two ideas presented.

For the purpose of this report, we conclude that the creation of new interface states is a fact, although the physical origin of the states is still uncertain. In any case it is shown experimentally that the buildup of new states with dose will also go into saturation not unlike the buildup of positive charges. It is claimed, however, that the buildup of the new states is independent of the applied gate bias during irradiation in MOS structures.(5)

2.2.1.2 Degradation of Transistor Parameters

Next, we would like to discuss the expected degradation of a passivated planar transistor in terms of the surface changes caused by ionizing irradiation presented previously. The two main degradations we are concerned with are the increase of I_{CBO} and the decrease of h_{FE}. To be more general, we will talk about the increase in the reverse current, I_R. Also, instead of the degradation of h_{FE} we will discuss the increase of the base current, I_B. These latter two events are equivalent because

$$h_{FE} = \frac{I_C - I_{CEO}}{I_B} = \frac{I_C}{I_B}\left(1 - \frac{I_{CBO}}{I_B}\right)$$

where

$$I_{CEO} = \left(\frac{I_C}{I_B}\right) \times I_{CBO}$$

Since I_C changes very little during ionizing irradiation it is the increase in I_B which is primarily responsible for the gain loss.

Now we wish to find out the controlling variables of currents I_R and I_B in order to assess and understand the effect of the charge accumulation and the creation of new interface states on the appropriate variables hence on currents I_R and I_B. Reiterating some of the results of semiconductor device physics it is well established that in terms of their physical origin I_R and I_B are given by:(6)

$$I_R = \sum_i I_R^i = \sum_i I_{gen}^i \quad \text{and} \quad I_B = \sum_i I_B^i = \sum_i I_{rec}^i \qquad (2)$$

The equations above tell us first that both I_R and I_B are made up of several different components designated as I_R^i and I_B^i, each component having a different spatial origin in the transistor. The regions in question are: bulk of the emitter and of the base; surface of the emitter and of the base; bulk of the junction transition region; surface of the transition region; channel (inversion) region, if present. (The appropriate components originating at the surface of the junction will be designated as I_B^s, I_R^s, I_{rec}^s, I_{gen}^s.) The relative importance of these regions in contributing to I_B or I_R depends on many factors including the injection level (for I_B). As an example, it is the surface of the transition region which is the most important in determining the value of I_B thus the current gain at low injection. More will be said about the empirical equations representing the different I_B components in section 2.2.1.3.

It is also shown in Equation (2) that the separate components can be identified with thermal generation (I_{gen}^i) and recombination (I_{rec}^i) currents respectively as to their physical origin. Equations (2) then simply express the fact that in a given region of the transistor a thermal generation current will result whenever the thermal generation rate of hole-electron pairs is made excessive over the recombination rate of those pairs. (The thermal generation is due to the electromagnetic radiation, called "thermal radiation", present in any material at temperature T.) Similarly, a recombination current will result whenever the recombination rate becomes excessive over the generation rate. In thermal equilibrium these two rates are equal of course, but by external means (e.g. reverse bias, forward bias, illumination....) the balance can be destroyed and one ends up either with current sources furnishing the I_R or with current sinks representing I_B.

By taking into account the fact that according to the Shockley-Read-Hall theory the generation and recombination of hole-electron pairs takes place through some energy levels located in the forbidden energy band, serving as "stepping stones" for the particular process, we can now list the variables controlling I_R and I_B.

$$J^{i}_{rg} = f\ (N_t, E_t, \sigma_e, \sigma_h, n_o, p_o, T, V, n, p) \qquad (3)$$

where J^{i}_{rg} is the recombination or generation current density in a given region of the transistor (hence $J^{i}_{r} = I^{i}_{B}$ and $J^{i}_{g} = I^{i}_{R}$). By writing J_{rg} instead of J_r and J_g we want to emphasize the intimate relation between J_r and J_g since the same energy levels serve as stepping stones for either the recombination or the generation process.

N_t: Density of energy levels in the energy gap promoting the generation and recombination; E_t is their energy position; σ_{el}, σ_h are the electron and hole capture cross-sections respectively

n_o, p_o: Equilibrium electron and hole concentrations in the bulk

T: Temperature

V: Applied voltage

n, p: Electron and hole concentrations in the particular region in question

The explicit functional form of J^{i}_{rg} is somewhat different in different regions of the transistor it is also different for J^{i}_{r} and J^{i}_{g} (i.e. for I^{i}_{B} and I^{i}_{R}). At the surface of the transition region for both J^{s}_{r} and J^{s}_{g} the dependence on N_t is linear. The dependence on n and p is much more complicated, containing hyperbolic cosine functions. J^{s}_{r} will have a maximum when $n = p \cong n_i \exp(q|V_F|/2KT)$ and J^{s}_{g} has a maximum when $n, p \ll n_i$ i.e. for a depleted surface. n_i is the intrinsic carrier concentration, V_F is the applied forward bias. Incidentally, the semi-empirical expressions for $(J^{s}_{r})_{max}$ and $(J^{s}_{g})_{max}$ are[7]

$$(J^{s}_{g})_{max} = q \times S_o \times n_i \qquad (4)$$

where S_o has been defined as the surface recombination velocity of a depleted surface. It is proportional to the density of the interface states. (Actually $S_o = S_{max}$ here since the n_s, $p_s \ll n_i$ condition made S reach its maximum value in the reverse biased case. Of course S_o is still a function of N_t, E_t, σ_{el}, σ_h, T, n_o, p_o as listed in Equation (3).) Also,

$$(J_r^s)_{max} \simeq \frac{2}{\pi} \times q\ S_o \times n_i \frac{q|V_F|}{2KT} \exp\ (q|V_F|/2KT) \qquad (5)$$

$$\text{for } |V_F| \gg KT/q$$

It is significant to note that surprisingly $(J_g^s)_{max}$ i.e. $(I_R^s)_{max}$ is independent of the reverse voltage in Equation (4).

Another interesting result comes by taking the ratio of Equations (5) and (4).

$$\frac{(J_r^s)_{max}}{(J_g^s)_{max}} = \frac{2}{\pi} \times \frac{q|V_F|}{2KT} \exp\ (q|V_F|/2KT) \qquad (6)$$

I.e. the ratio of $(I_B^s)_{max}/(I_R^s)_{max}$ is a constant at a given forward bias and temperature. Consequently if, for example, the maximum surface generation current, $(I_R^s)_{max}$, increases by a factor of two because of new interface states then so does approximately the maximum surface recombination current, $(I_B^s)_{max}$. (Hence the h_{FE} will also decrease by a factor of two.) Similar approximate results are obtained by taking the ratios I_B^i/I_R^i for other current components, signifying a close relation between them, although the ratio in those cases will depend on the reverse bias, V_R, as well.

Having found the variables controlling I_B and I_R in Equation (3) we can now discuss the effect of the charge accumulation and of the new interface states on these currents in terms of their variables.

The introduction of the new interface states will increase the density of the recombination - generation levels, N_t, in Equation (3). Consequently both I_R and I_B will be enhanced since their surface components I_B^s and I_R^s are increased linearly with N_t. Although the energy positions and respective capture cross-sections of the new levels may be different from those of the levels originally present, it is an experimental fact that the new energy levels themselves are very efficient recombination-generation states. It should be pointed out that whenever I_B^s is affected seriously as the case here, then the gain degradation is most significant at low injection levels where usually $I_B \simeq I_B^s$ even before irradiation.

<u>The effect of the charge accumulation</u> (either within or on the SiO_2 or both) on I_B and I_R in terms of their variables will be somewhat different in the following cases therefore treated separately in turn:

i) <u>No inversion</u>, only depletion of the substrate Si occurs. The charge accumulation will modify n and p at the surface of the transition region (n_s, p_s) in Equation (3) by changing the surface potential hence J_r^s or J_g^s will be modified. I_B^s and I_R^s may or may not reach maximum as a function of the surface potential (thus n_s and p_s) depending upon the extent of depletion of the substrate.

ii) <u>Inversion</u> of the substrate Si occurs, thus a junction, called the "field induced junction", is formed. This case has to be divided into the following three subcases: (In the first two it is assumed that the extent of inversion is not sufficient to cause "channel" formation discussed in γ).

α) There is no breakdown across the field induced junction during applied bias:

The two new regions which affect I_B and I_R in this inversion case are the surface of the inversion layer and the bulk transition region of the field induced junction. However, the effect of the surface decreases rapidly with surface inversion and will be negligible under large inversion.[8] (Since J_r^s and J_g^s as functions of the surface potential has already passed their maximum when the inversion set in.) On the other hand, the bulk transition region of the field induced junction will serve as an extra source of current for either I_R or I_B thus contributing to their degradation.

β) There is a voltage breakdown of the field induced junction during applied bias:

The breakdown can be either an avalanche or a Zener breakdown depending upon the surface doping of the inverted substrate.[9] Avalanche occurs below approximately 3×10^{18} cm^{-3}. Zener breakdown or tunneling occurs when the surface doping is approximately between 3×10^{18} cm^{-3} and 8×10^{18} cm^{-3}. Either of these breakdowns give rise to a tremendous increase in I_R. In addition, the tunneling can significantly increase I_B hence degrade h_{FE} both at low and high injection levels. This effect, when it occurs, is so drastic that it overrides every other cause of gain degradation especially at high injection levels.

γ) "Channel" or ohmic path formation between the contacts of the base-emitter, base-collector, emitter-collector.

This event specifically refers to the case of base inversion of such an extent in area that a direct ohmic path between the different terminals of the transistor develops. Depending upon the size of the channel the resulting increase in I_{CBO} or I_{CEO} may completely disrupt further device operation. (Fortunately the effect of a channel across the base-emitter junction alone is not too serious for gain degradation because this junction is forward biased and the channel path is usually highly resistive.)

Since the accumulated charges in the SiO_2 are positive it follows that the depletion and inversion occurs on a P type substrate only. This is the base of an NPN transistor and the emitter and collector of a PNP transistor. Therefore, a different response is expected to ionizing irradiation by NPN and PNP transistors. The difference in behavior is further amplified by the fact that the surface doping of the base and emitter regions is quite different. The emitter region is usually very highly doped ($> 10^{20}$ cm^{-3}), consequently only a very narrow region in the vicinity of the junction, where there is a lateral concentration gradient, can be depleted and inverted. Nonetheless, since tunneling can usually occur through part of the small inverted region, the degradation of I_B hence h_{FE} can still be very significant for a PNP transistor as we will see later during the presentation of our experimental results.

2.2.1.3 Empirical Equations for I_B^i

Previously in Equation (3), we indicated the variables controlling I_B^- by taking into account the physical mechanisms causing the current. Next we write down some empirical equations for I_B^i, which say very little about the physical origin of the current but emphasizes its approximate voltage and temperature dependence.

$$I_B = \sum_i I_B^i \qquad \text{and} \qquad I_B^i = I_O^i \exp \frac{qV}{n_i(V,T)kT} \tag{7}$$

where I_O^i is an empirical constant for the i^{th} component of the base current, $n_i(V,T)$ is the "identifying" component number for the i^{th} component. In general, it may be a function of injection level and of temperature. The value or the range of values of n for the different base current components are as follows:

- $n = 1$: Bulk recombination current in the emitter and base region. Or, surface recombination current on the emitter and base region.
- $1<n<2$: Bulk recombination current in the junction transition region. Or, surface recombination current over the transition region. It is significant to note that in this important case the meaning of a given n value is unfortunately ambiguous, unless complemented by some other measurements.
- $2<n<4$: Recombination current in the channel (inversion) regions, if present, and the adjacent bulk material.

In a given V and T range it is usually true that one of the base current components is dominant. Then by determining the n value we may be able to identify the component in question. The identification of the spatial origin of the current is usually important in complementing and supplementing the conclusions of some other measurements. Two different techniques were used to obtain "n":

i) V_{BE} analysis: n can be determined from the slopes of the log I_B vs. V_{BE} plots as seen from Equation (7) and is well discussed in the literature. We emphasize again that a changing n value at different V_{BE} points may still represent one dominant I_B component. The variation in n in such a case may simply reflect its injection level dependence.

ii) $1/h_{FE}$ vs. I_C plots: n can also be determined from the slopes of the log $1/h_{FE}$ vs. log I_C plots at a given fluence since

$$\frac{1}{h_{FE}} \cong \frac{I_B}{I_C} \cong \text{constant } I_C^{\frac{1}{n} - 1} \tag{8}$$

This is valid if the base current consists of one dominant component, i.e. $I_B = I_{BO} \exp (qV/nkT)$. Then since $I_C = I_{CO} \exp (qV/KT)$ we can write I_B = constant $I_C^{1/n}$ and consequently obtain Equation (8).

If one is interested in identifying only the additional base current component(s) introduced by the irradiation then the log $(\Delta 1/h_{FE})$ vs. log I_C plots have to be used instead. In practice there was very little difference between this and the log $1/h_{FE}$ vs. log I_C plot when I_B increased by a factor of 20 or more.

Although method i) is more precise in obtaining n it is also far more tedious and time consuming than ii). In contrast the data necessary for method ii) are relatively easily obtained on a high speed automatic transistor gain tester like the Fairchild Series 500. Nevertheless, method i) also furnishes actual I_B vs. V_{BE} data while ii) does not. In certain analyses the knowledge of the I_B values is just as important as the knowledge of the "n" values.

2.2.2 Analysis of Devices from the Special Group

The special measurements are the ones discussed in 2.1.2.2 and listed in Table 1. Typical examples on the interpretation of these measurements are given below for certain devices where each device is a representative of a small group.

More than that, we believe that the devices discussed are actually good representatives of the four main groups of transistors used in our experiment namely, the passive and active NPN's and PNP's. At least, the measurements which were common to all transistors (h_{FE}, I_{EBO}, I_{CBO}) seem to bear this assumption out. Consequently the conclusions drawn below should essentially apply to the particular group containing the device in question.

The measurements will be interpreted on the basis of the theoretical discussion given in the previous section. I.e., the data are analyzed in terms of the effect of the charge accumulation and of the creation of the new interface states on the Si surface where possible. Since the effect of the charge accumulation is different in the presence or absence of inversion, we will always start the discussion of the figures with the C_{BE} vs. fluence measurements. These curves can tell us immediately whether or not inversion has taken place. Conclusions drawn then can be substantiated by other measurements.

In discussing parameters such as I_B, I_R, h_{FE}, which are affected by both charge accumulation and interface states, we have to be content with considering only the combined effects of these two events since on the basis of our measurements their effects cannot be separated. One can nevertheless draw some indirect conclusions about their relative importance under certain conditions.

The gain degradation is expressed in terms of $\Delta 1/h_{FE}$ vs. $\emptyset$ curves. Actually $\Delta 1/h_{FE} \cong \frac{\Sigma I_B^x}{I_C}$ where ΣI_B^x is the sum of the extra base current components induced by the irradiation, and I_C is the collector current at which the gain was measured. The pros and cons of other methods of presenting the gain degradation data will be discussed in Section 2.2.4.

NPN-unbiased during irradiation: As discussed earlier it is the p type base which is affected primarily by the positive charge accumulation and the new interface states, thus leads to transistor degradation in an NPN structure.

The C_{BE} and C_{BC} vs. Φ curves are shown in Figure (4) for Fairchild 2N1613, device #1. For passive 2N1613 transistors there was no indication of any inversion of the base surface due to the accumulated charge since C_{BE} and C_{BC} remained approximately constant. The absence of inversion is also supported by the I_B vs. V_{BE} curves of the type shown in Figure (5) where the slopes yield n values ≤ 1.9 (n comes from equation (7)).

I_B vs. Φ (Figure (6)), or what is essentially the same, $\Delta 1/h_{FE}$ vs. Φ (Figure (7)) and the I_{EBO} vs. Φ, I_{CBO} vs. Φ curves (Figure 8) can be qualitatively understood by assuming an increased surface recombination velocity due to irradiation on the base surface, in the vicinity of the junctions. This assumption as the reason for increased I_B, is in accordance with the n values determined from Figure (5), where $1.4 \leq n \leq 1.9$. There seems to be some discrepancy, however, if we also assume that I_{EBO} was likewise dominated by the surface generation current. Namely, such a current component is presumed to be approximately independent of voltage.[6] In the I_{EBO} vs. reverse voltage, V_R curves of Figure (9) this is true only above 0.2 volts. Essentially similar arguments apply for the I_{CBO} vs. V_R curves of Figure (10).

NPN - biased during irradiation: (Bias: $V_{CB} = 10$ V, $I_E = 10$ ma).

Just as in the passive NPN case, it is the surface condition of the base, affected by the positive charge accumulation and the new interface states which determines the transistor degradation. However, due to the active bias on the transistor during exposure, the amount of charge accumulation can be significantly increased due to the fringing electric fields influencing charge migrations. It is not yet clear how the creation of the new interface states is affected by biases across the junctions. Although it is claimed to be independent of the electric field[5], it could conceivably be injection dependent. All in all, the combined effect of the charge accumulation and of the new interface states on active NPN transistors

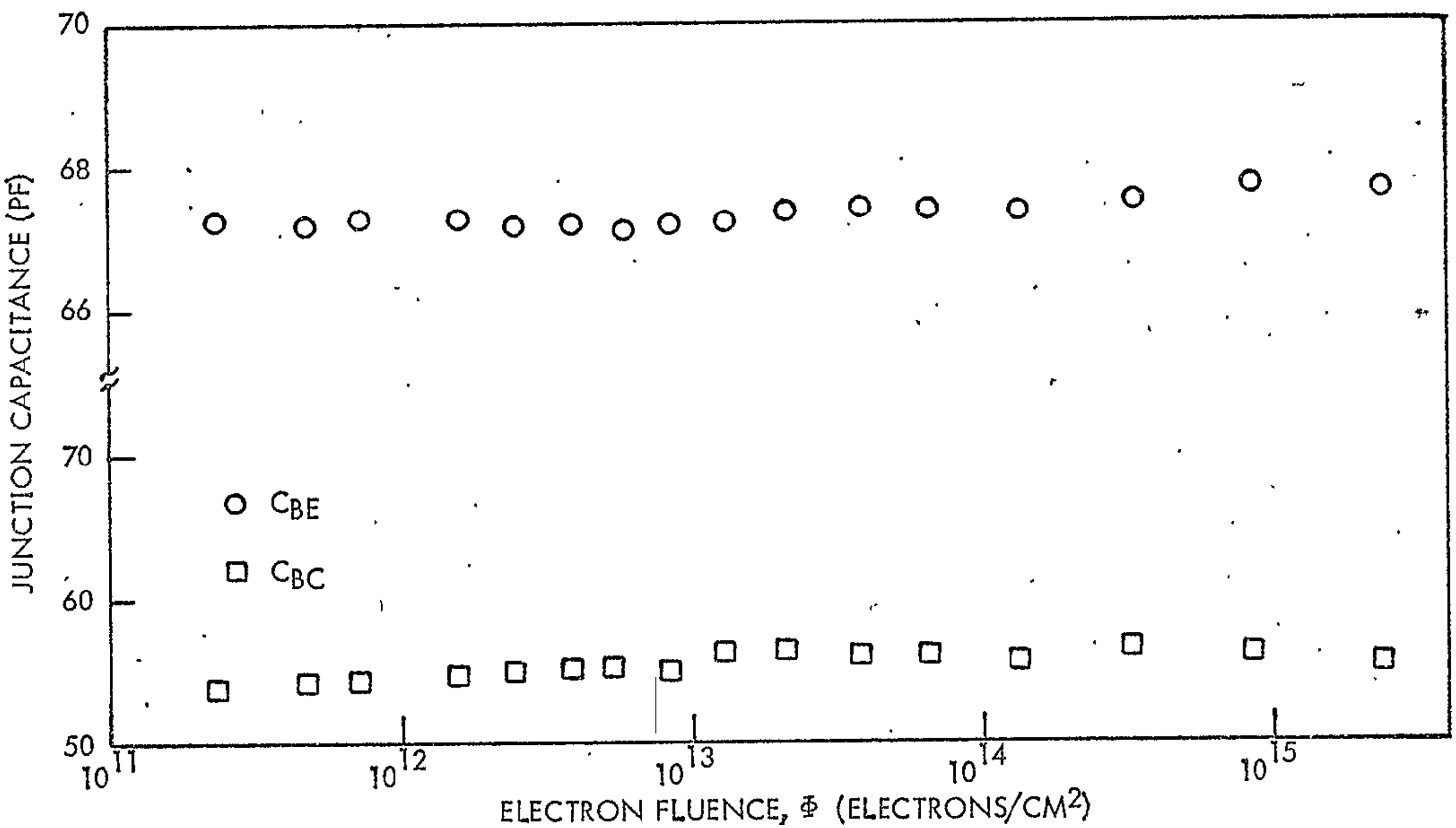

Figure 4. C_{BE} and C_{BC} (Zero Bias) Versus Fluence (Fairchild 2N1613, Passive During Irradiation)

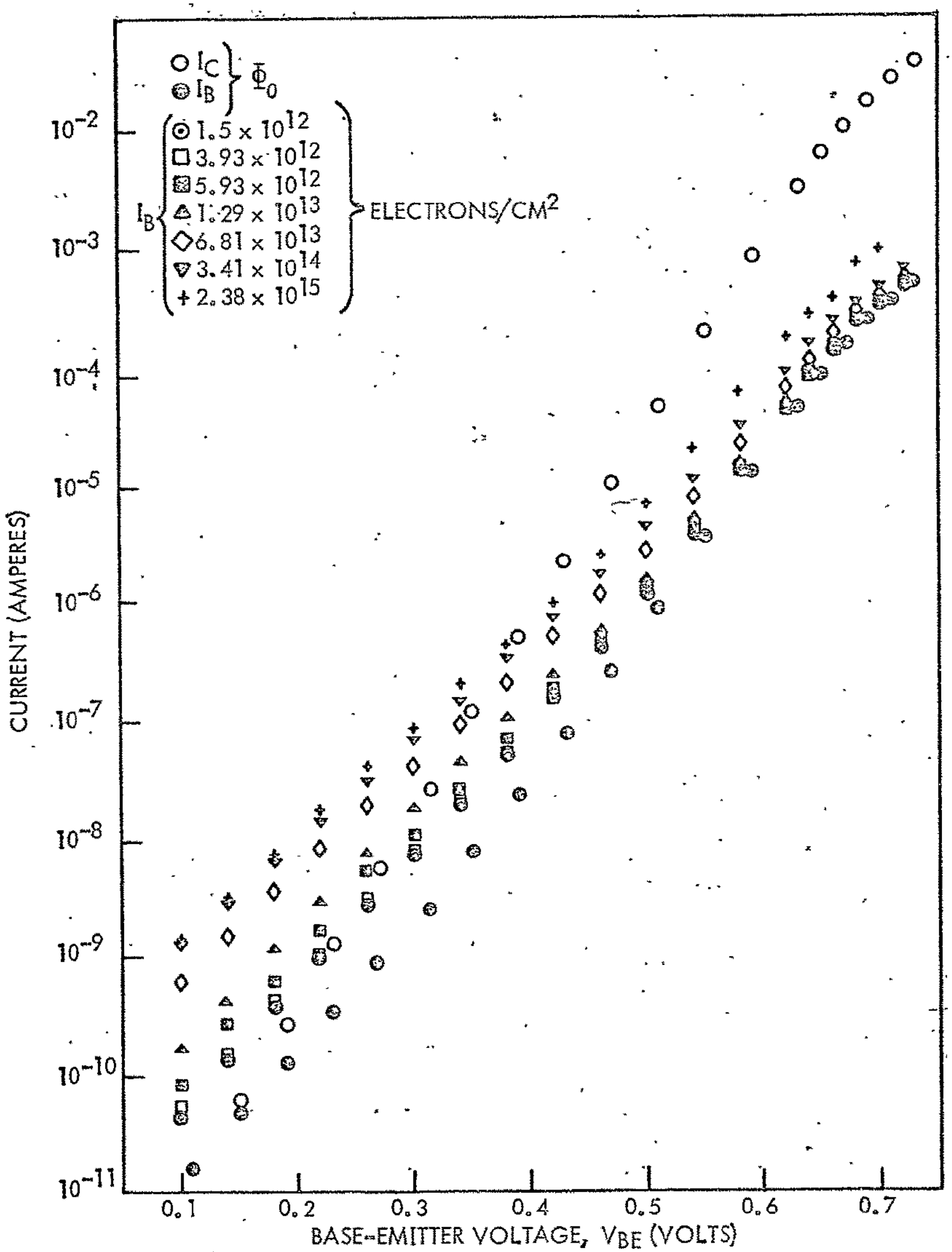

Figure 5. I_B and I_C Versus V_{BE} Curves, Taken at Different Stages During Exposure (Fairchild 2N1613, Passive During Irradiation)

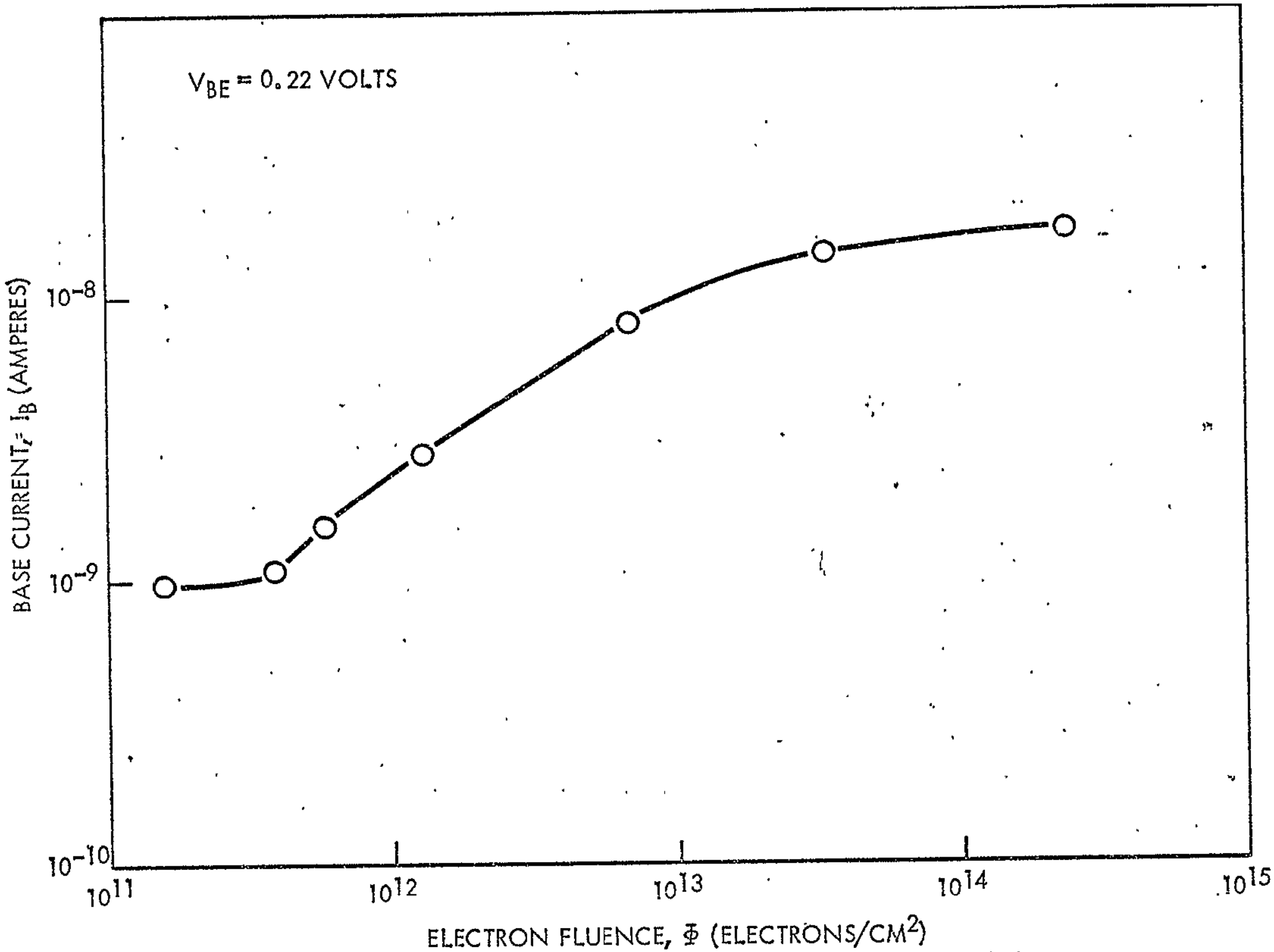

Figure 6. I_B Versus Fluence (Fairchild 2N1613, Passive During Irradiation)

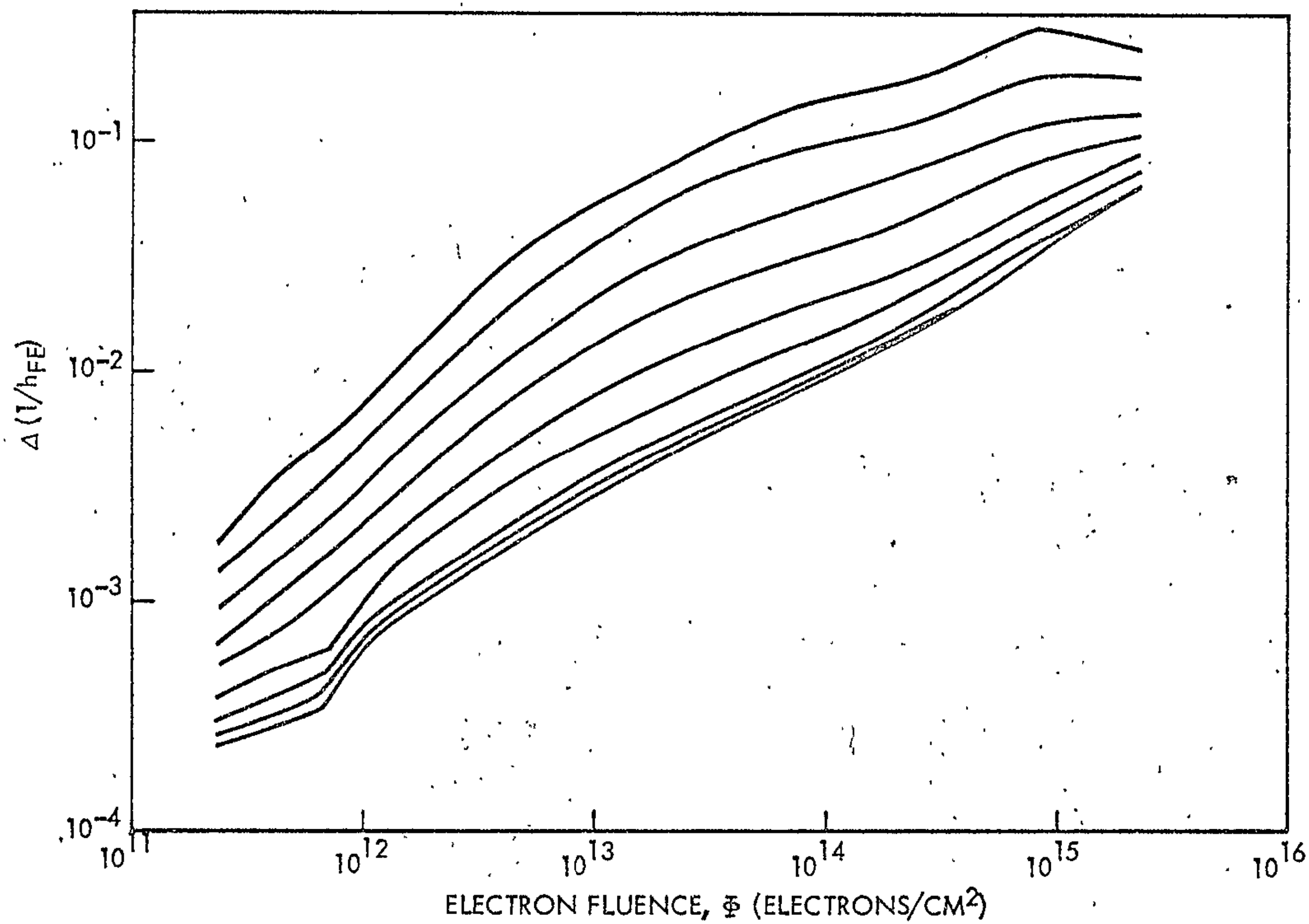

Figure 7. $\Delta(1/h_{FE})$ Versus Fluence (Fairchild 2N1613, Passive During Irradiation)
(Measurement Current, I_E, From Top to Bottom: 10μa, 30μa, 100μa, 300μa
1 ma, 3 ma, 10 ma, 20 ma, 40 ma)

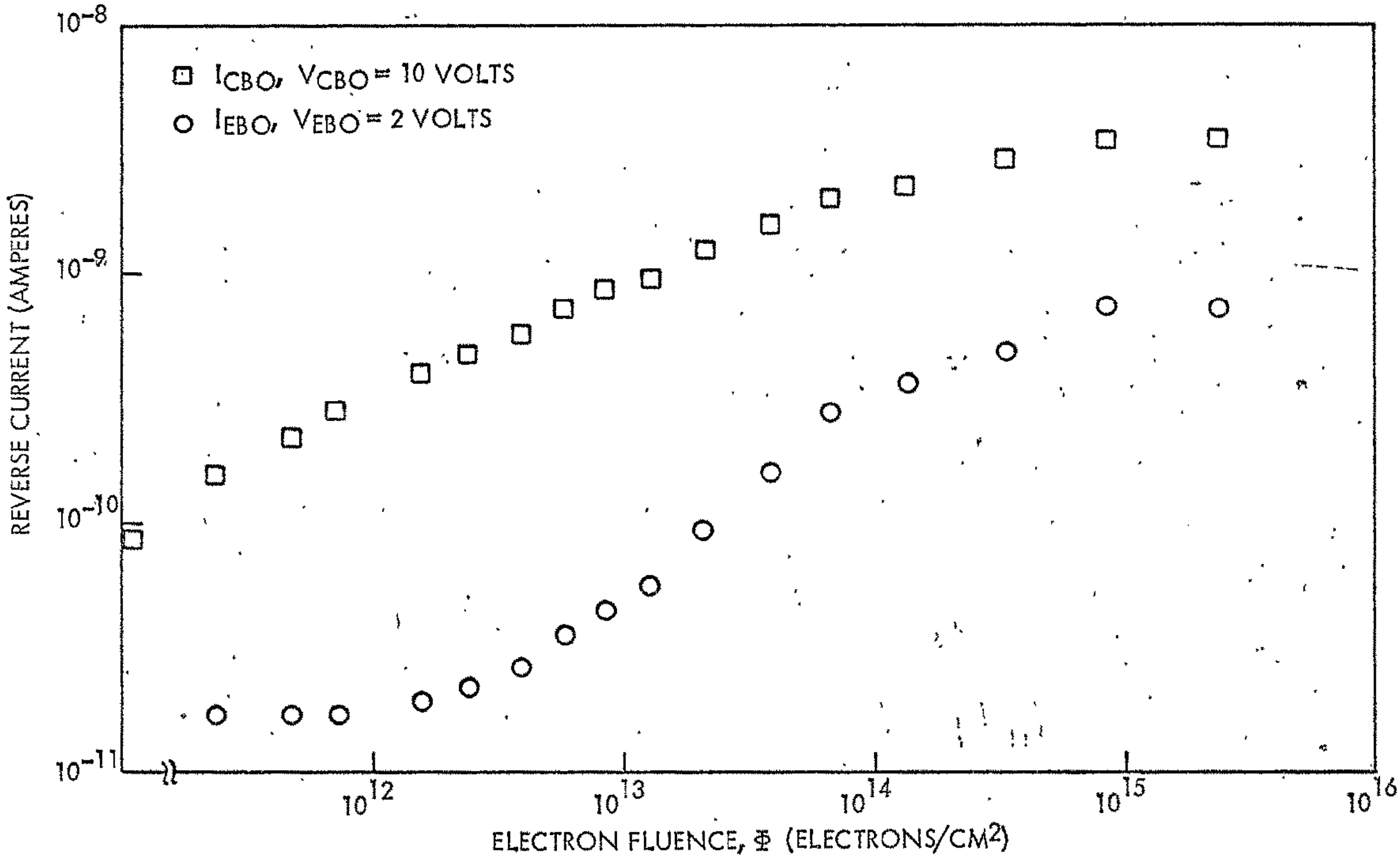

Figure 8. I_{EBO} and I_{CBO} Versus Fluence (Fairchild 2N1613, Passive During Irradiation)

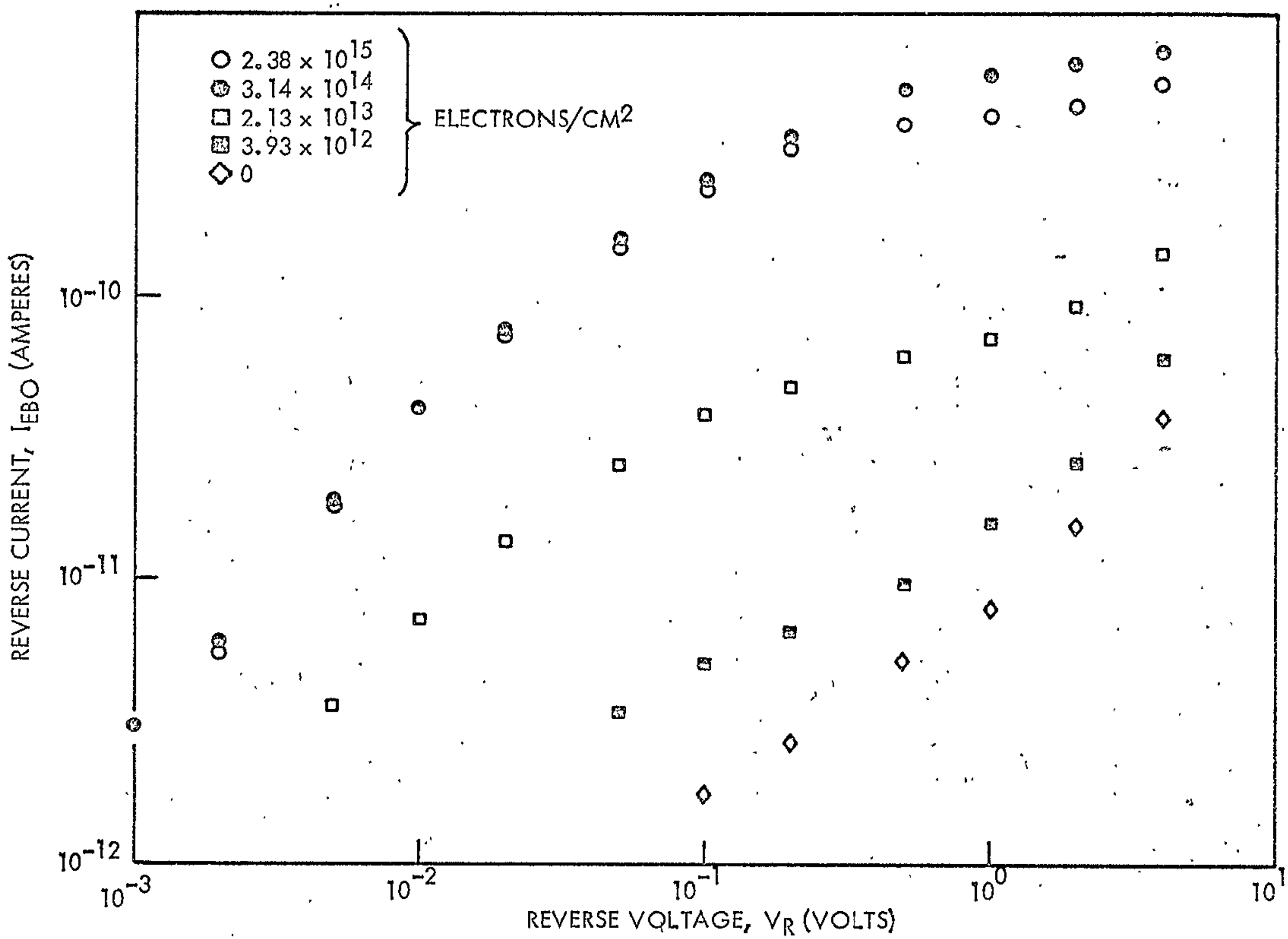

Figure 9. I_{EBO} Versus Reverse Voltage, V_R, Curves, Taken at Different Stages During Exposure (Fairchild 2N1613, Passive During Irradiation)

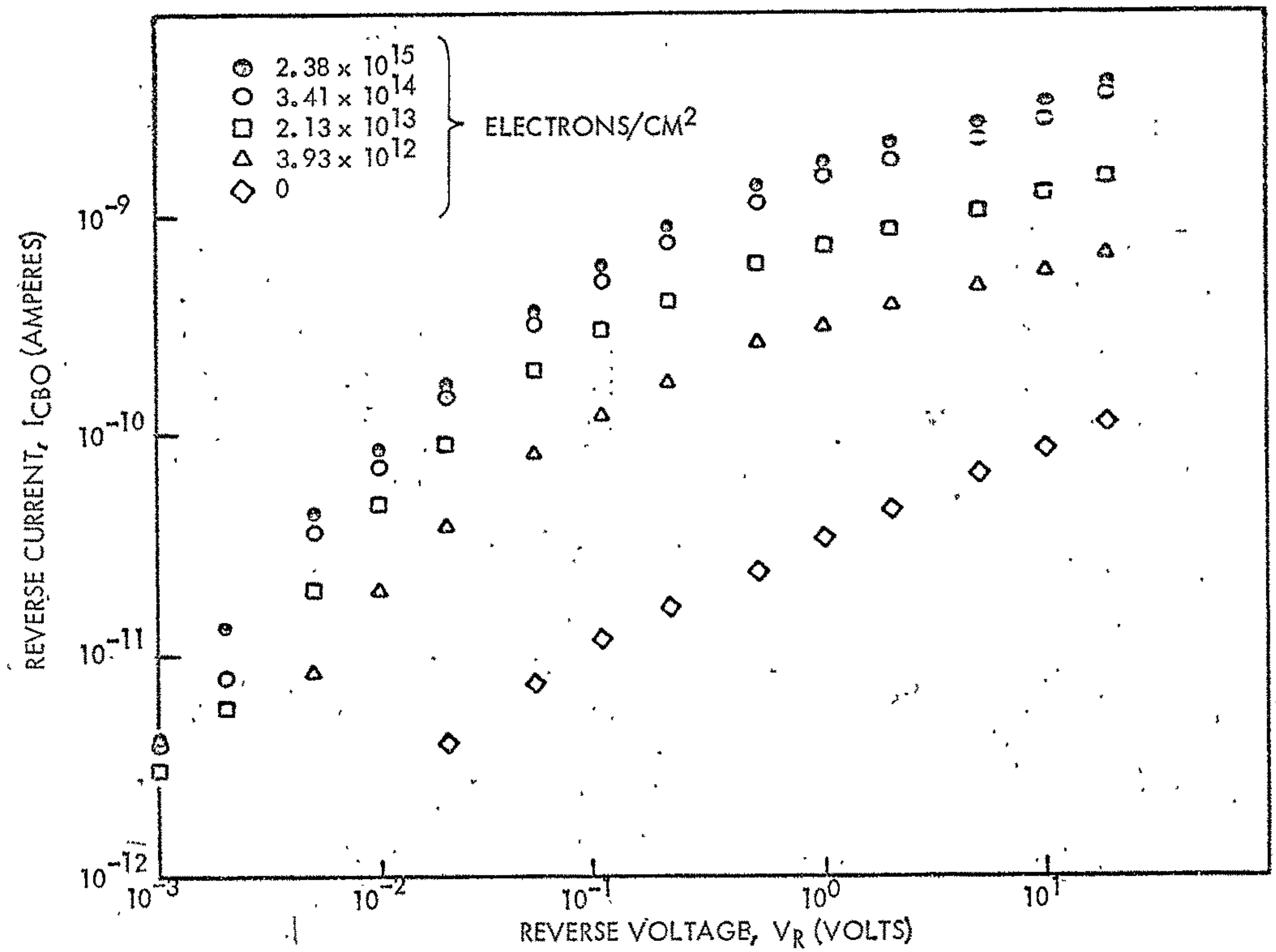

Figure 10. I_{CBO} Versus V_R Curves, Taken at Different Stages During Exposure (Fairchild 2N1613, Passive During Irradiation)

is drastic indeed. E.g., the $\Delta 1/h_{FE}$ vs. ϕ figures will exhibit a significantly faster gain degradation with exposure than those for the respective passive devices. Also the formation of an inversion layer over the base will be noted.

C_{BE} vs. ϕ curve in Figure (11) shown for Fairchild 2N1613, device #13, indicates inversion layer formation and also the receding of the layer with fluence. Inversion layer formation results in a substantial increase of the junction capacitance since the capacitance due to the field induced junction will add to that of the metallurgical junction. The reason for the receding of the inversion layer is discussed shortly; it is indicated by the broken lines in Figures 11 and 13. This conclusion is in accordance with the n values determined from the I_B vs. V_{BE} curves of Figure (12) where $n > 2$ in the similar fluence region.

The effect of inversion in I_{EBO} is strikingly illustrated by the similarity of the I_{EBO} vs. Φ curve of Figure (13) to the C_{BE} vs. ϕ plot. The physical mechanism by which the inversion affected I_{EBO} appears to be channeling, it will be treated shortly. The initial, substantial rise in I_{EBO} prior to inversion is due to the increased surface recombination velocity caused by the irradiation. Incidentally, the values of I_{EBO} became quite high above $\phi \approx 5 \times 10^{14}$ electrons/cm^2 and one might wonder if tunneling took place across the field induced junction. This speculation is ruled out, however, because the presence of a breakdown voltage associated with tunneling (value expected is approximately 0.5-volt for our base doping) of the field induced junction was not observed as shown in the I_{EBO} vs. V_R curves, Figure (14). In fact, the shape of these curves did not change at all by the onset of inversion.

Now the question arises whether the positive charges inducing the observed inversion layer originated within or on the SiO_2. It appears that most of them were collected on the outer surface of the oxide layer (through the ionization of the gas inside the transistor can and the electric field between the base and the can which was connected to the collector). Namely we observed quite significant "Telstar type" effects, i.e., slow drifts, resulting in recovery of the transistor parameters with time after the irradiation was stopped and the bias was disconnected. These effects are indicated in Figures (11) and (13) by the broken lines as mentioned earlier. The recoveries of C_{BE} and I_{EBO} with time after-exposure were often substantial. (Such effects were observed essentially on all biased NPN devices.) In the past, such effects were found to be related to the redistribution of charges on the outer surface of the SiO_2.

Note by comparing Figure (11) and Figures (15) or (16) that quite significantly most of the gain degradation took place before the onset of inversion since $\Delta 1/h_{FE}$ or I_B went into saturation above $\approx 2 \times 10^{13}$ electrons/cm^2. Although the amount of positive space charge on the SiO_2 kept changing as indicated by the onset and the recession of the inversion layer, the correspondingly changing surface potential did not appreciably affect the rate of surface recombination thus I_B. All these can be qualitatively understood since the surface effects play a dominant role on I_B and I_R only before inversion occurs, after inversion their role becomes less and less significant because then the effects by the bulk transition region of the field induced junction take over. However, this latter event is usually not too serious in affecting I_B and I_R unless tunneling occurs.

Now since tunneling was absent nevertheless I_{EBO} was drastically affected during inversion, "channeling" or the formation of an ohmic path between base and emitter must have taken place. This would explain the large changes in I_{EBO} as well as the relative constancy of I_B, thus h_{FE}, during inversion, because channeling does not have much effect on a forward biased junction.

The C_{BC} vs. ϕ data in Figure (11) show an absence of inversion, also confirmed by I_{CBO} vs. ϕ on Figure (13), for device constructional reasons. According to the manufacturer the base metal contact overlaps the collector-base junction hence prevents charge accumulation on the surface of the oxide.

Although the assumption of an increased surface recombination velocity explains the increase in I_{CBO} with fluence (Figure 13) it is partially at variance with the I_{CBO} vs. V_R curves on Figure (17). Namely, I_{CBO} is approximately voltage independent only above ≈ 0.2 volt and not over the whole measurement range as it is theoretically claimed.

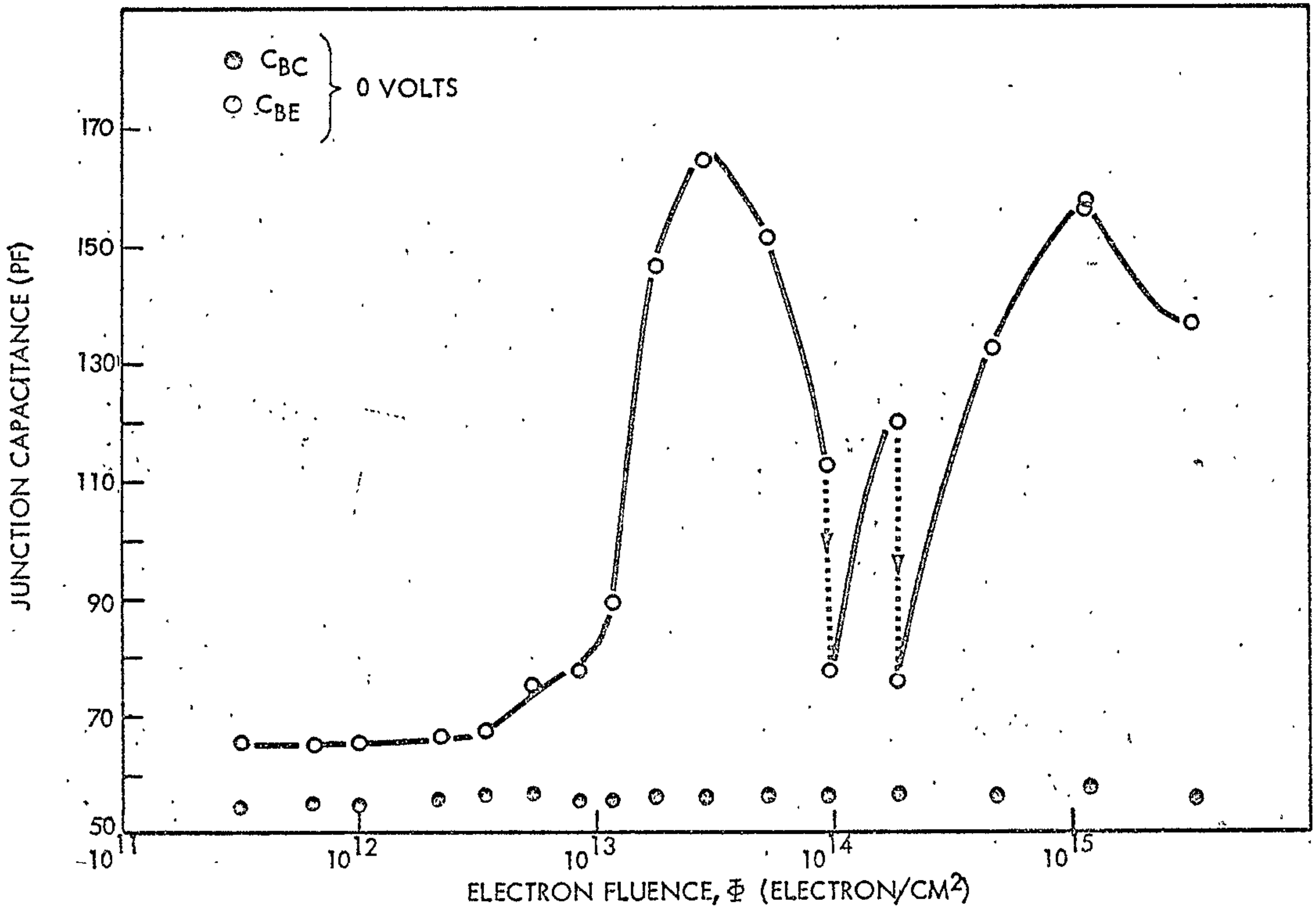

Figure 11. C_{BE} and C_{BC} (Zero Bias) Versus Fluence (Fairchild 2N1613, Active Bias During Irradiation $V_{CB} = 10$ V, $I_E = 10$ ma)

The broken lines indicate "Telstar-type" transient changes with time (usually overnight) after the irradiation has stopped and the bias was turned off.

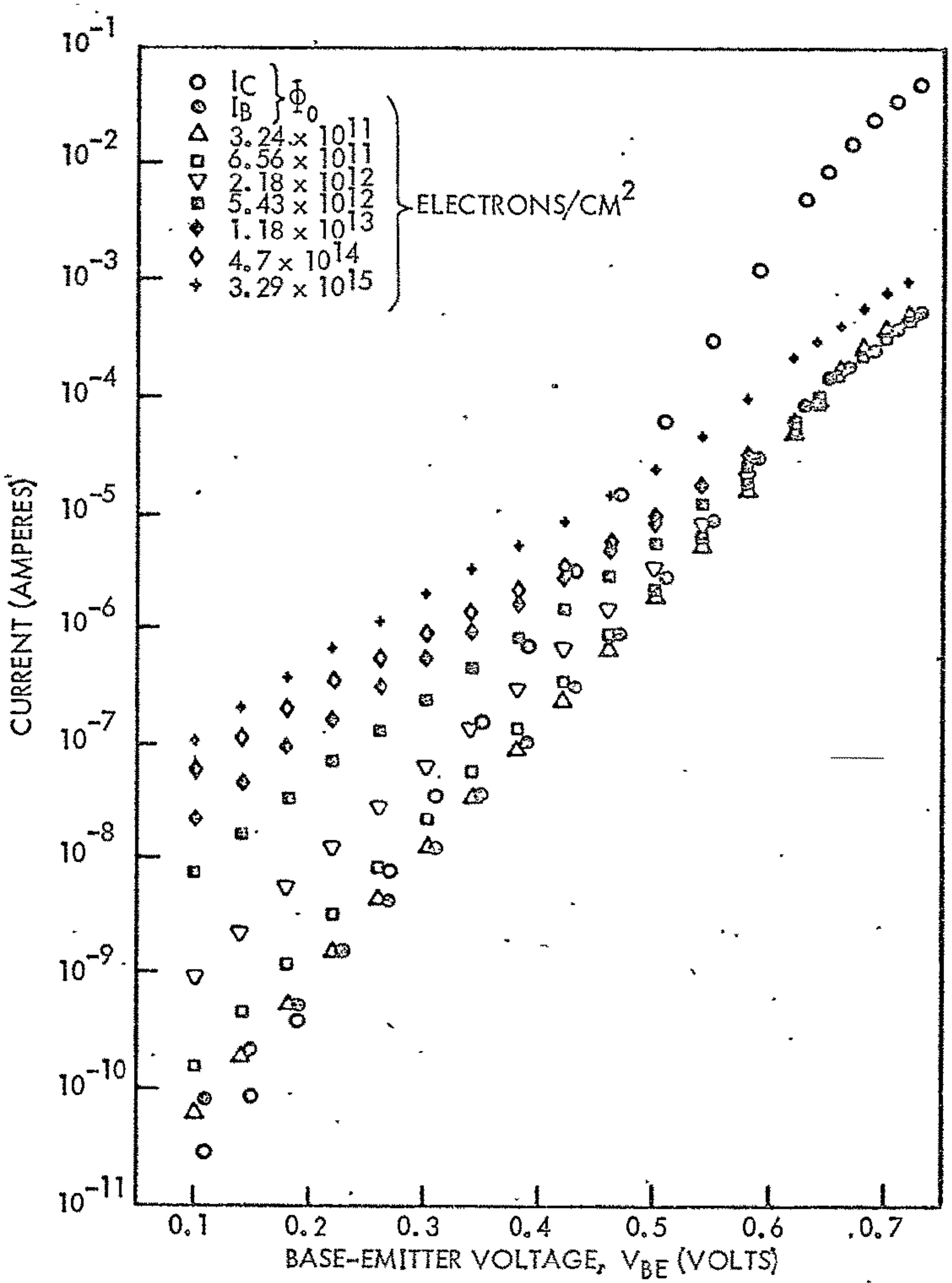

Figure 12. I_B and I_C Versus V_{BE} Curves, Taken at Different Stages During Exposure (Fairchild 2N1613, Active Bias During Irradiation: $V_{CB} = 10$ V, $I_E = 10$ ma)

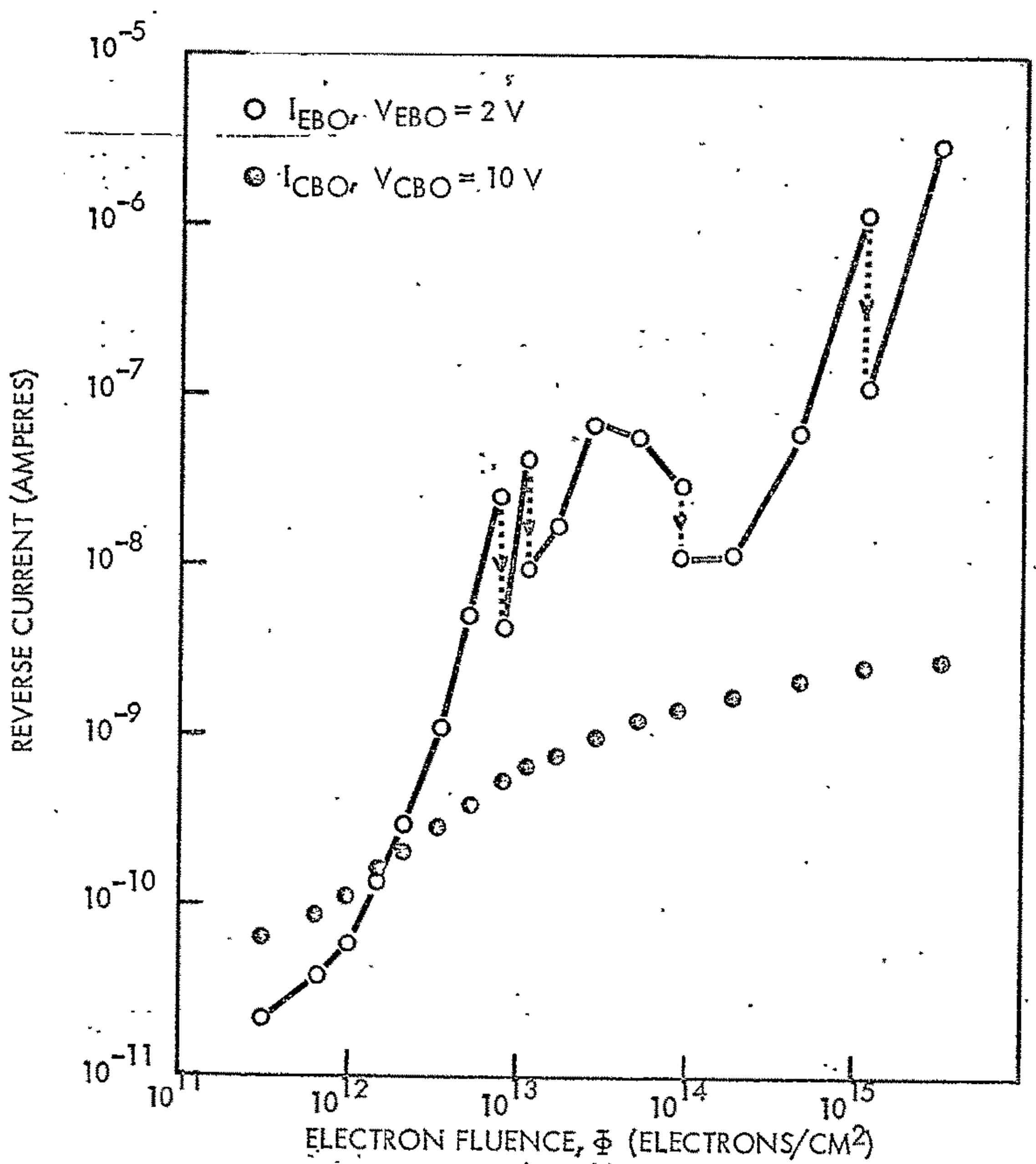

Figure 13. I_{EBO} and I_{CBO} Versus Fluence (Fairchild 2N1613, Active Bias During Exposure)

The broken lines indicate "Telstar-type" transient changes with time (usually overnight) after the irradiation has stopped and the bias was turned off.

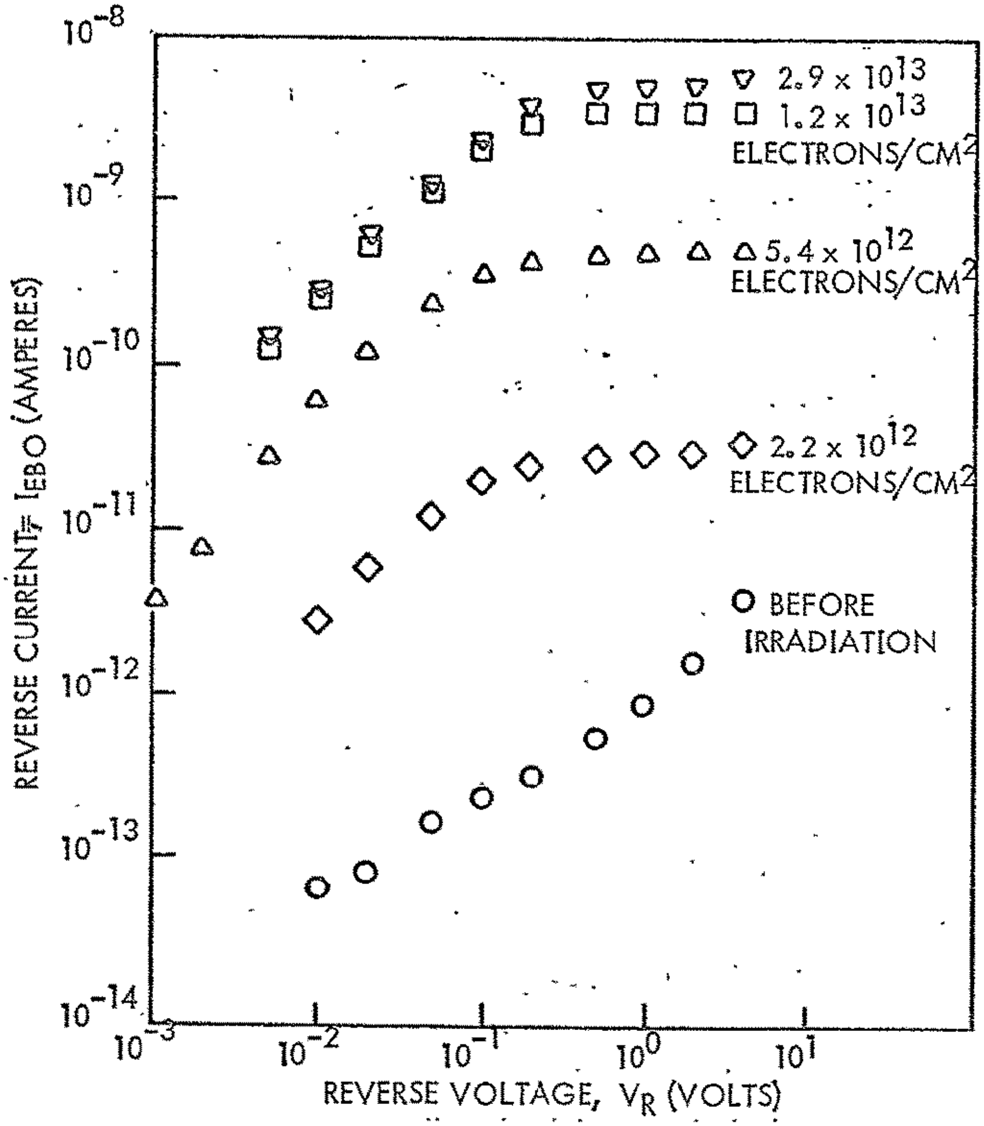

Figure 14. I_{EBO} Versus V_R Curves, Taken at Different Stages During Exposure (Fairchild 2N1613, Active Bias During Irradiation: $V_{CB} = 10V$, $I_E = 10$ ma)

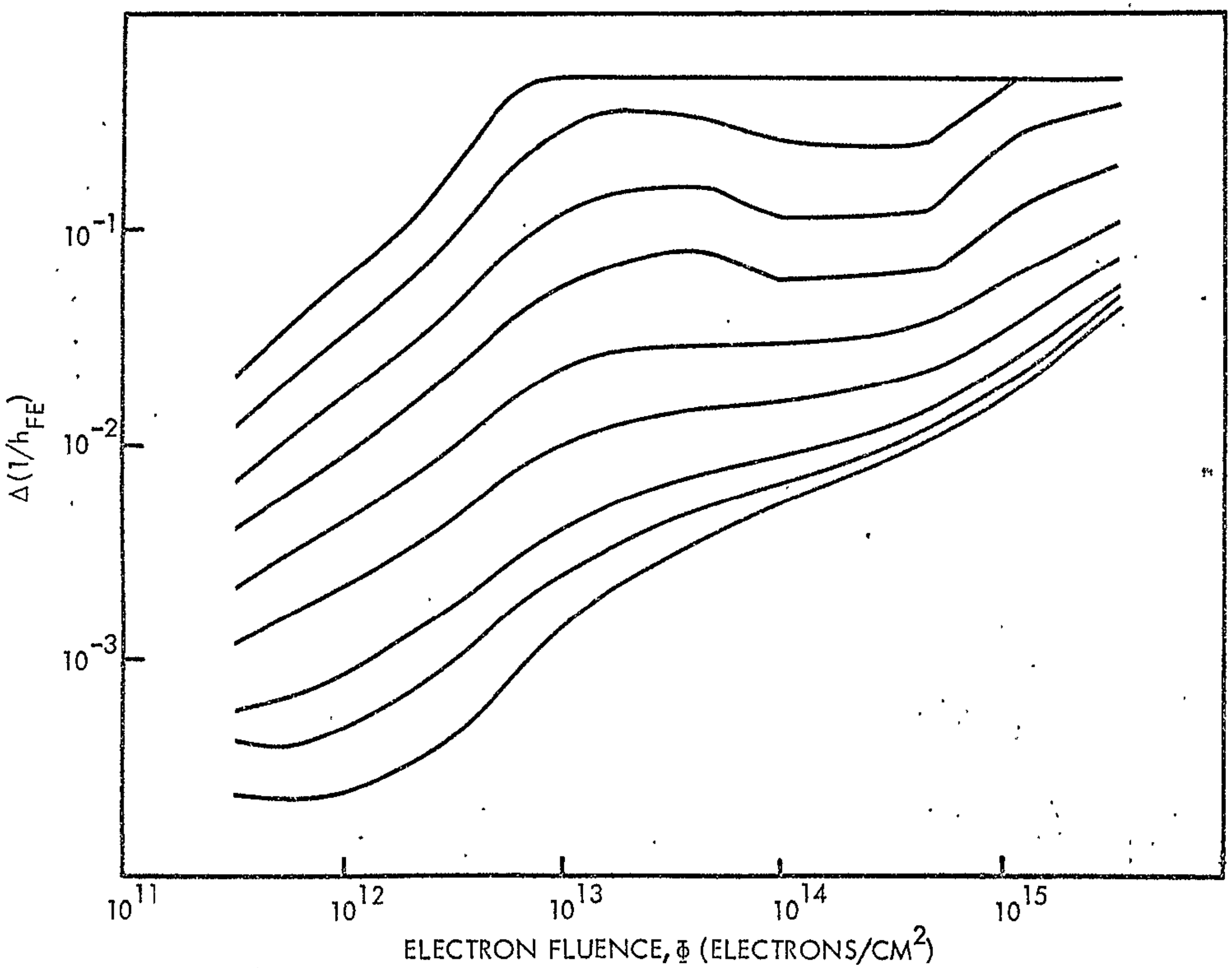

Figure 15. $|\Delta(1/h_{FE})$ Versus Fluence (Fairchild 2N1613, Active Bias During Irradiation: V_{CB} = 10 V, I_E = 10 ma; Measurement Current, I_E, From Top to Bottom: 10μa, 30μa, 100μa, 300μa, 1ma, 3ma, 10ma, 20ma, 40 ma)

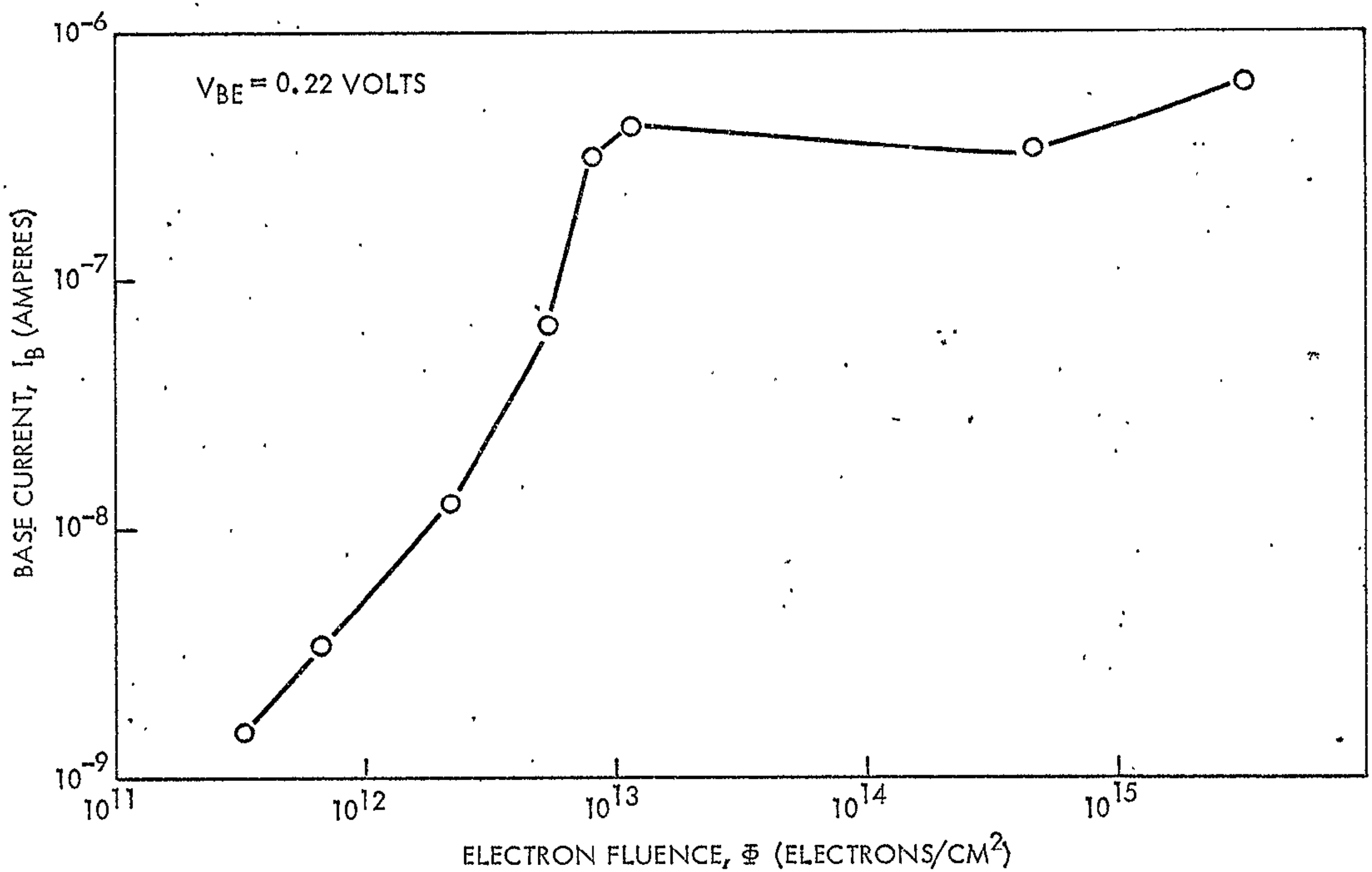

Figure 16. I_B Versus Fluence (Fairchild 2N1613, Active Bias During Irradiation: V_{CB} = 10 V, I_E = 10 ma)

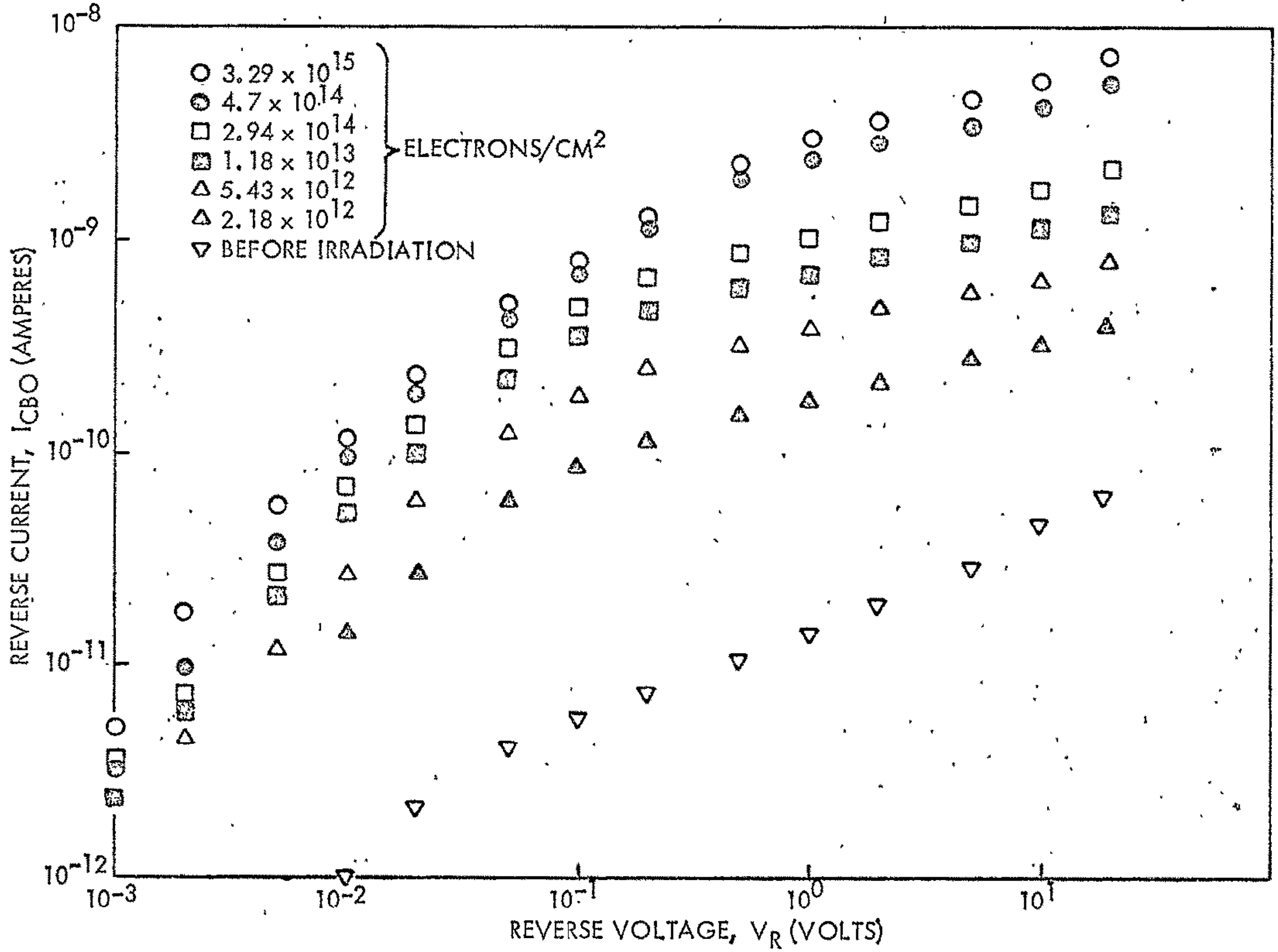

Figure 17. I_{CBO} Versus V_R Curves, Taken at Different Stages During Irradiation (Fairchild 2N1613, Active Bias During Irradiation: V_{CB} = 10 V, I_E = 10 ma)

PNP - unbiased during irradiation: As stated earlier, it is a small part of the emitter region (close to the base-emitter junction) which is primarily affected by the positive charge accumulation and the new interface states, and subsequently leads to gain degradation in a PNP structure. For I_{CBO} degradation the collector surface in the vicinity of the base-collector junction is the important region.

C_{BE} vs. ϕ is shown in Figure (18) for Raytheon 2N1132, device #111. There is no sign of inversion of part of the emitter region. This is in accordance with the n values of 1.24 - 1.55 obtained from the I_B vs. V_{BE} curves (Figure 19). Similarly, inversion is apparently absent over the collector region, (see C_{BC} vs. ϕ on Figure 18), which is somewhat surprising in view of the low surface doping normally found in collectors. Increases in I_B, $\Delta 1/h_{FE}$, I_{EBO}, I_{CBO} as a function of ϕ shown on Figures (20), (21), and (22) respectively, can be qualitatively understood in terms of increased surface recombination over the respective junctions. This assumption is in accordance with the $1.24 \leq n \leq 1.55$ values obtained from Figure (19). However, the I_{EBO} vs. V_R (Figure 23) and I_{CBO} vs. V_R (Figure 24) curves show very little if any saturation tendency with voltage which is at variance with the theoretical predictions of the voltage independence of the surface generation component of current.

PNP - biased during irradiation (Bias: V_{CB} = 10 V, I_E = 0.1 ma):

We saw previously the tremendous difference in irradiation behavior between the passive and active NPN devices. No such significant differences were observed between the passive and active PNP transistors. It is true that, due to the reverse biased collector base junction, an increased charge accumulation thus more severe I_{CBO} degradation was expected and indeed observed in active PNP devices (see Figures 22 and 29). Differences, however, practially disappeared when the gain degradation curves were compared. Although the detailed arguments to account for this observation are not clear, at present, certain tentative ideas can be presented. For one thing, the charge accumulation on the SiO_2 surface must surely be different from the NPN case, since the direction of the fringing electric field between the can and the base or the emitter surface (due to the reverse biased collector base junction) is such now that the positive gas ions, generated inside the

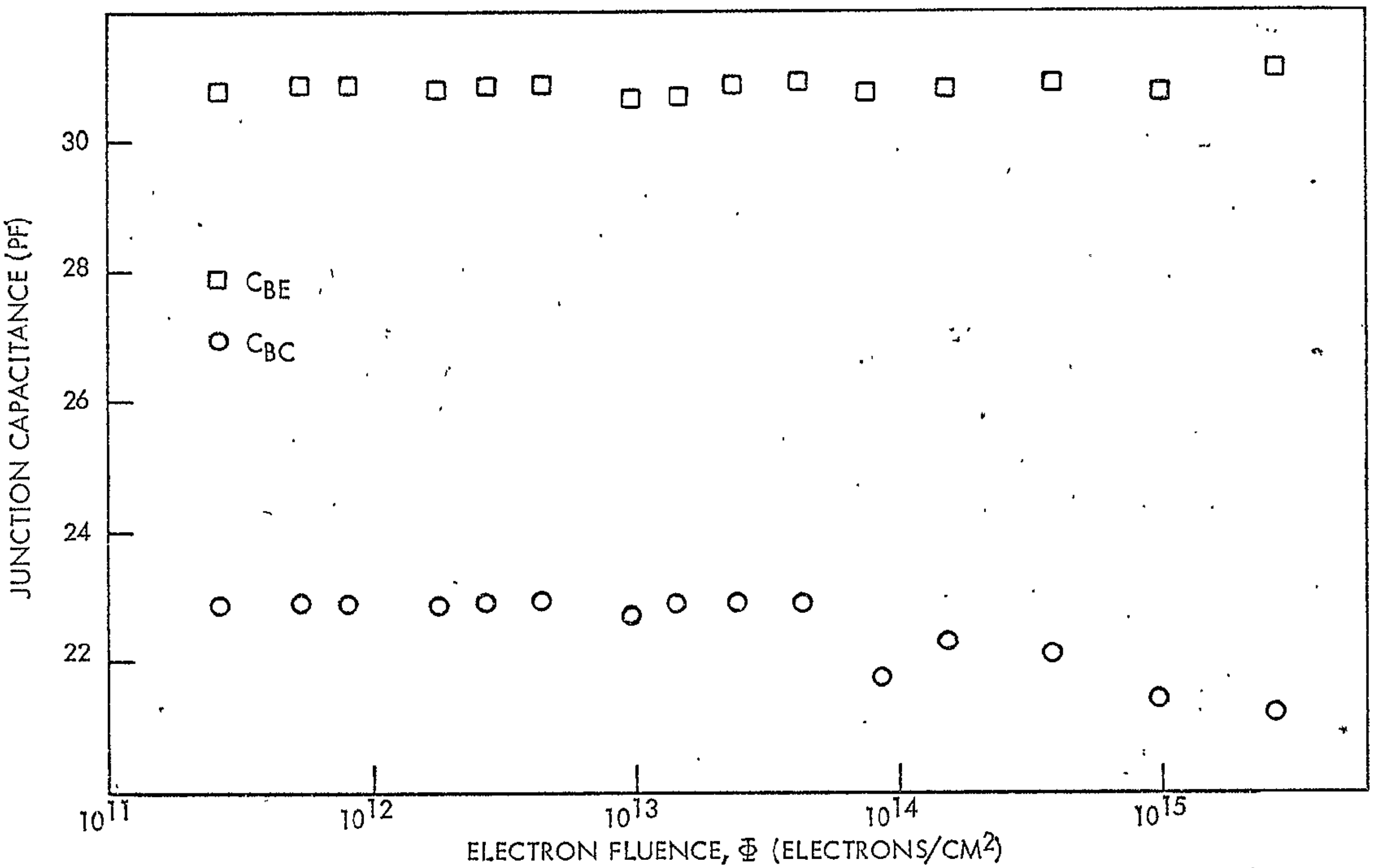

Figure 18. C_{BE} and C_{BC} (Zero Bias) Versus Fluence (Raytheon 2N1132, Passive During Irradiation)

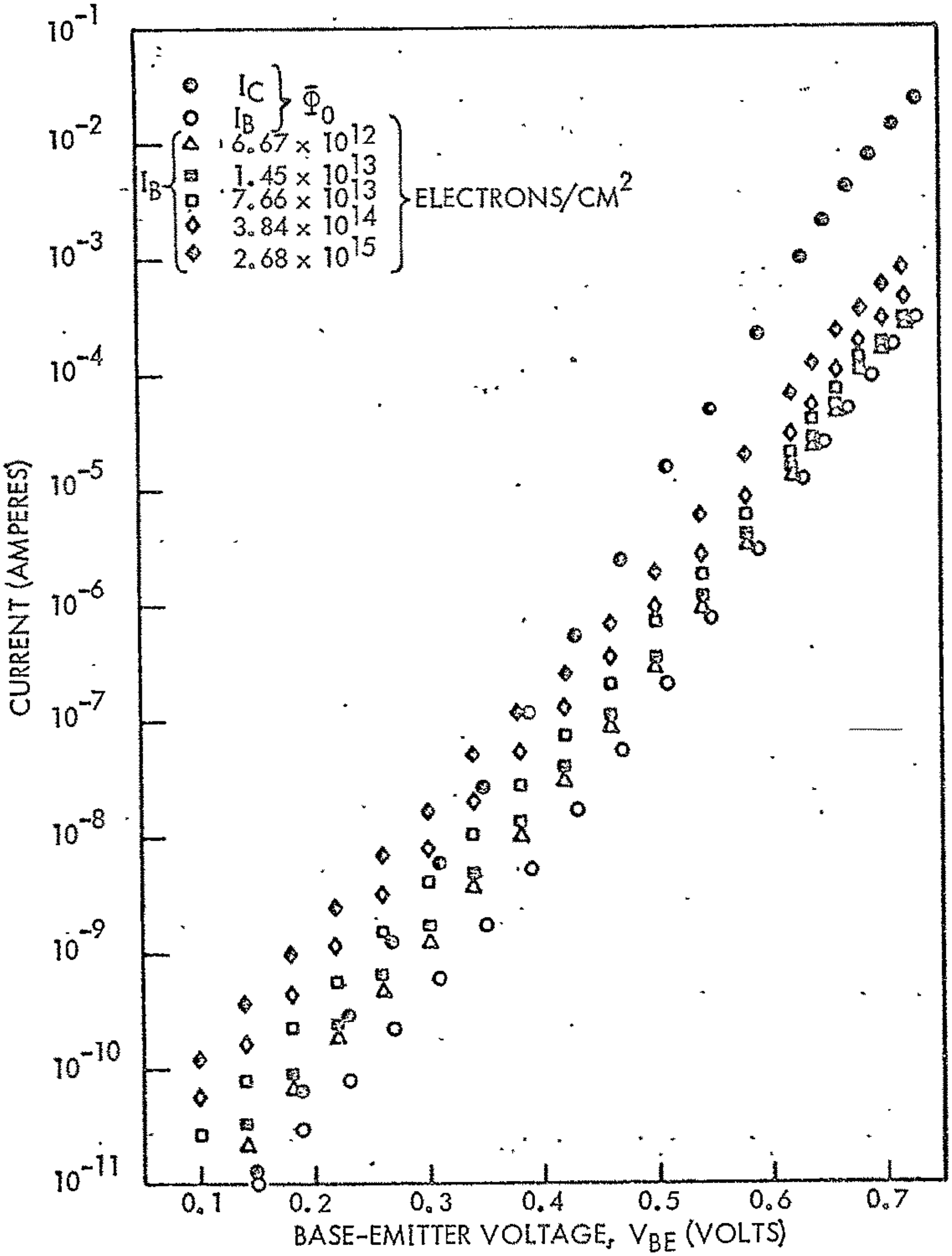

Figure 19. I_B and I_C Versus V_{BE} Curves, Taken at Different Stages During Exposure (Raytheon 2N1132, Passive During Irradiation)

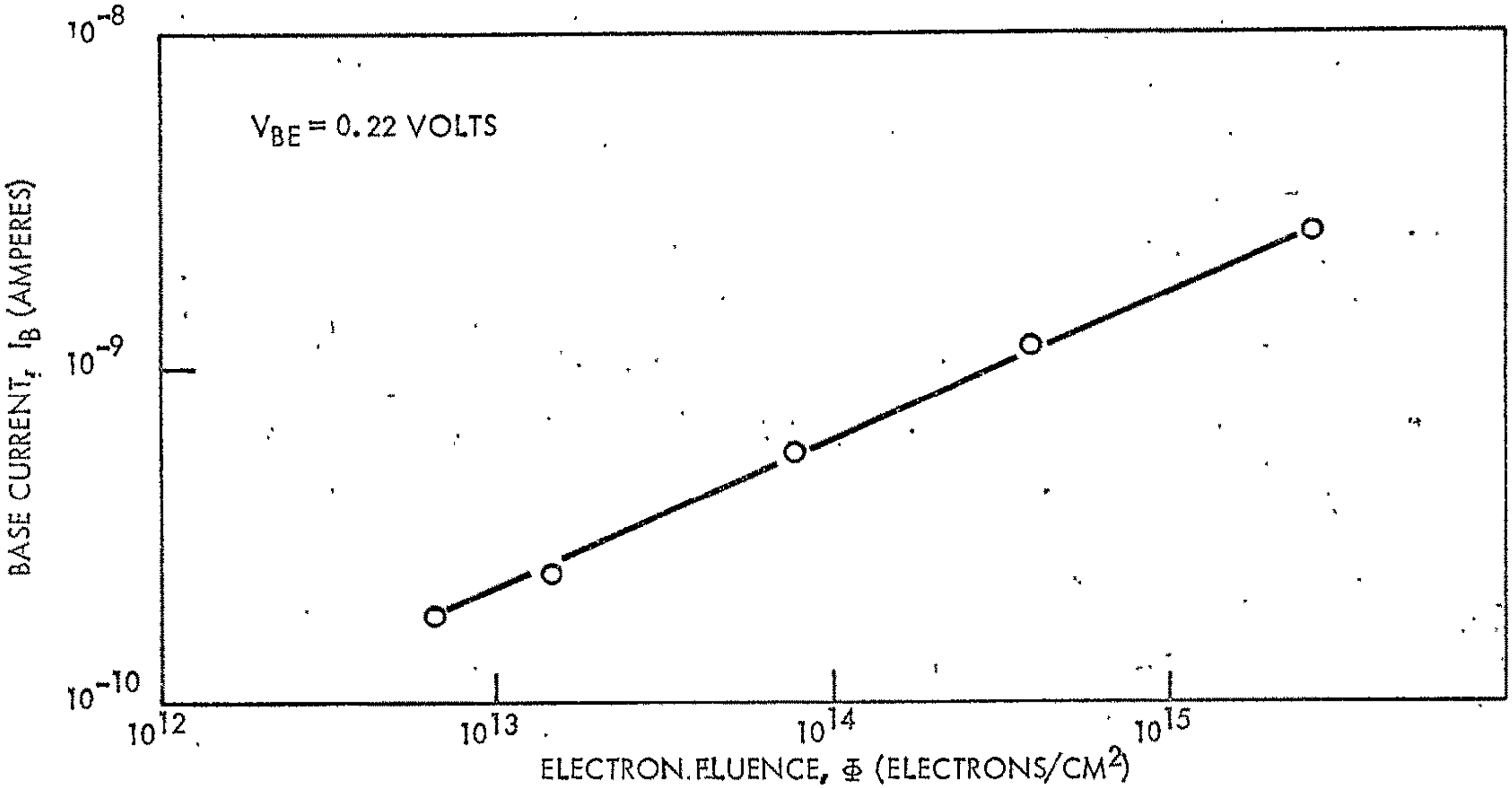

Figure 20. I_B Versus Fluence (Raytheon 2N1132, Passive During Irradiation)

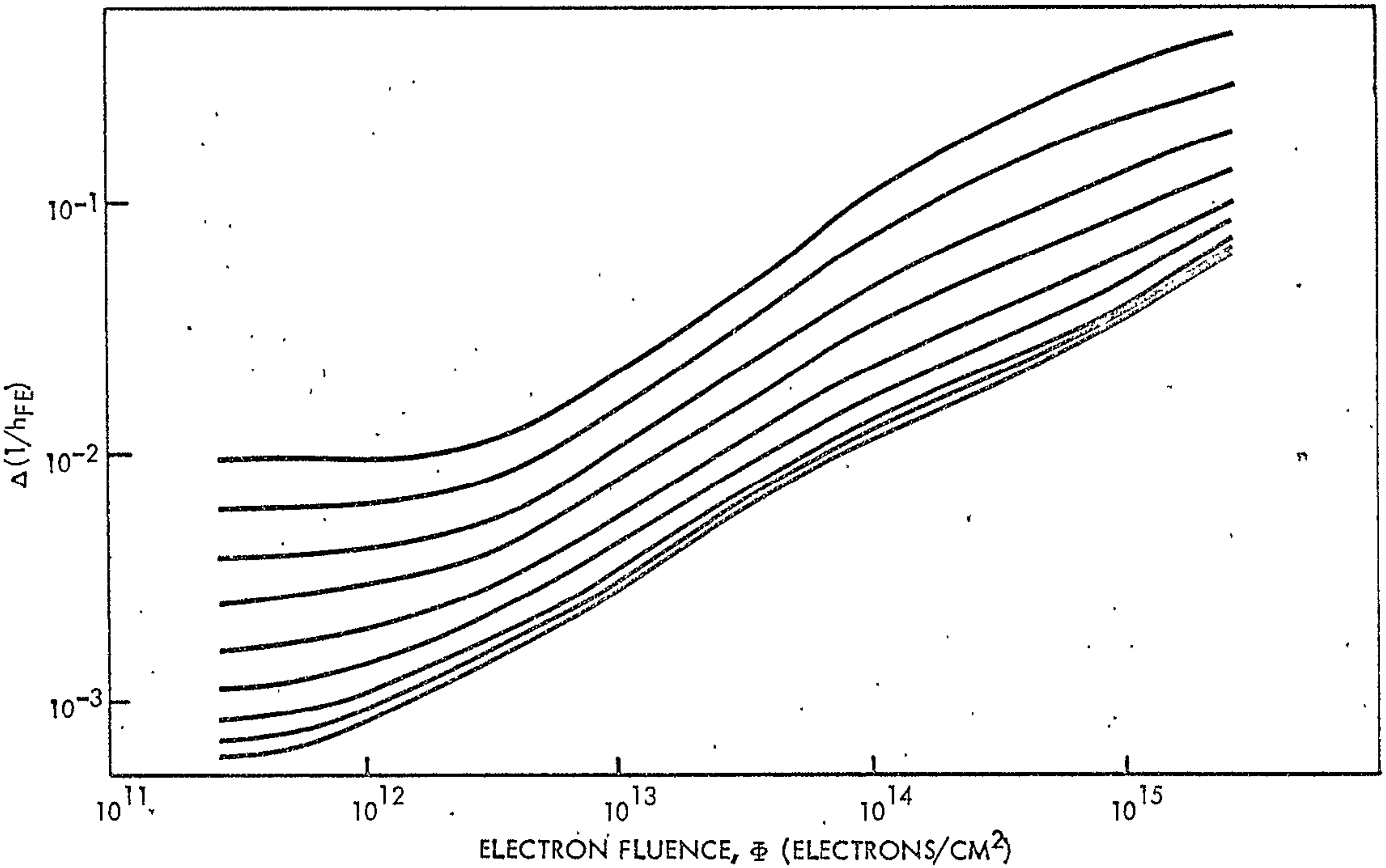

Figure 21. $\Delta(1/h_{FE})$ Versus Fluence (Raytheon 2N1132, Passive During Irradiation) (Measurement Current, I_E, From Top to Bottom: 10μa, 30μa, 100μa, 300μa, 1ma, 3ma, 10ma, 20ma, 40ma)

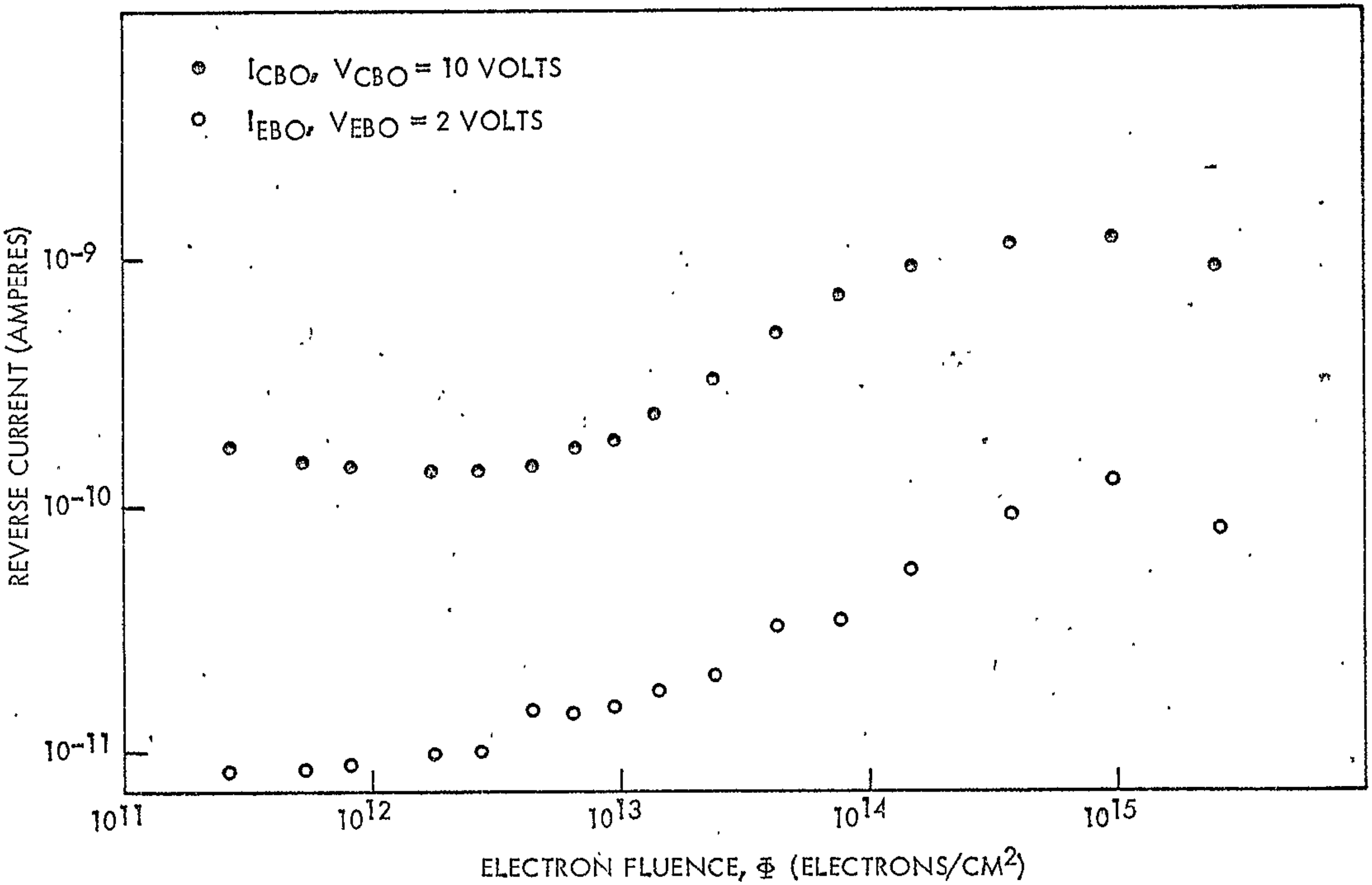

Figure 22. I_{EBO} and I_{CBO} Versus Fluence (Raytheon 2N1132, Passive During Irradiation)

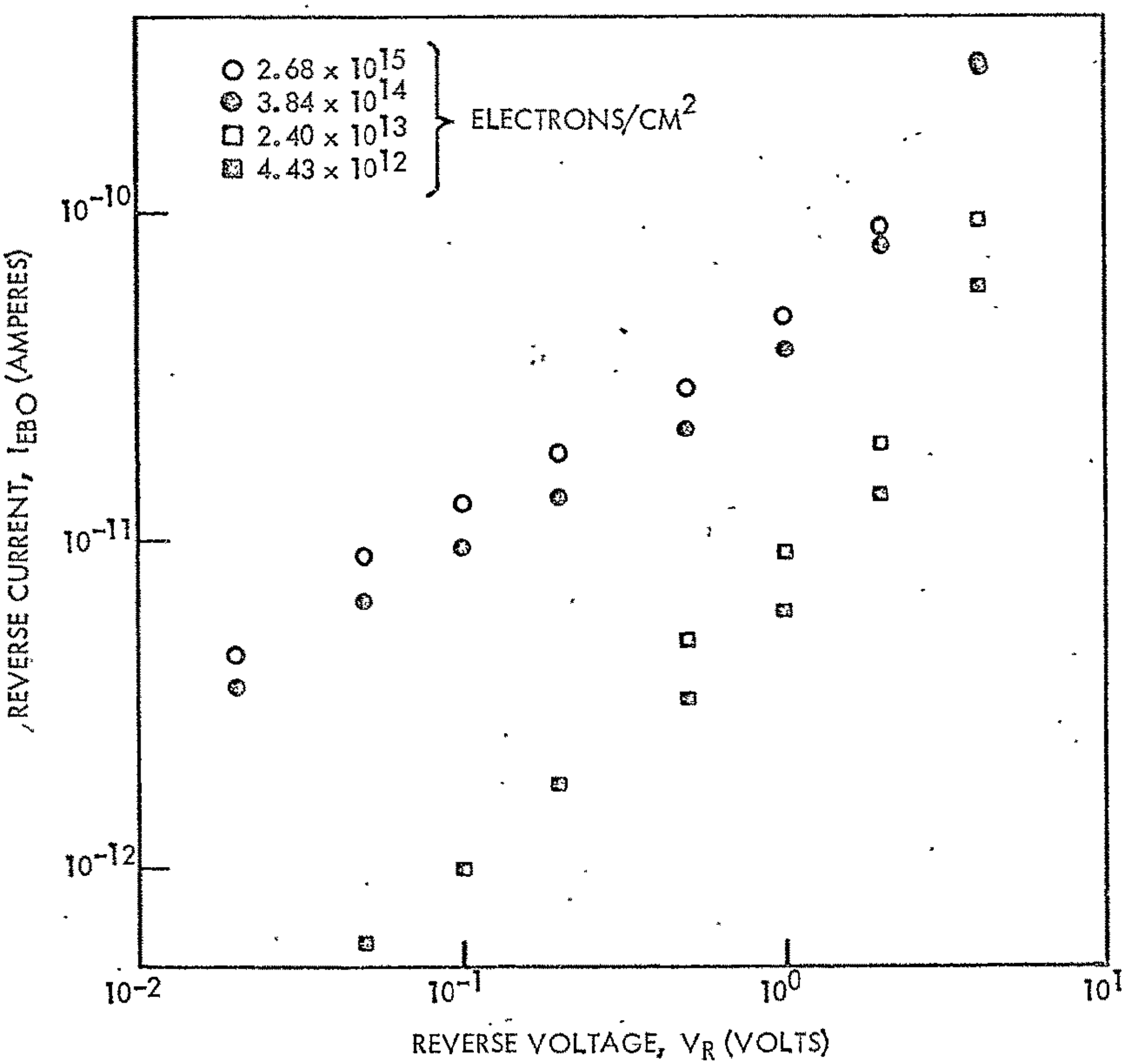

Figure 23, I_{EBO} Versus V_R Curves, Taken at Different Stages During Exposure (Raytheon 2N1132, Passive During Irradiation)

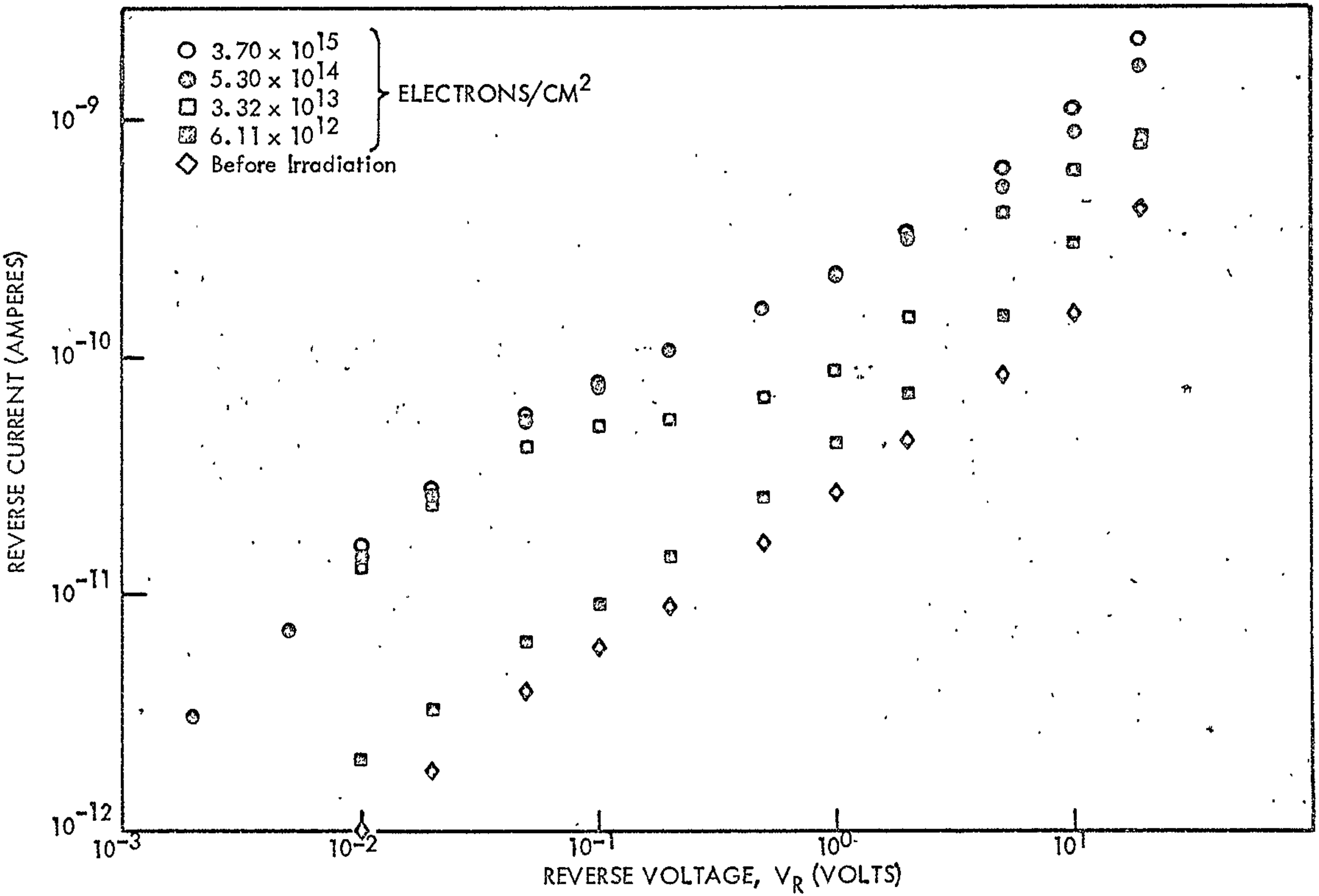

Figure 24. I_{CBO} Versus V_R Curves, Taken at Different Stages During Exposure (Raytheon 2N1132, Passive During Irradiation)

can, are moved toward the transistor can. But then the positive charge accumulation on the SiO_2 could be small which is essentially the case also for the passive PNP devices. Secondly, in an NPN device the depletion of the silicon surface and the creation of new interface states occur coincidentally at the base surface. Hence their effect can reinforce each other significantly. This may not be the case for the emitter region of a PNP device. If, e.g., the creation of the new interface states over the base of an active NPN structure were enhanced by electron injection then such an enhancement would not occur in the emitter region of an active PNP transistor, due to the absence of such an injection. Then the differences in irradiation response between passive and active PNP transistors could be restricted essentially to slight differences in charge accumulation within the SiO_2, the net effect of which might be small. Clearly, further speculation is not justified without the benefit of additional experimental data.

The remarks on the figures are very similar to the PNP - unbiased case. Both C_{BE} vs. ϕ and C_{BC} vs. ϕ (Figure 25), shown for Raytheon 2N1132, device #121, indicate the absence of inversion in the emitter and collector regions respectively. The n values of 1.25 - 1.64 obtained from the I_B vs. V_{BE} curves (Figure 26) support the conclusion. The assumption of increased surface recombination over the junctions as the main reason for the increase in I_B (Figure 27), $\Delta 1/h_{FE}$ (Figure 28), I_{EBO} (Figure 29), I_{CBO} (Figure 29) are also in accordance with the quoted n values. However, the presumed voltage independence of the surface dominated I_{CBO} is demonstrated on the I_{CBO} vs. I_R curves in Figure (30) only above 0.1 volt (at large fluences). Worst yet, the I_{EBO} vs. V_R curves in Figure (31) are at variance with the theoretical predictions over the whole voltage range.

In closing this section we would like to mention the preliminary results of the transit time measurements on the passive devices: The majority of the Fairchild 2N1613 showed an <u>increase</u>, most of the Raytheon 2N1613, 2N1132 and the Fairchild 2N1132 showed a <u>decrease</u> in the base transit time with exposure. The reverse behavior of the Fairchild NPN devices with respect to the rest is very intriguing. However, the analysis of these data is not sufficiently developed yet to warrant further discussion.

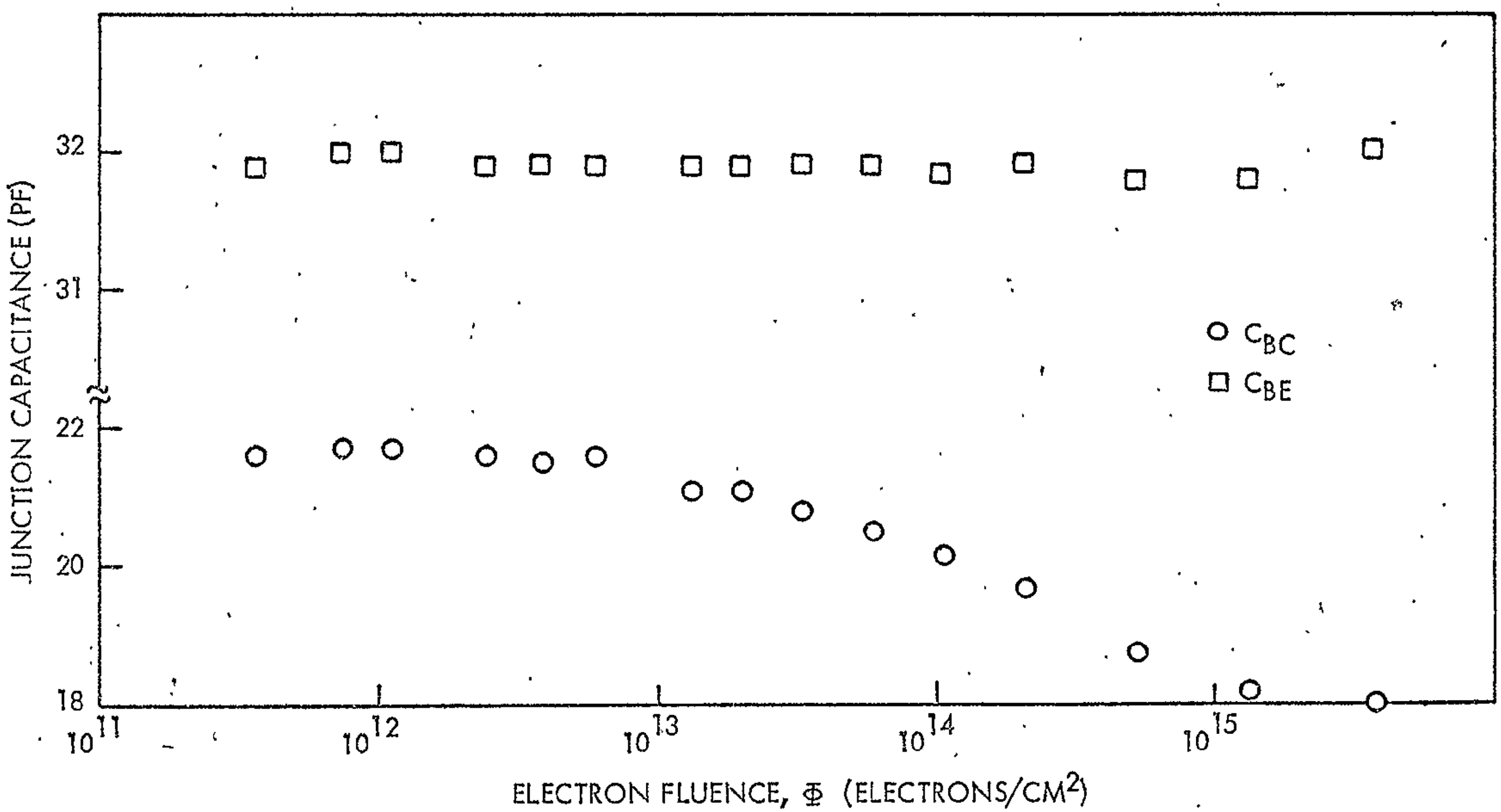

Figure 25. C_{BE} and C_{BO} (0 Volts) Versus Fluence (Raytheon 2N1132, Active Bias During Irradiation: $V_{CB} = 10$ V, $I_E = 0.1$ ma)

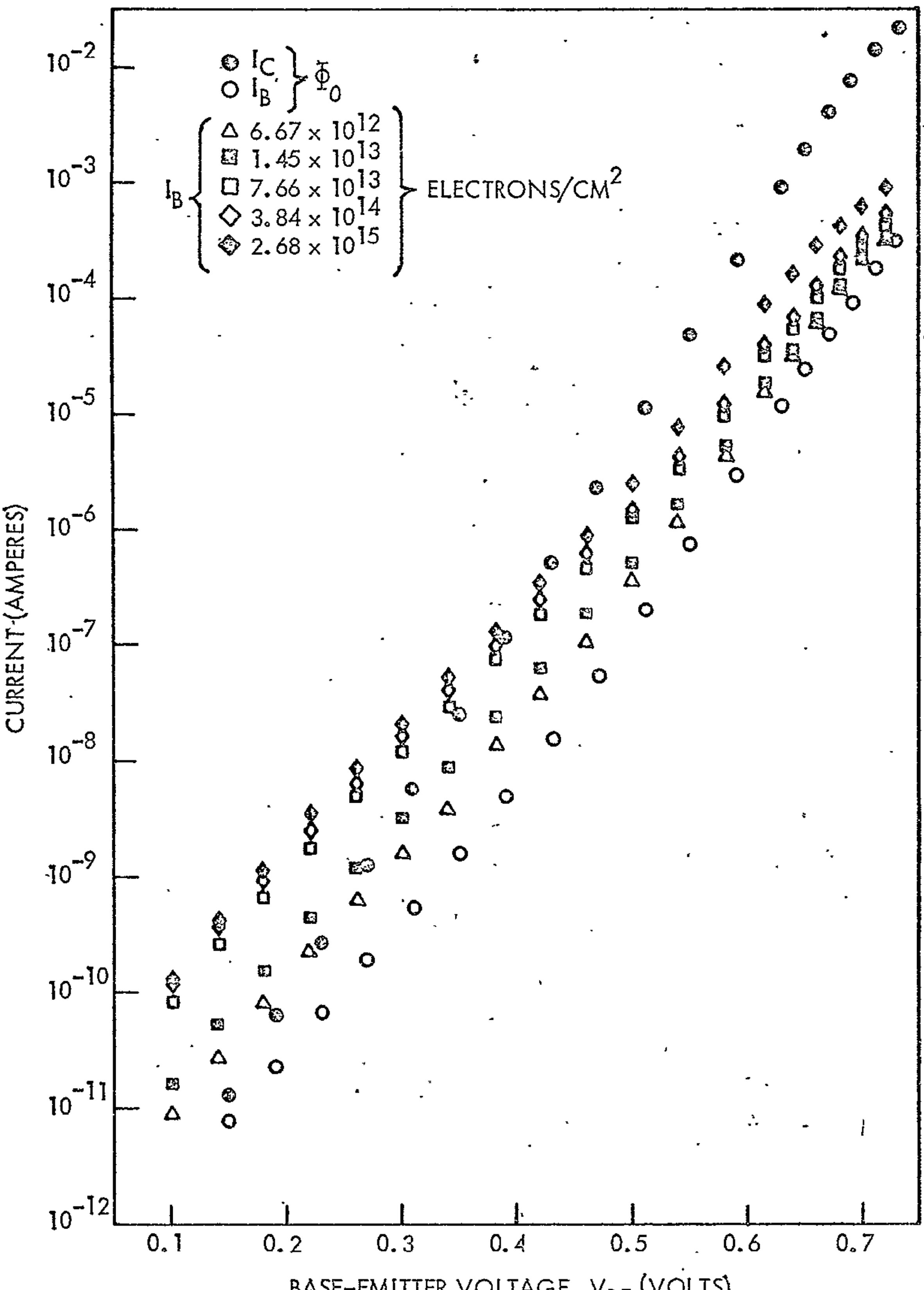

Figure 26. I_B and I_C Versus V_{BE} Curves, Taken at Different Stages During Exposure (Raytheon 2N1132, Active Bias During Irradiation: $V_{CB} = 10$ V, $I_E = 0.1$ ma)

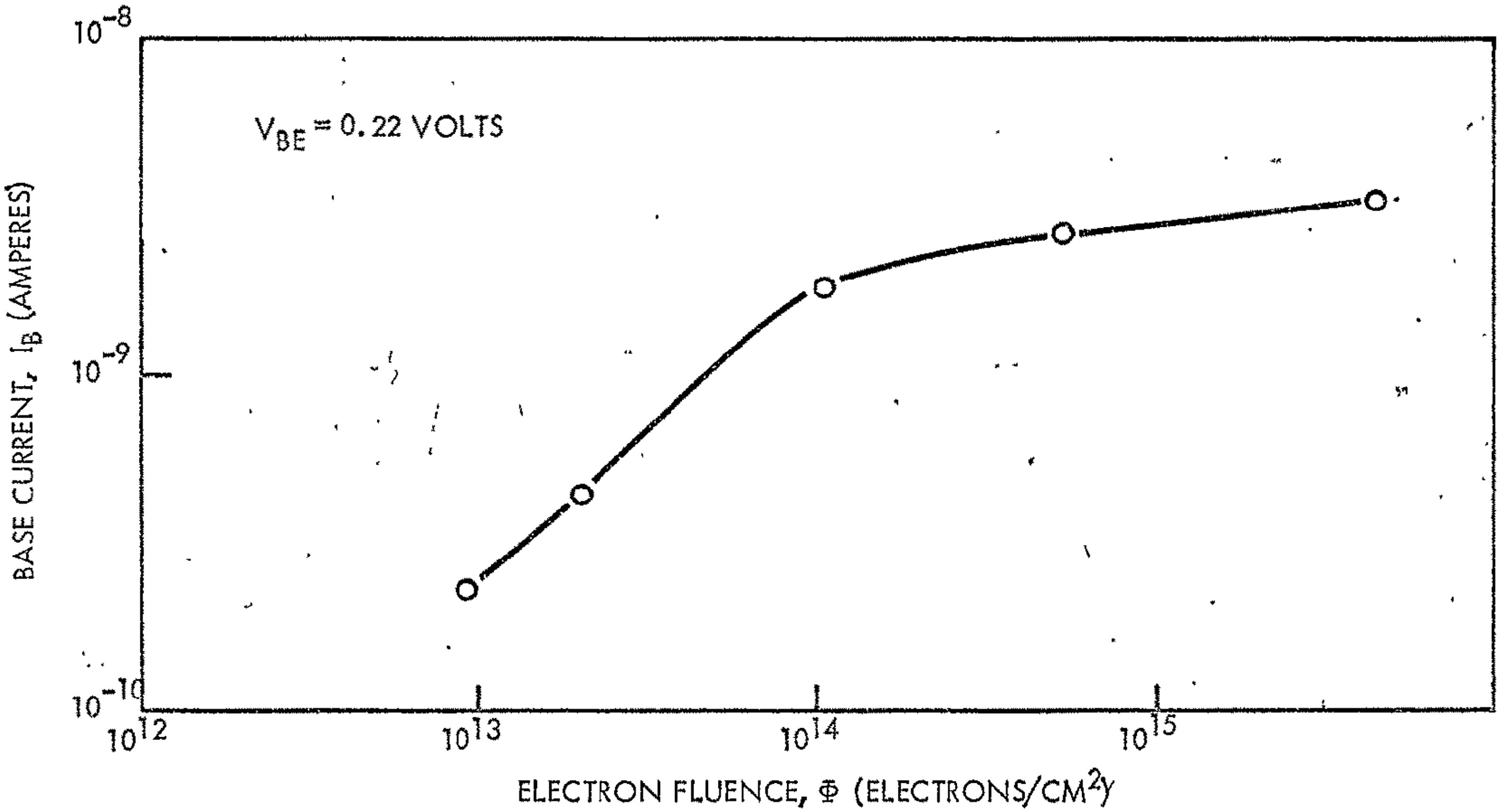

Figure 27. I_B Versus Fluence (Raytheon 2N1132, Active Bias During Irradiation: $V_{CB} = 10$, $I_E = 0.1$ ma)

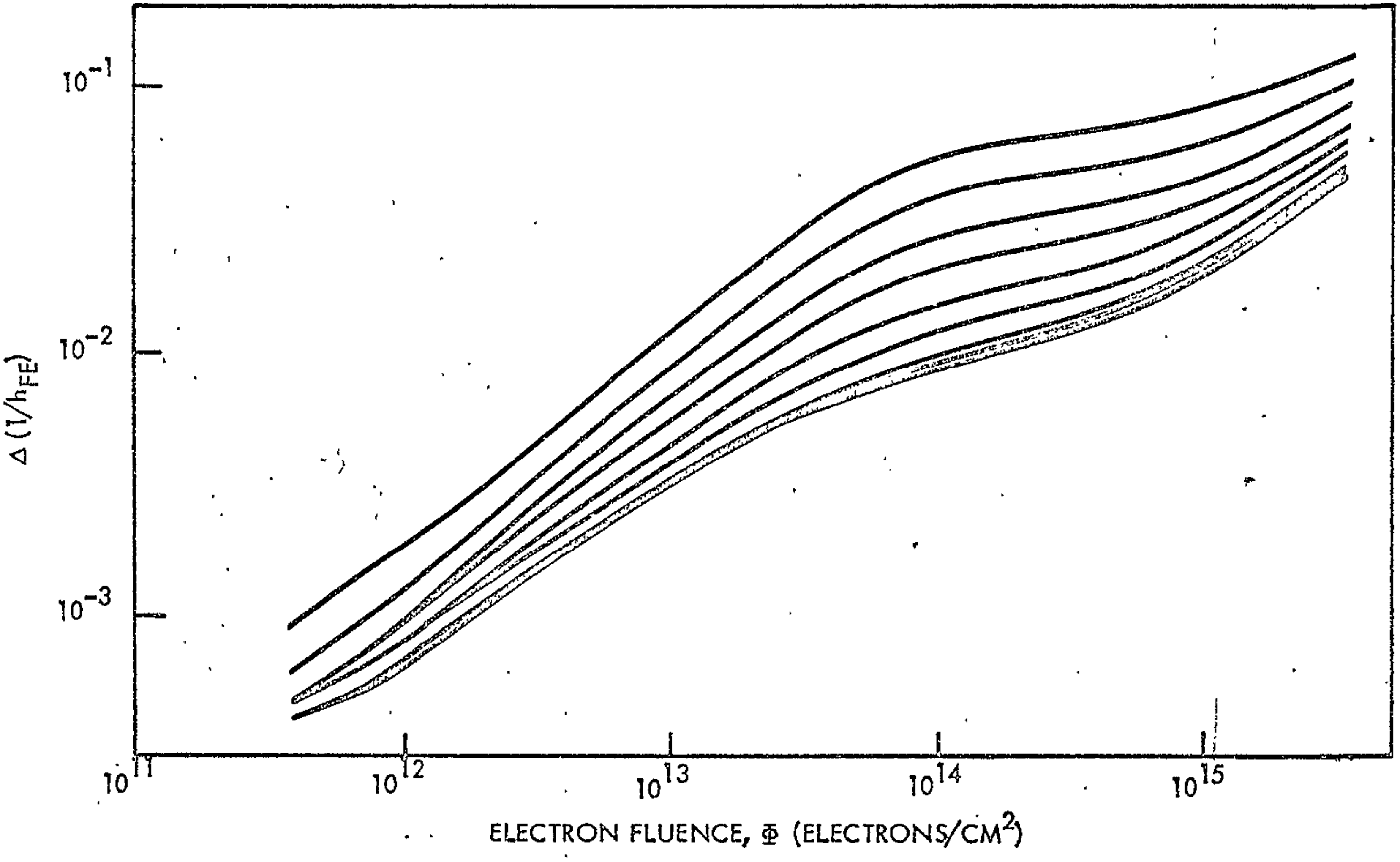

Figure 28. $\Delta(1/h_{FE})$ Versus Fluence (Raytheon 2N1132, Active Bias During Irradiation: $V_{CB} = 10$ V, $I_E = 0.1$ ma; Measurement Current, I_E, From Top to Bottom: 10μa, 30μa, 100μa, 300μa, 1 ma, 3 ma, 10 ma; 20 ma, 40 ma)

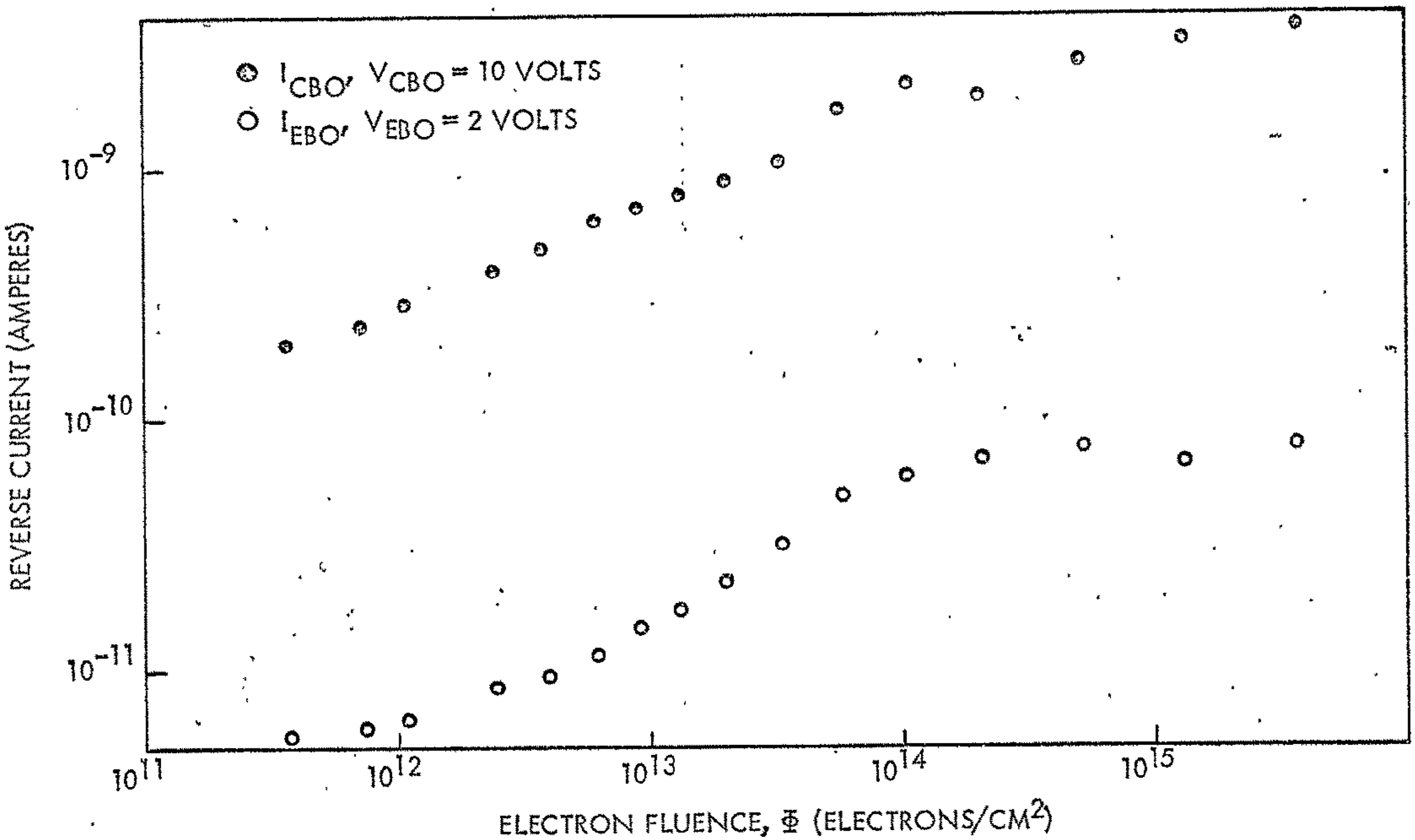

Figure 29. I_{EBO} and I_{CBO} Versus Fluence (Raytheon 2N1132, Active Bias During Irradiation: V_{CB} = 10 V, I_E = 0.1 ma)

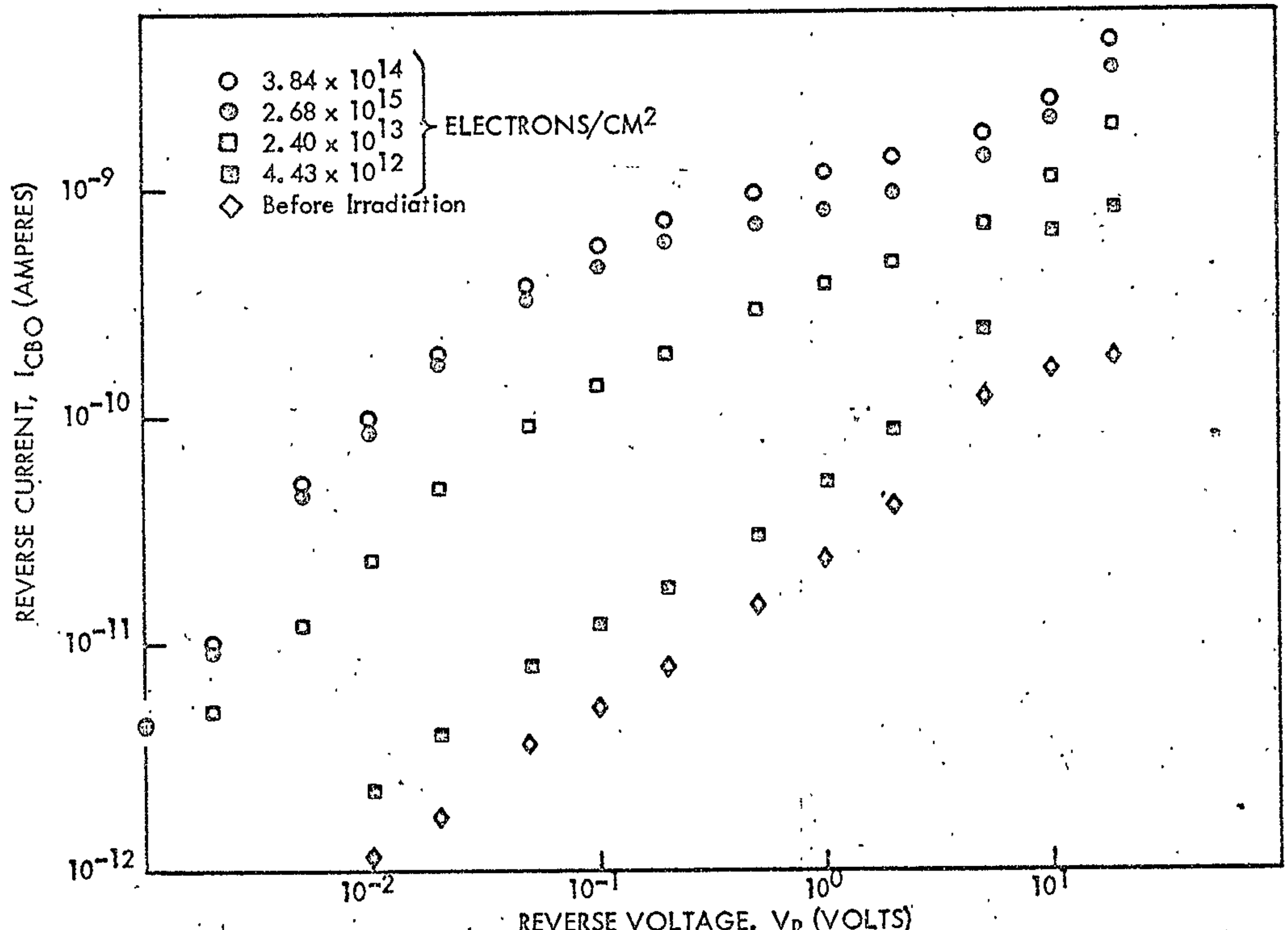

Figure 30. I_{CBO} Versus V_R Curves, Taken at Different Stages During Exposure (Raytheon 2N1132, Active Bias During Irradiation: $V_{CB} = 10$ V, $I_E = 0.1$ ma)

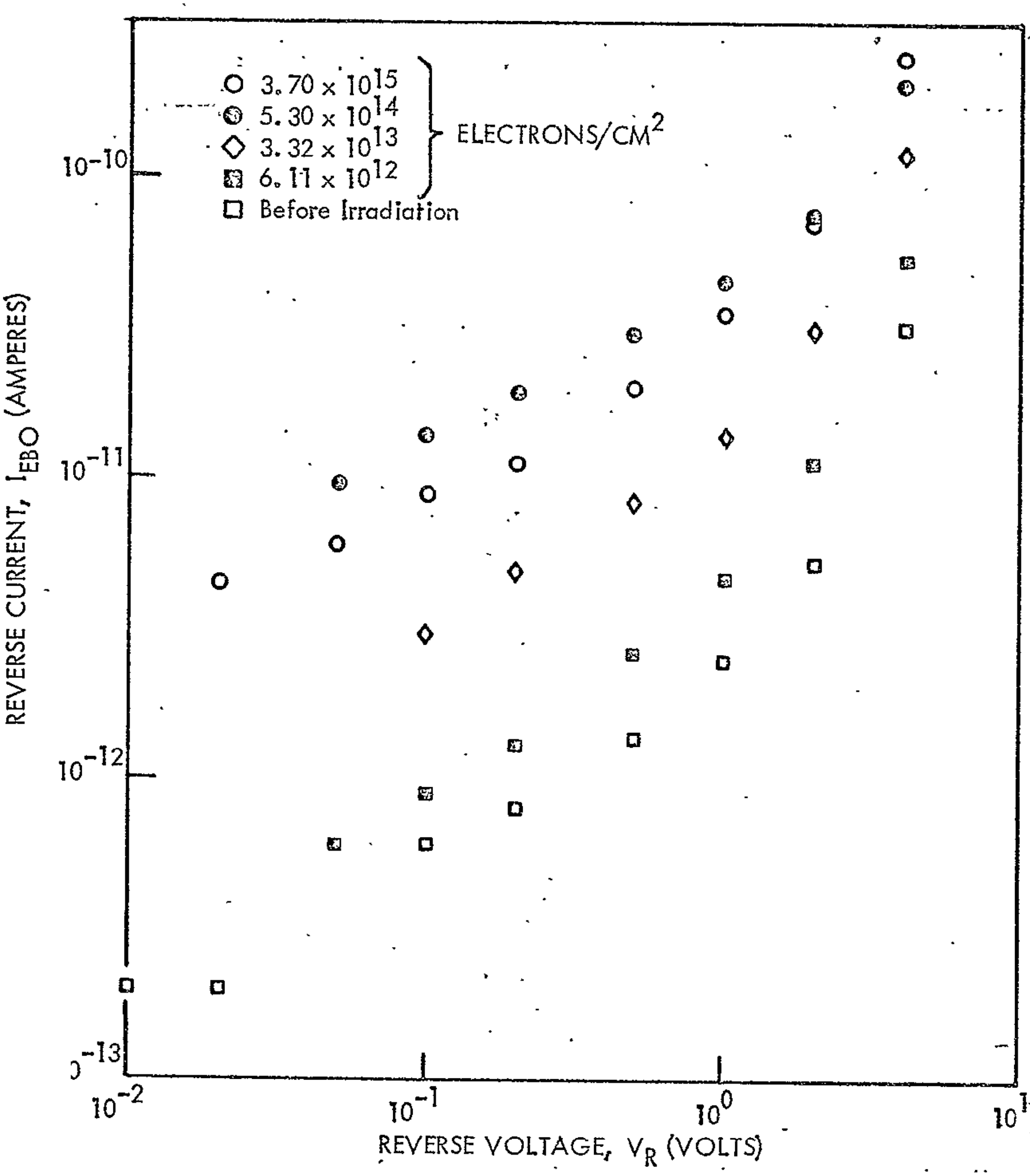

Figure 31. I_{EBO} Versus V_R Curves, Taken at Different Stages During Exposure (Raytheon 2N1132, Active Bias During Irradiation: $V_{CB} = 10$ V, $I_E = 0.1$ ma)

2.2.3 Analytical Form of the Damage Buildup with Dose

Displacement damage on transistor gain is often called linear damage because the buildup of $\Delta 1/h_{FE}$ is proportional to the fluence, Φ. Surface damage on transistor gain on the other hand is often called nonlinear damage because the relation between $\Delta 1/h_{FE}$ and Φ is not linear. Of course, for the purpose of predicting gain degradation with dose, it is of fundamental importance to know what the actual relation is; i.e., is it a power law like D^x (at least before saturation) where x is some number and D is the dose; or perhaps an exponential relation like constant $(1 - e^{-\beta D})$ where β is a constant? One paper claims[10] that for 125 keV electron irradiation

$$\Delta 1/h_{FE} = K \ln(\Phi/\Phi_o) \tag{9}$$

where both K and Φ are some constants. Actually, for practical reasons there is no theoretical prediction on the $\Delta 1/h_{FE}$ vs. D or Φ relation.

First, the electric field intensity and its distribution within the SiO_2 has to be known for the exact description of the charge accumulation with dose. However, the fringing fields in the vicinity of the junctions due to biases are not very amenable to theoretical analysis.

Second, it is not possible to relate $\Delta 1/h_{FE}$ <u>directly</u> to the effect of irradiation in a general manner, since $\Delta 1/h_{FE}$ is affected by both the buildup of positive space charge in SiO_2 and the creation of new interface states. The relative importance of these two effects is still unsettled, probably depends on the particular experimental conditions. In any case, the theoretical prediction of the buildup of interface states with dose is still missing, as discussed in 2.2.1.1. Consequently, the buildup of the related quantity $\Delta 1/h_{FE}$ with dose cannot be predicted at present.

As far as the empirical curves of the $\Delta 1/h_{FE}$ vs. Φ curves are concerned we see later in Figures (35) through (46) that <u>there is a whole variety of curves</u> with very different shapes depending on transistor types, manufacturers, batches (or date codes), biasing conditions. For example, a simple power law of the form $\Delta 1/h_{FE}$ = constant Φ^x where $x < 1$, is exhibited in Figures (36) and (40), representing about 20 and 10 devices respectively. Not one of our curves follow the relation (9) so its validity is probably quite limited. Our main conclusion is that one cannot make a specific statement about the shapes of the $\Delta 1/h_{FE}$ vs. Φ curves, except perhaps emphasizing their wide variety.

We would like to stress this last point very strongly since one recent paper(11) claims a general validity of the simple power law representation of the buildup of the nonlinear damage with fluence or dose, i.e., it is claimed that

$$\Delta \frac{1}{h_{FE}} = \text{constant } \Phi^{x} \qquad 0 < x < 1 \qquad (10)$$

Now we said earlier that some of our passive devices indeed obeyed this simple relation. But <u>not</u> all of them. In fact, most of them did not, as Figures (35) through (46), representing most of our 218 devices (passive, active, NPN, PNP), will illustrate. Of course, within a small dose range many of the $\Delta 1/h_{FE}$ vs. Φ curves can be approximated by a simple power law. However, this approximation fails when the whole dose range, below damage saturation, is considered. The second point is that in the proposed power law representation of the nonlinear damage with dose, the exponent, x, is claimed to be always less or at most equal to 1. In our experiments, most of the active NPN transistors exhibited <u>faster</u> than linear rise ($x > 1$) in part of the $\Delta 1/h_{FE}$ vs. Φ plots. This means, of course, that in trying to predict nonlinear damage for such devices, in a given mission, with a less than linear power law, will badly underestimate the expected gain degradation. Due to the great importance of such prediction problems, further study would be clearly justified to clear up the discrepancies just discussed. (Interestingly enough, there appeared to be a slight voltage dependence of the exponent, x, being less than 1 or equal to 1 at the lower collector-base voltages. It is intriguing to speculate that the value of x, for whatever the power law approximation is worth, is dependent not only on device structure and processing variables, but also on the applied active biasing conditions. Note that in Reference (11) x is not assumed to be dependent on biasing, the authors simply increase the surface damage constant, k_s, to account for higher gain degradation of transistors with a reverse biased C-B junction.)

2.2.4 Correlation Studies

In trying to predict the response of bipolar transistors to ionizing irradiation it would be of considerable help if one could correlate certain initial and final parameters.

With this idea in mind, correlation studies were carried out between a number of initial and final parameters. Table 2 summarizes some of the results. Parameters in question are listed as well as the degree of correlation expressed in terms of the Rank coefficients.

As shown in Table 2 and in Figures (32), (33), and (34), good correlation was found only in one case, namely between the gain loss Δh_{FE} and the initial gain h^o_{FE}, especially for the Fairchild devices. In the strict sense of the word the relationship found in the quoted figures is not really a correlation. It may be nothing more than a useful relation for predicting gain loss subject to certain limitations. Nonetheless, the word "correlation" will be used, rather loosely, in this report, in the context described below.

Relation between Δh_{FE} and h^o_{FE}

$$h_{FE} \equiv \beta \qquad h^o_{FE} = \beta_o \qquad \Delta h_{FE} \equiv \Delta\beta$$

$\sum I^X_B$: sum of the extra base current components introduced by the irradiation.

$$\frac{\beta_o - \beta}{\beta_o} = 1 - \frac{\beta}{\beta_o} = 1 - \frac{I_c/(I^o_B + \sum I^x_B)}{I_c/I^o_B} = 1 - \frac{I^o_B}{I^o_B + \sum I^x_B} = \frac{\sum I^x_B}{I^o_B + \sum I^x_B}$$

$$\Delta\beta = \frac{\sum I^x_B}{I^o_B + \sum I^x_B} \cdot \beta_o = \frac{1}{1 + \frac{I^o_B}{\sum I^x_B}} \beta_o$$

$$\Delta\beta \simeq K \beta_o \quad \text{where } K \equiv \frac{1}{1 + \frac{I^o_B}{\sum I^x_B}} \tag{11}$$

Initial Parameter	β_o (10 V, 0.01 mA)				$1/I_{EBO}$ ($\frac{6}{4}$ volts)			
Final Parameter	β_f	$\Delta\beta$	$\Delta\beta/\beta_o$	$\Delta 1/\beta$	β_f	$\Delta\beta$	$\Delta\beta/\beta_o$	$\Delta 1/\beta$
<u>NPN</u>								
a) NPN Fairchild, unbiased	.82	.95	.46	-.63	.03	.22	.27	.09
b) NPN Fairchild, biased	.21	.89	.22	-.11	.12	.23	.00	-.07
c) NPN Raytheon, unbiased	.44	.47	.07	-.20	.03	.20	.16	.06
<u>PNP</u>								
d) PNP Fairchild, unbiased	.77	.83	.07	-.36	-.42	-.45	-.06	.16
e) PNP Raytheon, biased	.52	.81	.01	-.33	.34	.02	-.26	-.30
f) PNP Raytheon, unbiased	.44	.92	.42	.05	.37	.52	.29	.08

Table 2. RANK CORRELATION COEFFICIENTS

(β_f = final gain; I_{EBO} was measured at 4 volts for the Fairchild 2N1132 devices only)

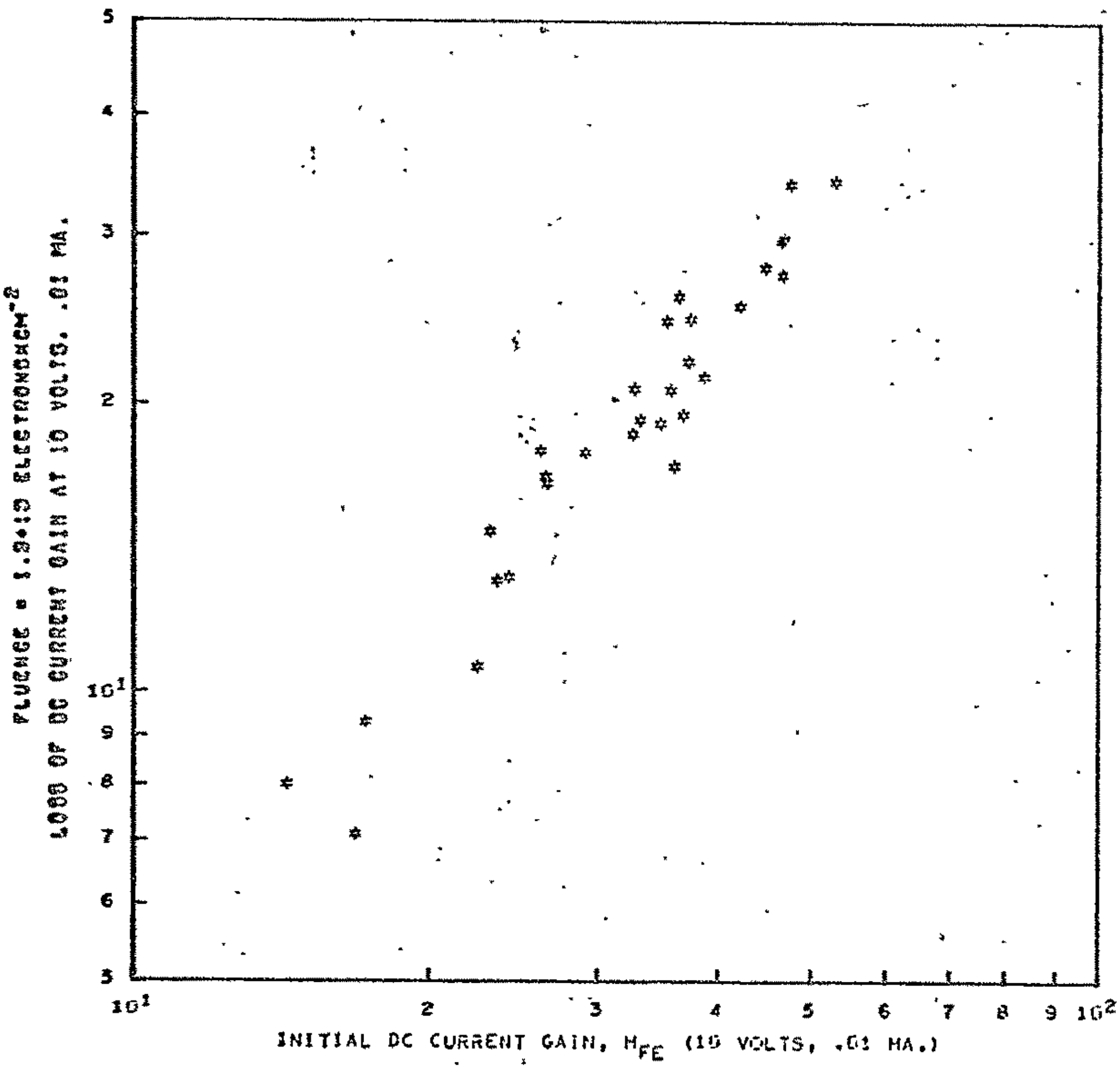

TYPE 2N1613, FAIRCHILD TRANSISTORS
NO BIAS APPLIED

RANK COEFFICIENT OF CORRELATION = .95

Figure 32: CORRELATION OF GAIN LOSS WITH INITIAL GAIN

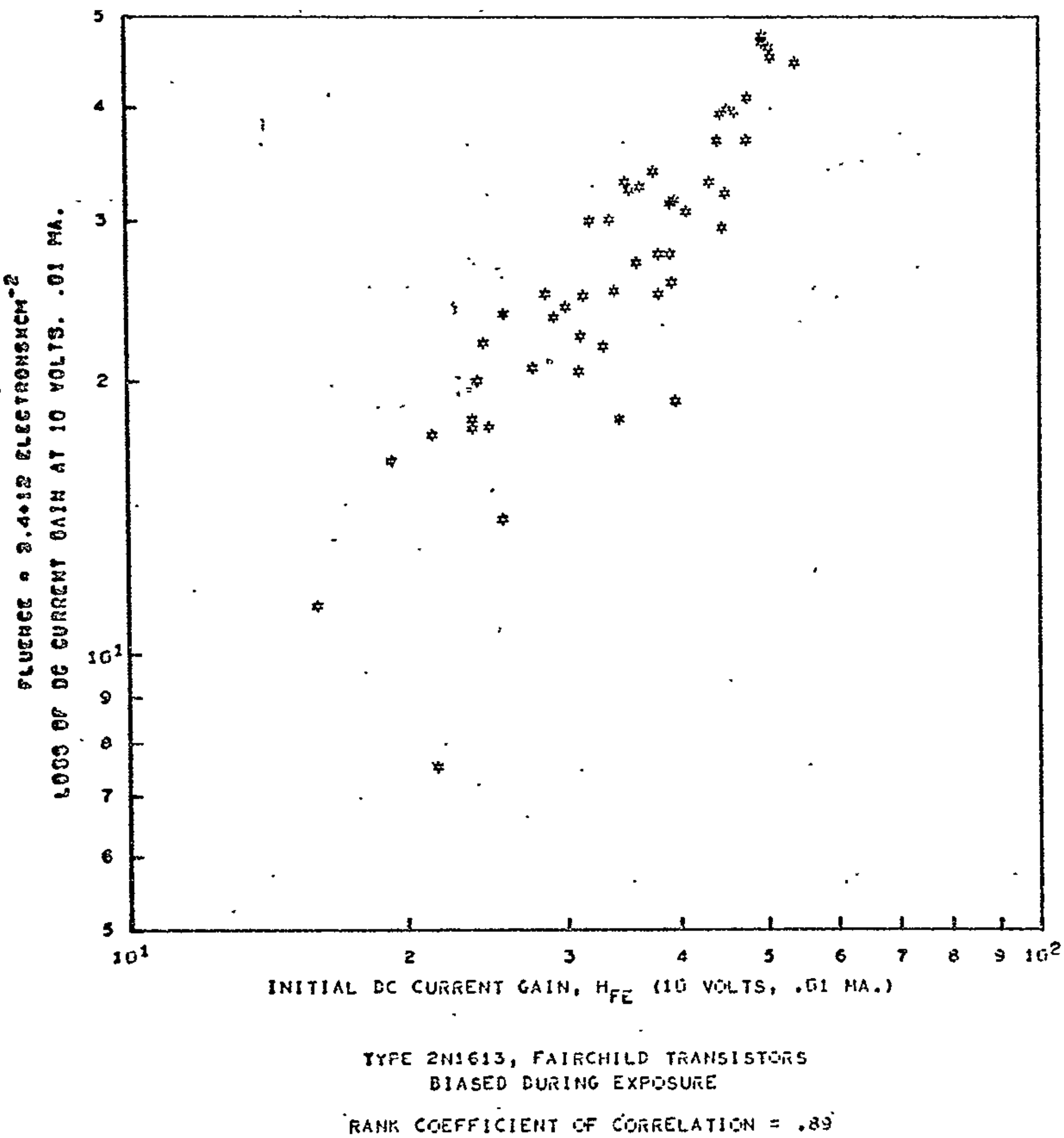

Figure 33: CORRELATION OF GAIN LOSS WITH INITIAL GAIN

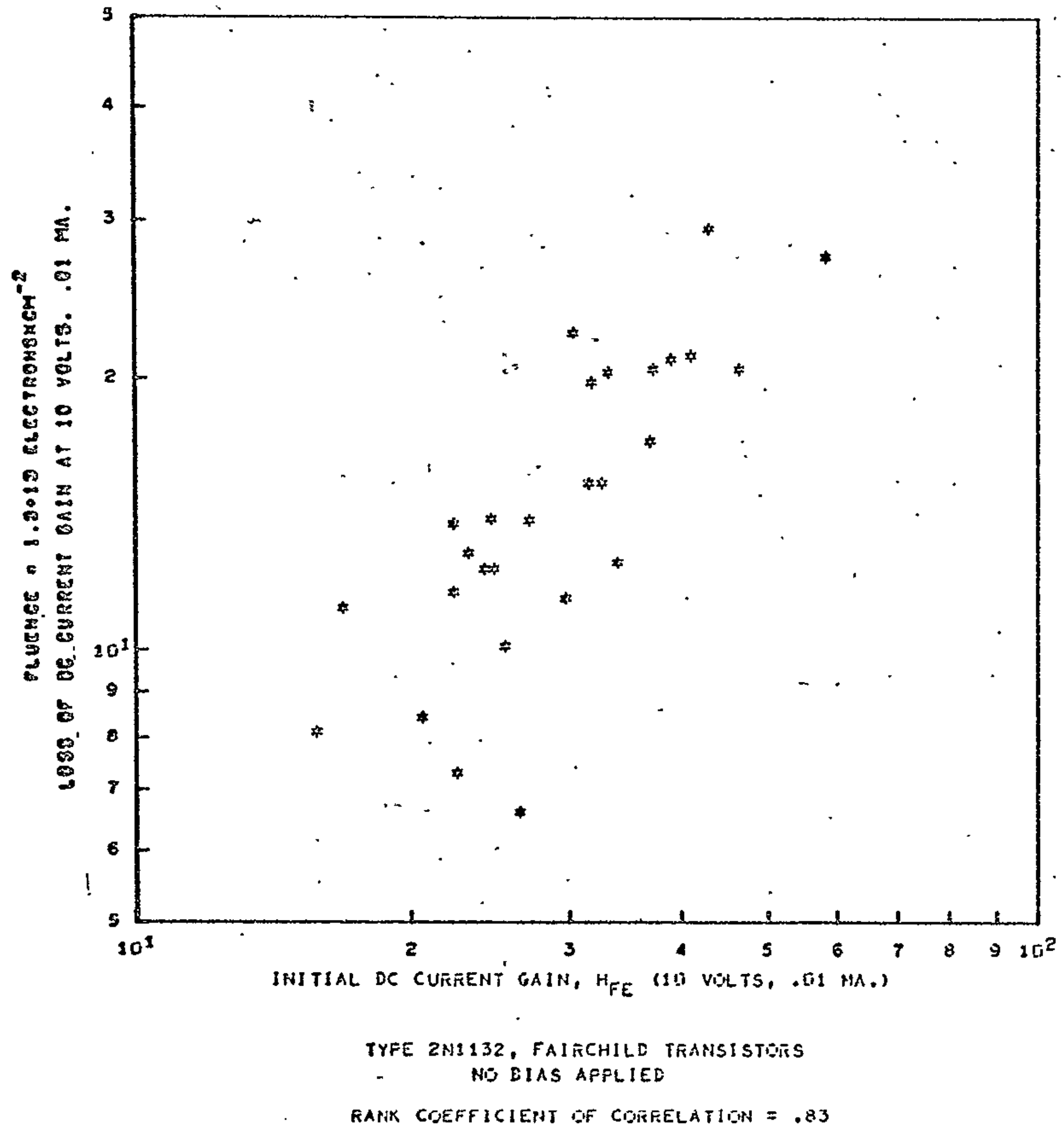

Figure 34: CORRELATION OF GAIN LOSS WITH INITIAL GAIN

This equation is simply an identity which applies to each device separately. Now, one may think that K is just as different among devices as the initial gains (excepting of course the very high dose case where $K \approx 1$ for all of them since $\sum I_B^x >> I_B^o$). Interestingly enough, in certain cases K turns out to be approximately constant among devices, even below the extreme high doses, as e.g., figures (32) through (35) testify. (Many other similar "correlation" plots were observed by Boeing personnel.) But then in a certain fluence range the prediction of the gain loss from the initial gain is possible within certain limits. In other words, the relative gain loss is approximately constant among devices regardless of the initial gains. This last sentence seems to imply that some sort of a "normalization" of the gain degradation of the different devices take place when the results are compared in terms of $\Delta\beta/\beta_o$. Whether this is indeed the case, is still subject to argument; other workers insist that the devices should be compared in terms of $\Delta 1/h_{FE}$. Let us discuss this problem in a little more detail.

In radiation damage studies one is quite often faced with the problem of comparing the radiation sensitivities of different devices to gain degradation. Then the question arises as to what quantity(ies) to use for a valid comparison. One such quantity widely used in nonlinear damage studies is $\Delta 1/h_{FE}$. Certainly $\Delta 1/h_{FE}$ appears to be a good selection for some of the comparison purposes since it is equal to $\sum I_B^x/I_c$, and $\sum I_B^x$ depends on the inherent radiation sensitivity of the device but not on the initial gain. However, we feel that when the devices to be compared have different geometries, e.g., coming from separate manufacturers, the quantity $\sum I_B^x/I_c$ has to be modified in order to normalize the devices to the same geometrical dimensions. It appears that an expression like $\sum I_B^x/I_B^o$ would be appropriate since then the different geometrical factors will drop out. (E.g., the lengths of the emitter-base junction perimeters. The previous statement is strictly correct if both I_B^o and $\sum I_B^x$ are dominated by the same base current component. This is, however, usually the case in practice, because of the dominant role of the surface component in nonlinear damage.) Actually any expression involving $\sum I_B^x/I_B^o$ would be equally good, e.g.

$$\frac{1}{1 + \frac{I_B^o}{\sum I_B^x}} = \frac{\Delta\beta}{\beta_o} \qquad \text{the relative gain loss}$$

or

$$\frac{1}{1 + \frac{\sum I_B^x}{I_B^o}} = \frac{\beta}{\beta_o} \qquad \text{the relative gain remaining}$$

Note however, that it is just as wrong not to normalize against certain pertinent factors as to normalize against others which have nothing to do with the resultant gain degradation. Therefore we propose that if there is no correlation between I_B^o and $\sum I_B^x$ (i.e., between h_{FE}^o and $\Delta 1/h_{FE}$), then the comparison of presumably identical devices should be done in terms of $\Delta 1/h_{FE}$, whereas the comparison of others with known geometrical differences should be done in terms of $\Delta\beta/\beta_o$. On the other hand, if correlation between I_B^o and $\sum I_B^x$ do exist then the comparison of devices in terms of $\Delta\beta/\beta_o$ should always be superior to that in terms of $\Delta 1/h_{FE}$.

In the final analysis, the experimental results should decide whether or not a correlation between I_B^o and $\sum I_B^x$ exist. In many of our experiments the quantity $\Delta\beta/\beta_o$ seemed to give a better normalization of the gain degradation, thus implying some degree of correlation between I_B^o and $\sum I_B^x$ or β_o and $\Delta 1/\beta$. However, direct tests indicated correlation between these two quantities only in a few cases. Needless to say the problem merits further consideration. In particular, a thorough experimental study of correlation problems is sorely needed.

2.3 Dependence of Nonlinear Damage on the Current Level During Gain Measurement (Task A1)

One of the major tasks of this contract was to evaluate empirically the dependence of nonlinear damage on the emitter current, I_E, at which the gain was measured. The degradation results are summarized in Figures (35) through (58) in three different graphical forms. Essentially all of our devices are represented in the following figures depicting their dependence of gain degradation on injection level. (Since the Fairchild Series 500 Transistor Tester programs I_C instead of I_E data curves are shown for the former. Also, the gain is measured as I_C/I_B. Correcting this expression for the leakage current, I_{CBO}, (see Equation (1) in 2.2.1.2) made very little difference in our data.)

The three different types of plots are discussed below. The fluence values, whenever they occur, (either as independent variables or as parameters) can easily be converted into dose if desired, by dividing with a conversion factor of 4.24×10^7. That is to say

$$\text{Dose (rads(Si))} = \frac{\text{Fluence (1 MeV electrons/cm}^2)}{4.24 \times 10^7 \cdot \left[\text{rads(Si)} \times \text{cm}^2\right]^{-1}}$$

Note that the quoted fluence values on all of our figures are meant on the Si chip and not on the transistor can. Namely, the transmission losses suffered by the electron beam when traversing the can were taken into account. This way one is able to better compare the irradiation response of devices coming from different manufacturers with different can thicknesses.

i) <u>$\Delta(1/h_{FE})$ vs.</u> Φ plots for a family of I_C values (Figures 35-46):

On this type of plot the "nonlinearity" of the gain degradation induced by surface effects is very apparent. The dependence of gain degradation on the measuring current is indicated in graphical forms by a family of curves for the nine different I_C values. Interestingly enough, these curves are almost parallel to each other and except for the very high current values, nearly equally spaced. This means, that at least for this type of a plot, measurements made at a smaller number of currents would also be sufficient to characterize the I_C dependence and enable one to predict the curve at intermediate I_C values.

The 12 figures selected make up essentially a complete set in showing all the different graphical forms of the $\Delta 1/h_{FE}$ vs. $\emptyset$ curves, obtained under different conditions, thus representing practically all of our 218 devices. This representation is possible with the relatively few figures of 12 since devices within a given batch had very similar curves hence on figure shown can represent the rest. More than that, sometimes one device can represent all the devices from several batches. Table 3 summarizes what devices in a given batch or batches are represented by a certain figure. Some other relevant information is also included.

The figures for the active NPN and PNP devices, #57, 71, and #129, 153 respectively, do not represent batches, they represent essentially all the devices within the biased NPN and PNP groups regardless of their specific batch number of specific bias conditions. No study was carried out to ascertain differences between batches under identical bias and exposure conditions in a comprehensive manner like that for the passive devices. (Two-two devices were selected to represent the biased NPN and the biased PNP group respectively, in order to illustrate some slight differences in the curves within the biased groups. The "flattening" of the 10 ua curve in Figure (38) above $\emptyset \approx 10^{13}$ electrons/cm^2 shows that the gain was reduced below 1.9 by the Fairchild 500 Tester. Similar "flattened out" regions will be seen in some of the other figures for the same reason. Although separate measurements of the gain values below 1.9 were also made by changing certain circuit modules on the Transistor Tester, it was not feasible to incorporate these data into the main deck of the computer data cards.

The tremendous difference in the $\Delta 1/h_{FE}$ vs. $\emptyset$ curves for passive and active NPN devices should be noted; it signifies the drastic effect of the active bias during exposure in enhancing nonlinear gain degradation.

As shown in the figures, the I_C dependence of the gain degradation seems to be very much the same for all the devices represented, in spite of the differences in the graphical forms of the $\Delta 1/h_{FE}$ vs. $\emptyset$ plots. This seems to be the case even for the passive and active NPN devices in spite of their large difference in the $\Delta 1/h_{FE}$ vs. $\emptyset$ curves, reflecting their difference in radiation sensitivity.

That the curves should be nearly parallel can be explained as follows: The quantity $\Delta 1/h_{FE}$, which is plotted against Φ, can be expressed as

$$\Delta 1/h_{FE} = \frac{\sum I_B^X}{I_C}$$

therefore for two different I_C values at a given Φ:

$$(\Delta 1/h_{FE})_1 = \frac{\sum I_{B1}^X}{I_{C1}} \quad \text{and} \quad (\Delta 1/h_{FE})_2 = \frac{\sum I_{B2}^X}{I_{C2}}.$$

The ratio of these two equations (i.e., the distance between them on log scale) is given by

$$\frac{(\Delta 1/h_{FE})_1}{(\Delta 1/h_{FE})_2} = \frac{\sum I_{B1}^X}{\sum I_{B2}^X} \; \frac{I_{C2}}{I_{C1}} \tag{12}$$

Now the question is whether or not this ratio varies with fluence; if it remained nearly constant then the $\Delta 1/h_{FE}$ vs. Φ curves with different I_C values would be approximately parallel on a log-log plot. Clearly I_{C2}/I_{C1} is independent of fluence. Actually, so is the ratio of the extra base currents, at least when they are dominated by the surface components, since the ratio depends only on V_{BE}'s necessary to get the desired I_C values. The effect of increasing the number of interface states (ΔN_t) with dose should drop out, since both I_{B1}^S and I_{B2}^S are proportional to ΔN_t.

That the parallel curves should also be nearly equally spaced, except at high I_C, simply follows from the particular selection of the I_C values, namely, from the fact that the ratios of the adjacent I_C values are approximately the same ($\frac{30 \text{ ua}}{10 \text{ ua}} \approx \frac{100 \text{ ua}}{30 \text{ ua}} \approx \ldots$ etc.), as can be seen from Equation (12) after some manipulation.

Incidentally, the figures of 35-46 are referred to several times. They are used not only to show the dependence of nonlinear damage on the measurement currents, I_C, but also to illustrate the wide variety of the

Table 3. Description of the Device Groups Represented in Figures 35 - 46.

Figure No.	Device No.	Type	Manufacturer	Passive or Active	Number of Batches Represented	Corresponding No. of Devices (10 dev./batch)
35	2	2N1613 NPN	Fairchild	Passive	1	10
36	36	2N1613 NPN	Fairchild	Passive	2	20
37	57	2N1613 NPN	Fairchild	Active	Biased Group	45
38	71	2N1613 NPN	Fairchild	Active		
39	82	2N1613 NPN	Raytheon	Passive	1	10
40	107	2N1613 NPN	Raytheon	Passive	2	20
41	146	2N1132 PNP	Raytheon	Passive	3	30
42	129	2N1132 PNP	Raytheon	Active	Biased Group	45
43	153	2N1132 PNP	Raytheon	Active		
44	198	2N1132 PNP	Fairchild	Passive	2*	20
45	206	2N1132 PNP	Fairchild	Passive		
46	215	2N1132 PNP	Fairchild	Passive	1	10

*Two figures are necessary to represent each of the two batches; i.e., each batch has two subgroups of devices which are similar to the two subgroups in the other batch.

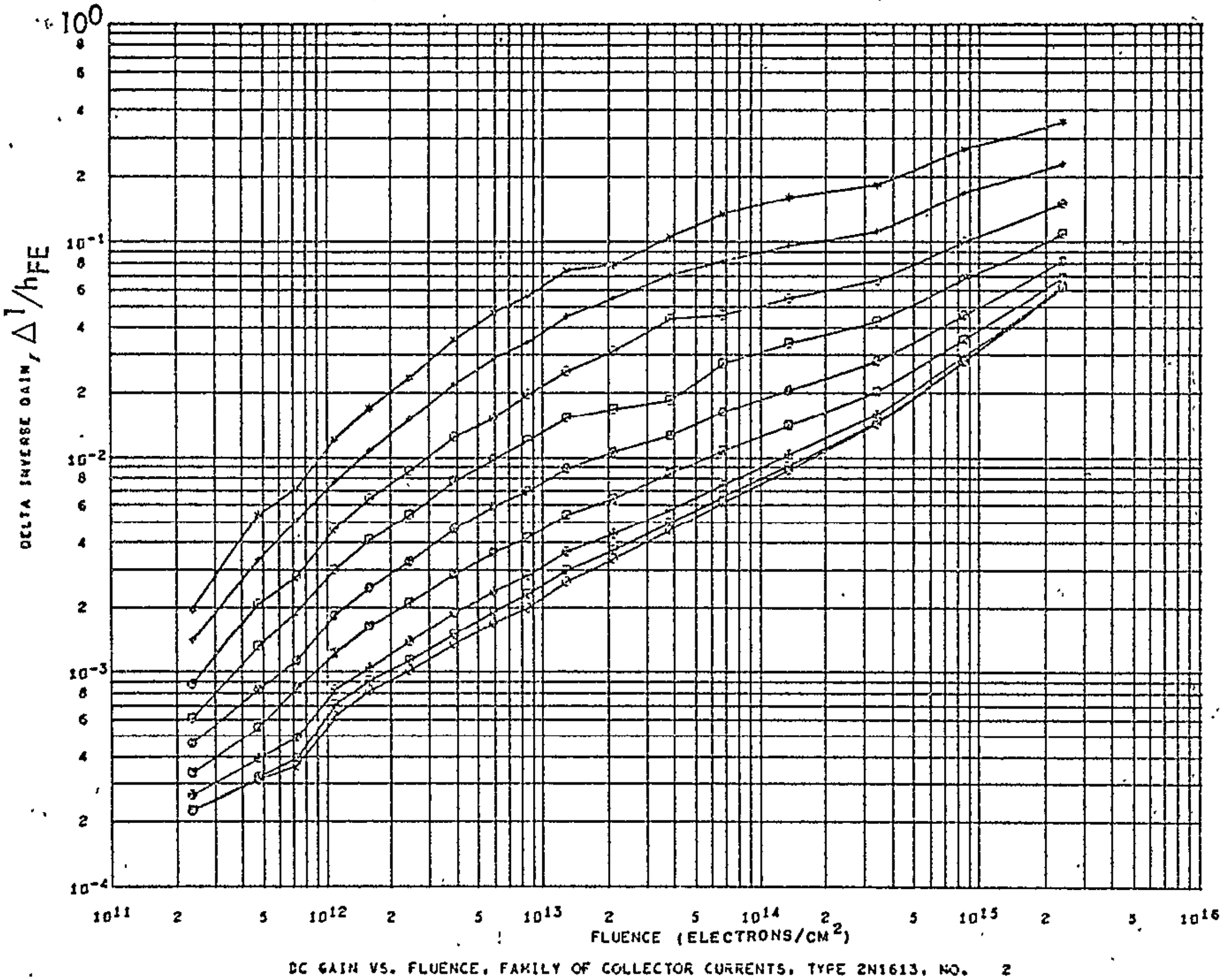

Figure 35: DEPENDENCE OF NONLINEAR DAMAGE ON INJECTION LEVEL DURING MEASUREMENTS IN PARAMETRIC FORM (FAIRCHILD 2N1613, PASSIVE, ONE BATCH; MEASUREMENT CURRENTS FROM TOP TO BOTTOM: 10-30-100-300 μa, 1-3-10-20-40 ma)

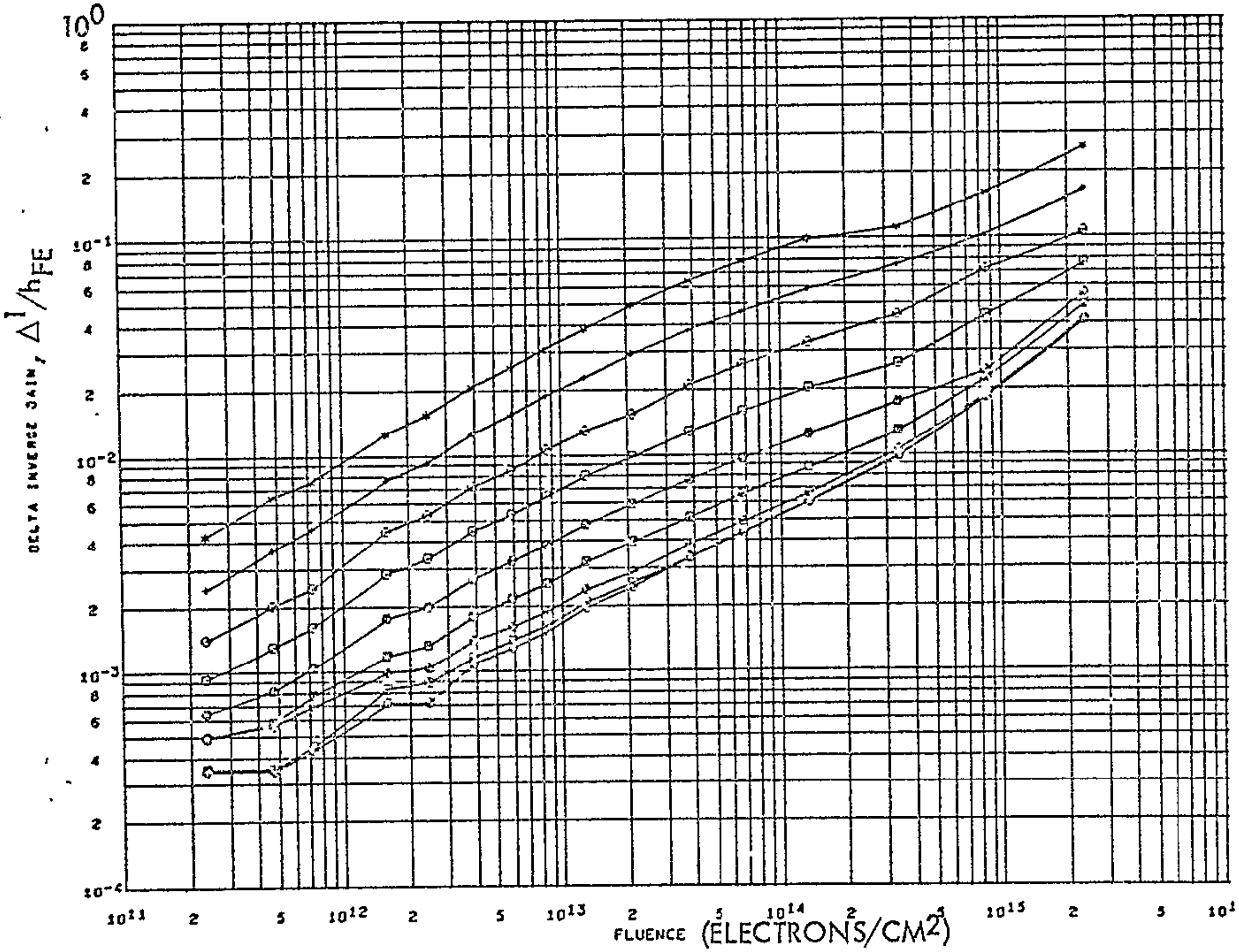

DC GAIN VS. FLUENCE. FAMILY OF COLLECTOR CURRENTS. TYPE 2N1613. NO. 36

Figure 36: DEPENDENCE OF NONLINEAR DAMAGE ON THE INJECTION LEVEL DURING MEASUREMENTS IN PARAMETRIC FORM (FAIRCHILD 2N1613 PASSIVE, TWO BATCHES; MEASUREMENT CURRENTS FROM TOP TO BOTTOM: 10-30-100-300 μa, 1-3-10-20-40 ma)

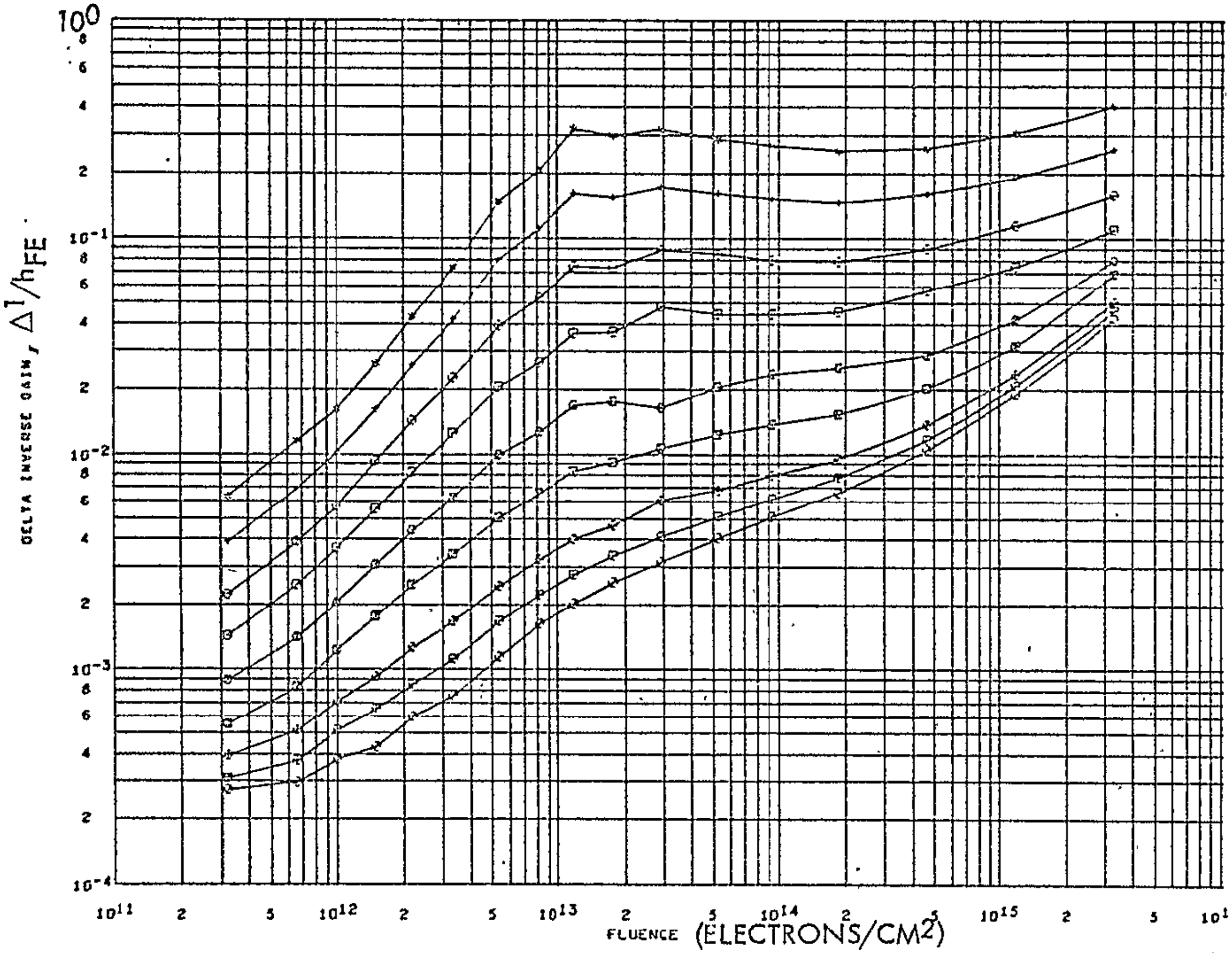

DC GAIN VS. FLUENCE. FAMILY OF COLLECTOR CURRENTS. TYPE 2N1613. NO. 57

Figure 37: DEPENDENCE OF NONLINEAR DAMAGE ON THE INJECTION LEVEL DURING MEASUREMENTS IN PARAMETRIC FORM (FAIRCHILD 2N1613 ACTIVE GROUP; MEASUREMENT CURRENTS FROM TOP TO BOTTOM: 10-30-100-300 μa, 1-3-10-20-40 ma)

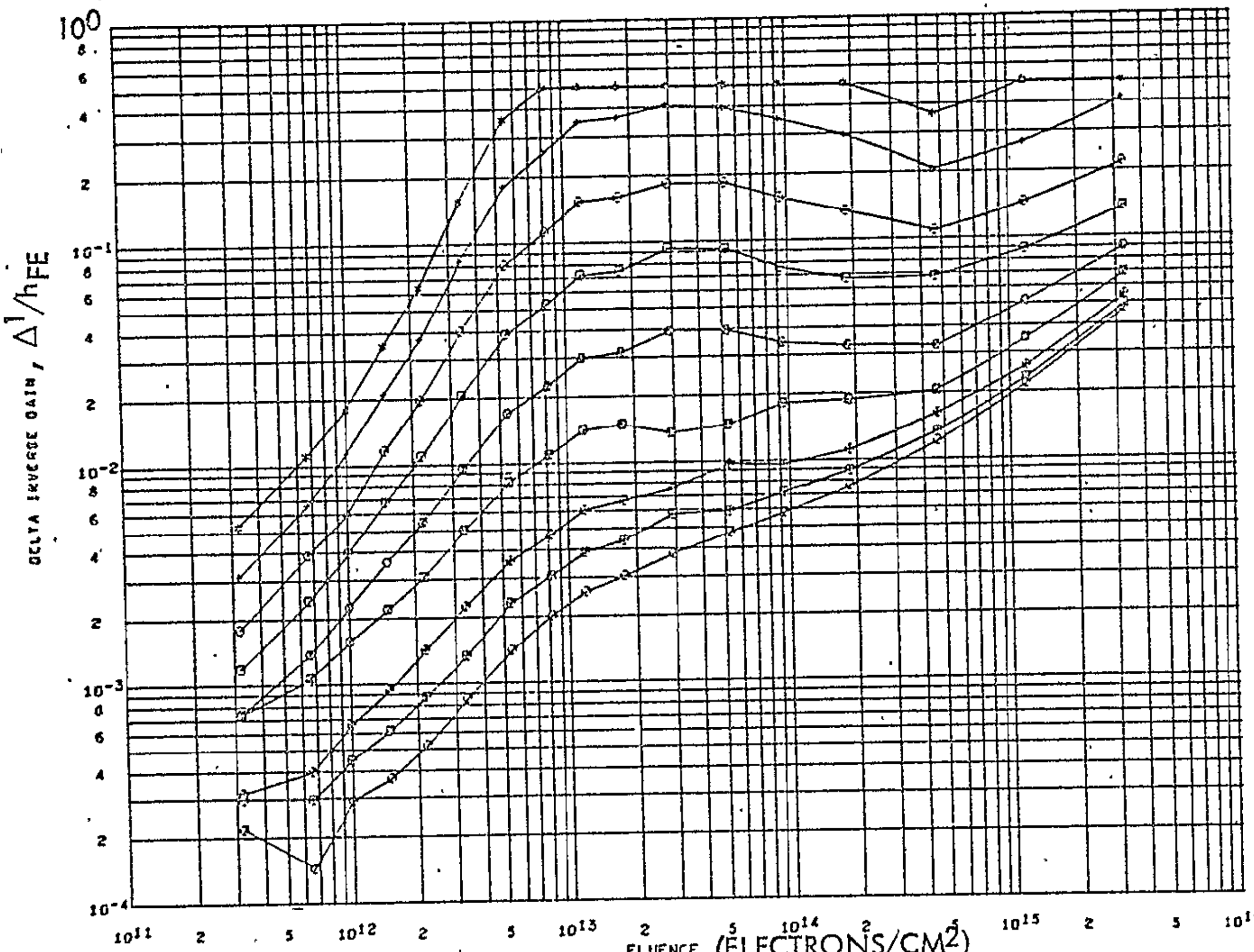

DC GAIN VS. FLUENCE, FAMILY OF COLLECTOR CURRENTS, TYPE 2N1613, NO. 71

(On the flattened out 10 µa curve see text)

Figure 38: DEPENDENCE OF NONLINEAR DAMAGE ON THE INJECTION LEVEL DURING MEASUREMENTS IN PARAMETRIC FORM (FAIRCHILD 2N1613 ACTIVE GROUP; MEASUREMENT CURRENTS FROM TOP TO BOTTOM: 10-30-100-300 µ-a-, 1-3-10-20-40 ma)

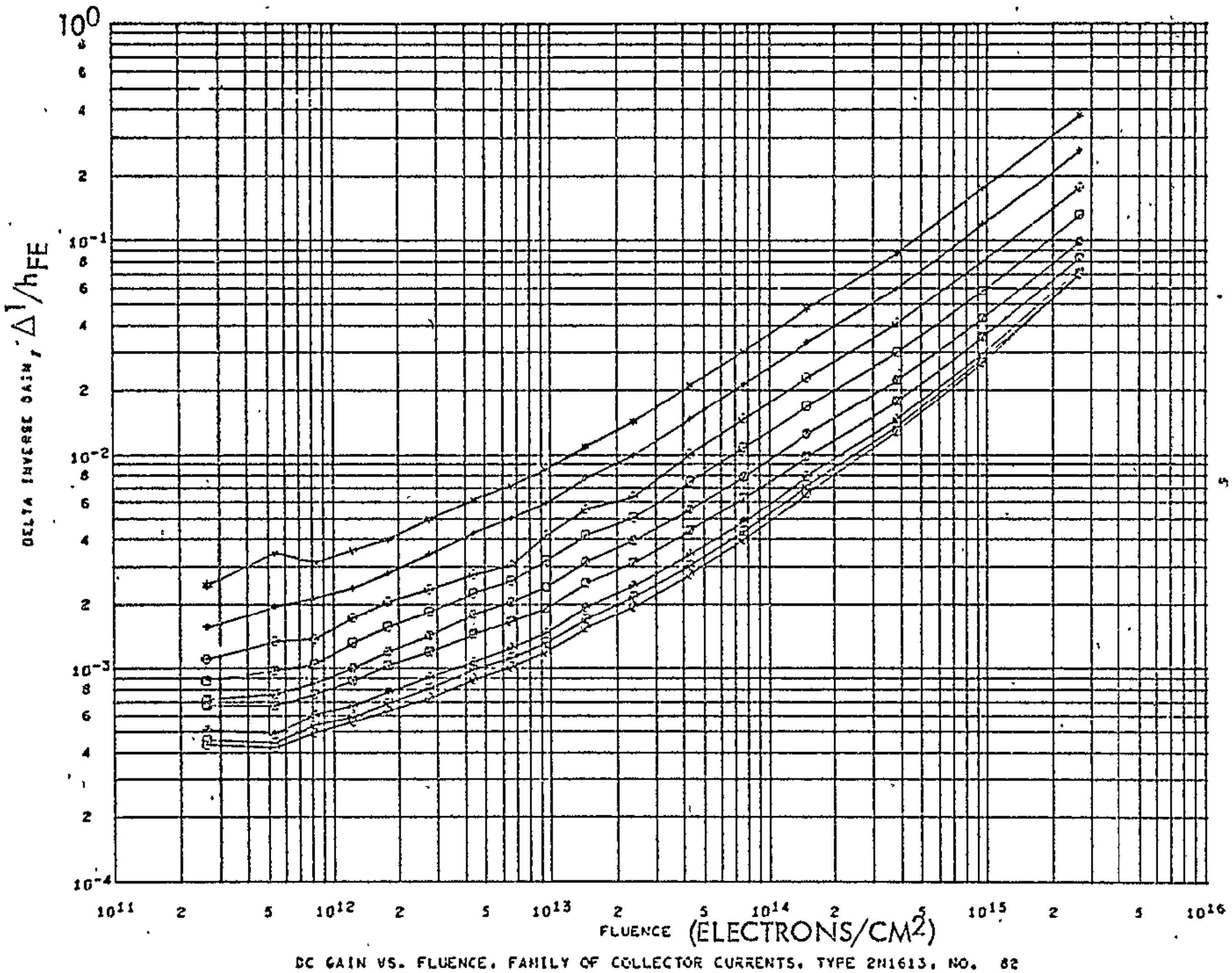

Figure 39: DEPENDENCE ON NONLINEAR DAMAGE ON THE INJECTION LEVEL DURING MEASUREMENTS IN PARAMETRIC FORM (RAYTHEON 2N1613 PASSIVE, ONE BATCH; MEASUREMENT CURRENTS FROM TOP TO BOTTOM: 10-30-100-300 µa, 1-3-10-20-40 ma)

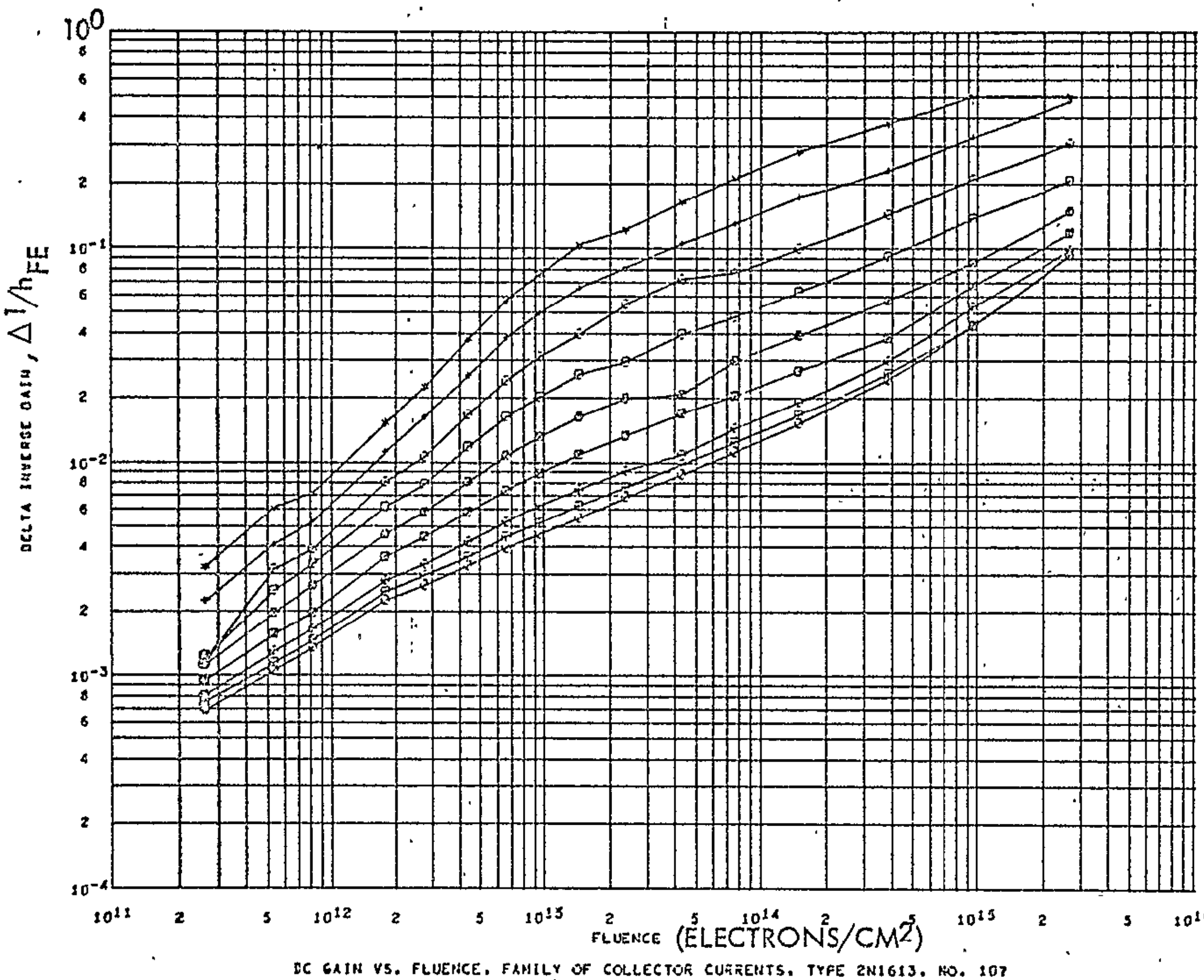

Figure 40: DEPENDENCE OF NONLINEAR DAMAGE ON THE INJECTION LEVEL DURING MEASUREMENTS IN PARAMETRIC FORM (RAYTHEON 2N1613, PASSIVE, TWO BATCHES; MEASUREMENT CURRENTS FROM TOP TO BOTTOM: 10-30-100-300 μa, 1-3-10-20-40 ma)

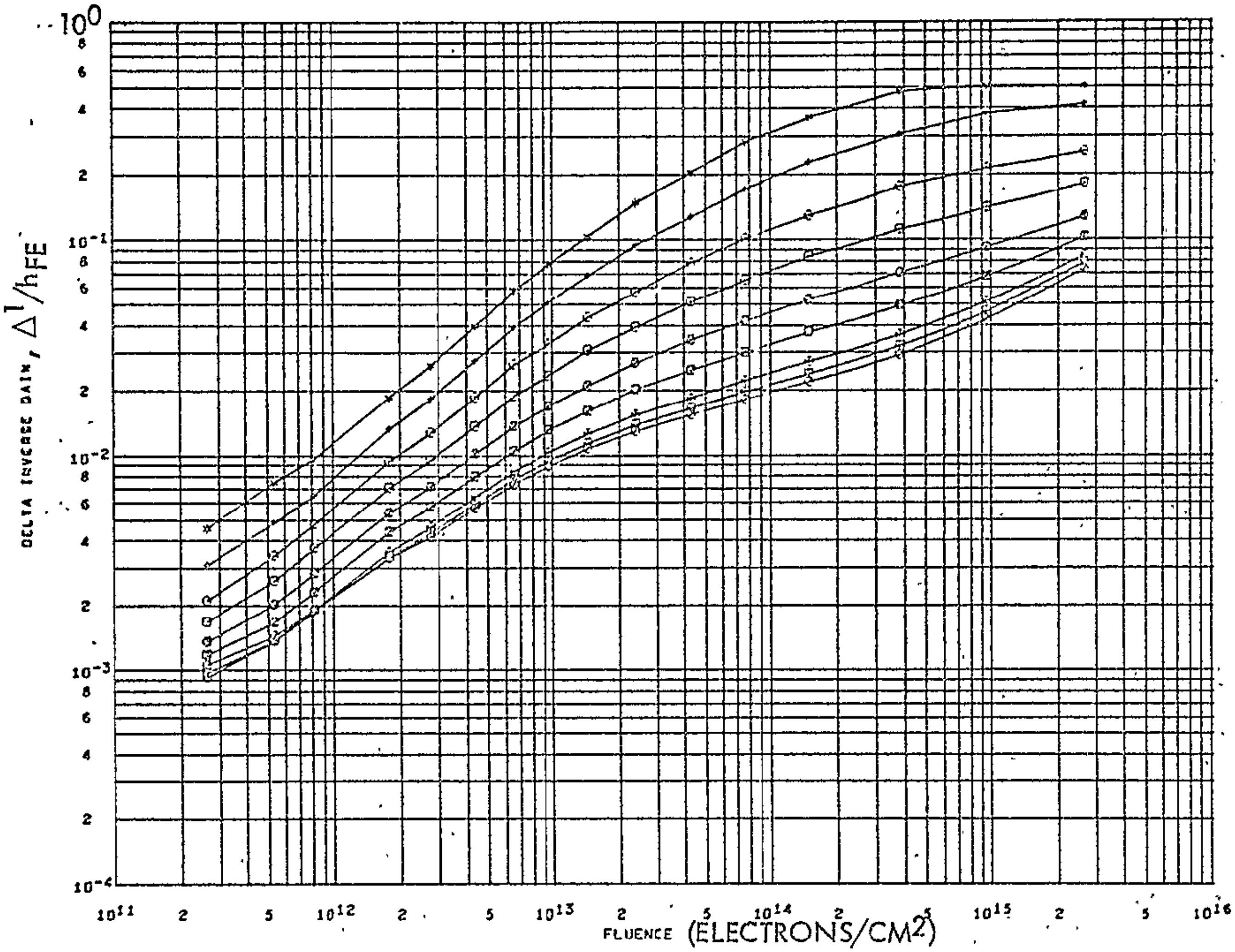

DC GAIN VS. FLUENCE. FAMILY OF COLLECTOR CURRENTS. TYPE 2N1132. NO. 146

Figure 41: DEPENDENCE OF NONLINEAR DAMAGE ON THE INJECTION LEVEL DURING MEASUREMENTS IN PARAMETRIC FORM (RAYTHEON 2N1132, PASSIVE, THREE BATCHES; MEASUREMENT CURRENTS FROM TOP TO BOTTOM. 10-30-100-300 μa, 1-3-10-20-40 ma)

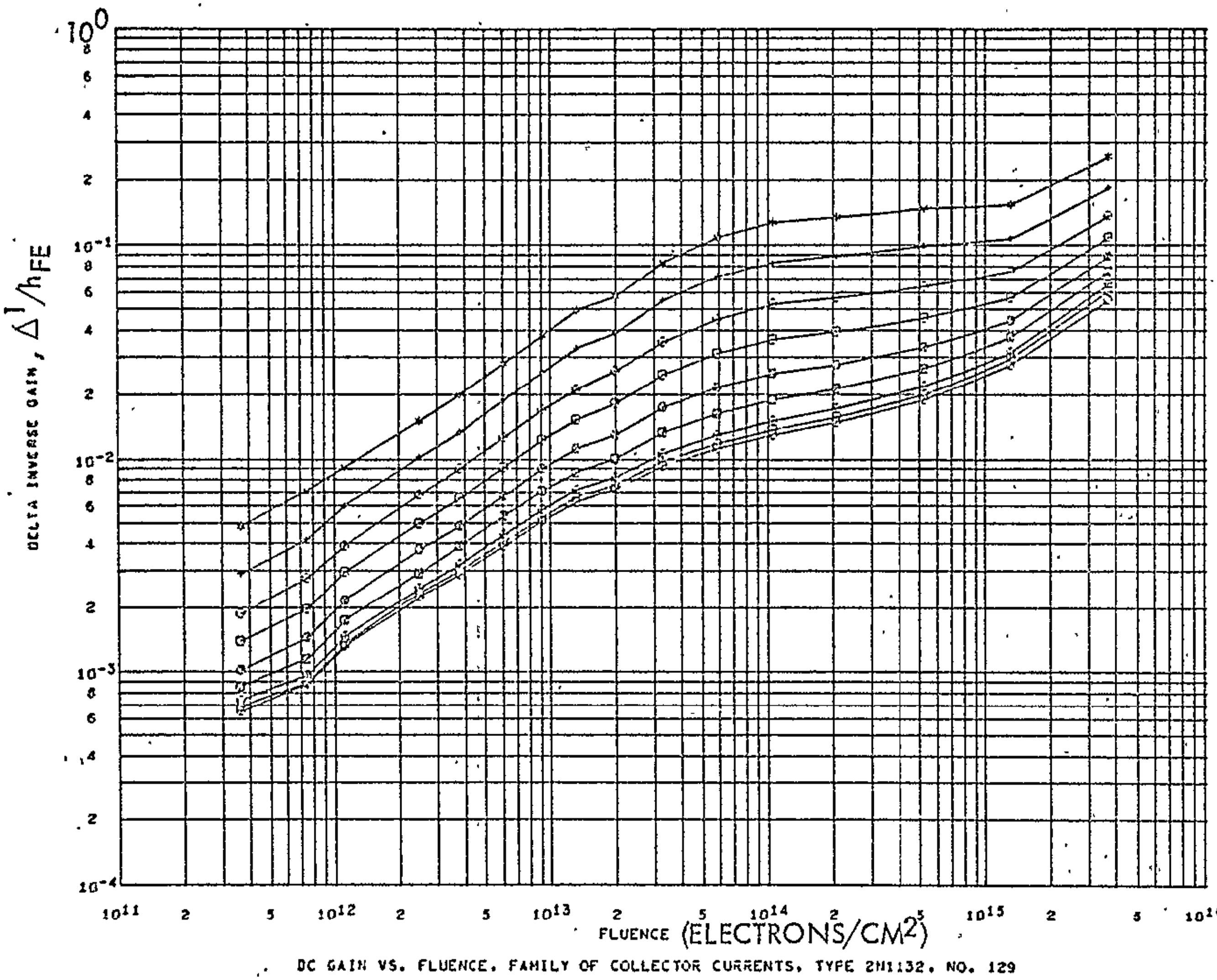

Figure 42: DEPENDENCE OF NONLINEAR DAMAGE ON THE INJECTION LEVEL DURING MEASUREMENTS IN PARAMETRIC FORM (RAYTHEON 2N1132, ACTIVE GROUP; MEASUREMENT CURRENTS FROM TOP TO BOTTOM: 10-30-100-300 μa, 1-3-10-20-40 ma)

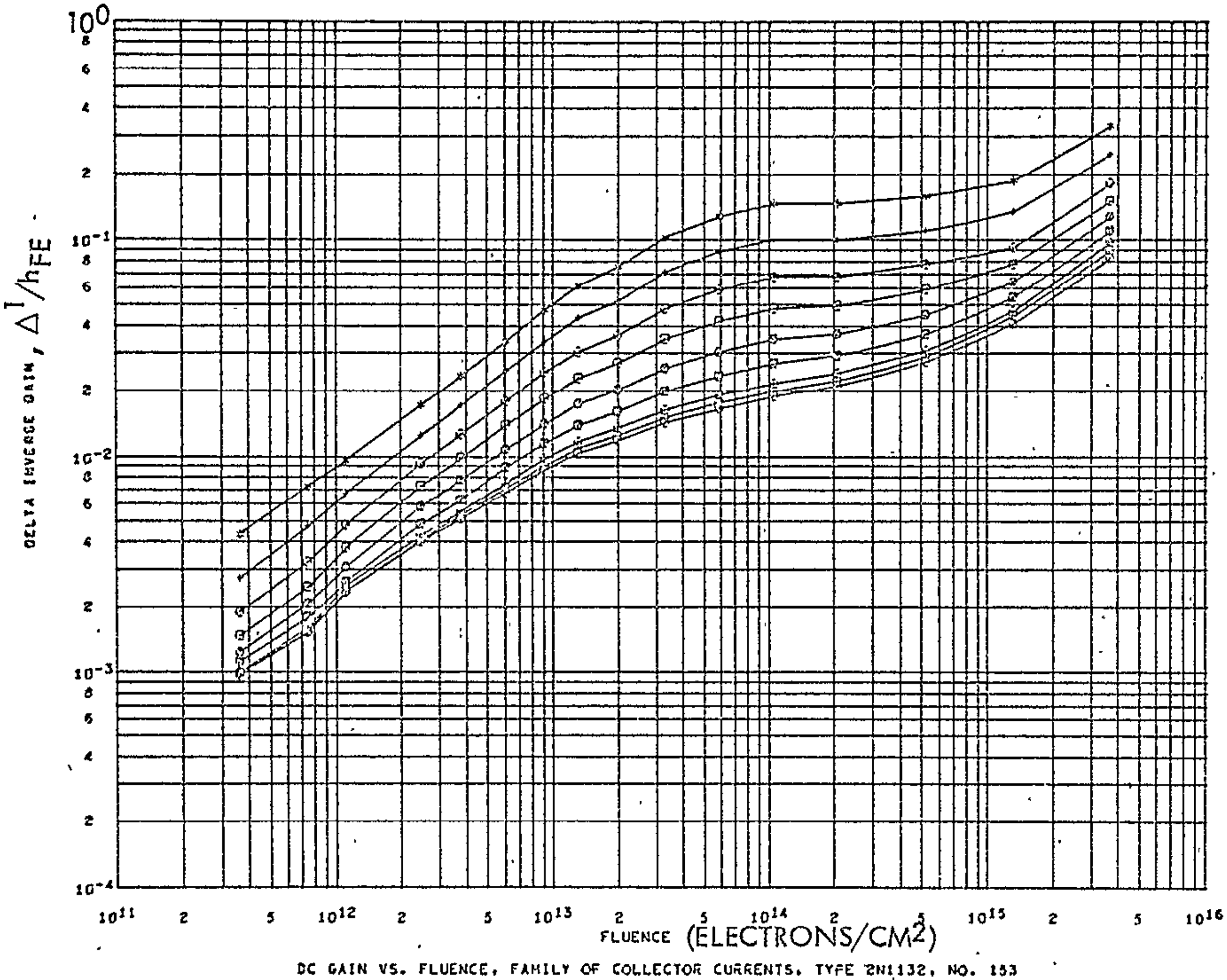

Figure 43: DEPENDENCE OF NONLINEAR DAMAGE ON THE INJECTION LEVEL DURING MEASUREMENTS IN PARAMETRIC FORM (RAYTHEON 2N1132, ACTIVE GROUP; MEASUREMENT CURRENTS FROM TOP TO BOTTOM: 10-30-100-300 μa, 1-3-10-20-40 ma)

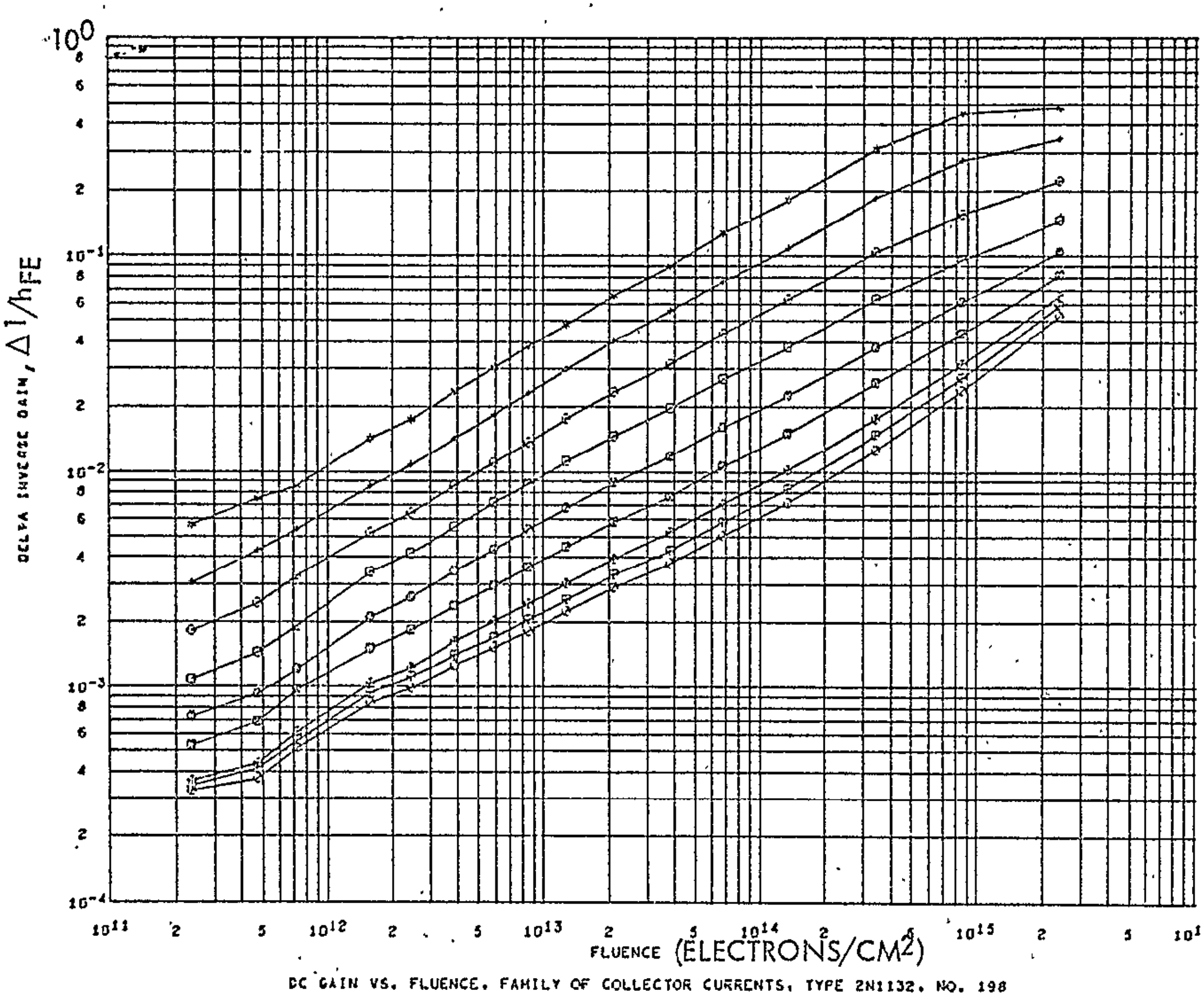

Figure 44: DEPENDENCE OF NONLINEAR DAMAGE ON THE INJECTION LEVEL DURING MEASUREMENTS IN PARAMETRIC FORM (FAIRCHILD 2N1132, PASSIVE, PART OF TWO BATCHES – SEE TEXT; MEASUREMENT CURRENTS FROM TOP TO BOTTOM: 10-30-100-300 μa, 1-3-10-20-40 ma)

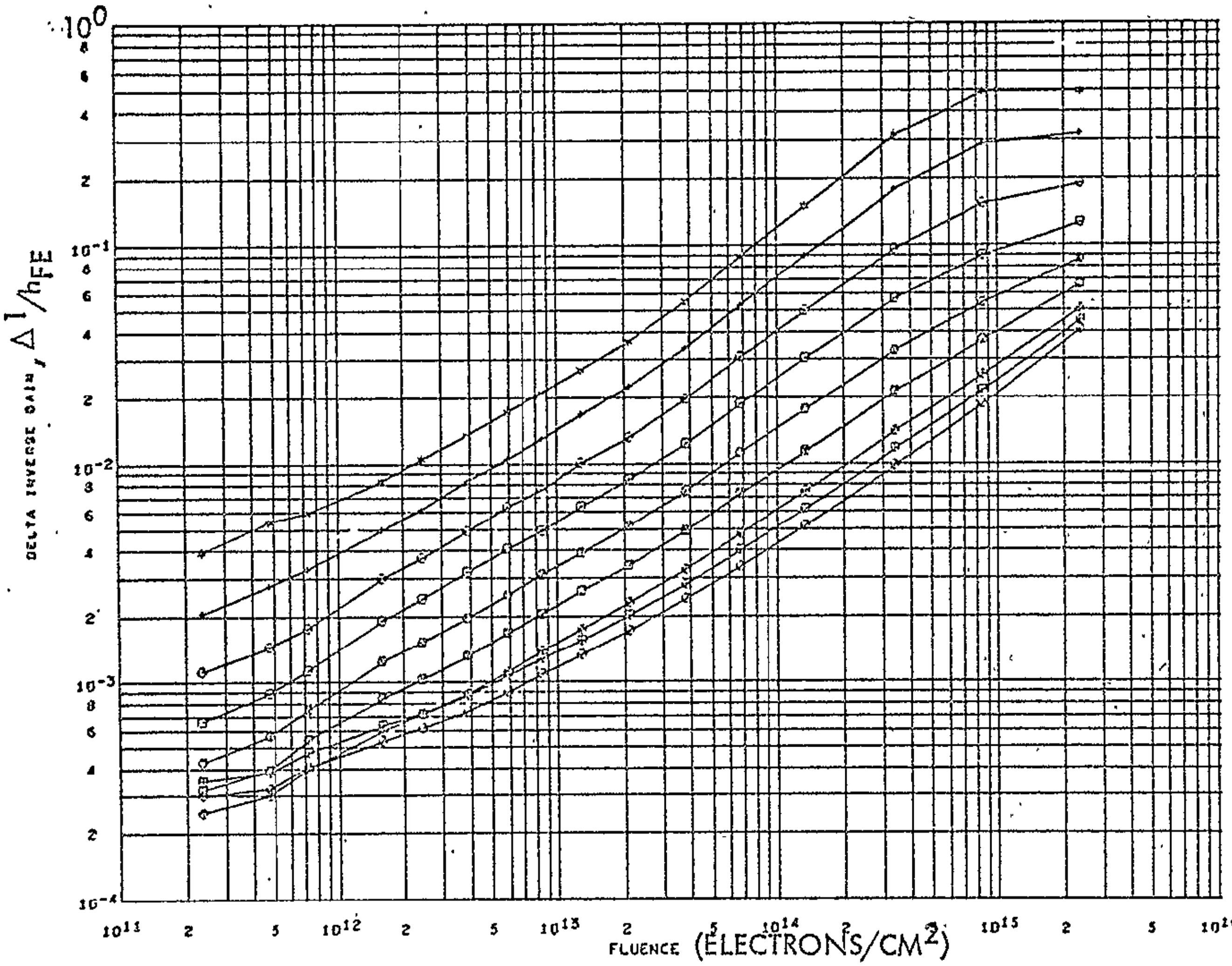

DC GAIN VS. FLUENCE. FAMILY OF COLLECTOR CURRENTS. TYPE 2N1132. NO. 206

Figure 45: DEPENDENCE OF NONLINEAR DAMAGE ON THE INJECTION LEVEL DURING MEASUREMENTS IN PARAMETRIC FORM (FAIRCHILD 2N1132, PASSIVE, PART OF TWO BATCHES - SEE TEXT; MEASUREMENT CURRENTS FROM TOP TO BOTTOM: 10-30-100-300 μa, 1-3-10-20-40 ma)

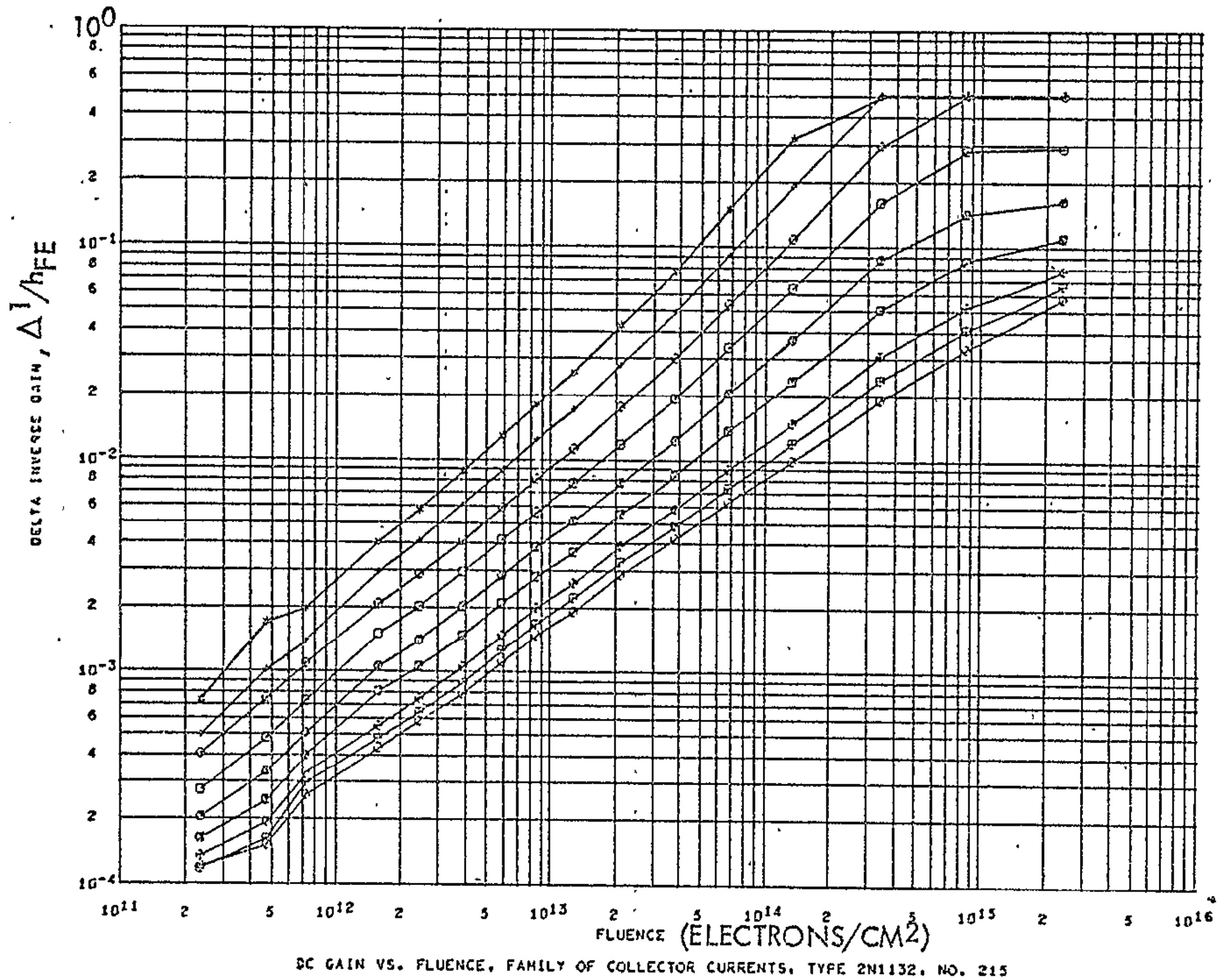

Figure 46: DEPENDENCE OF NONLINEAR DAMAGE ON THE INJECTION LEVEL DURING MEASUREMENTS IN PARAMETRIC FORM (FAIRCHILD 2N1132, PASSIVE, ONE BATCH; MEASUREMENT CURRENTS FROM TOP TO BOTTOM: 10-30-100-300 μa, 1-3-10-20-40 ma)

$\Delta 1/h_{FE}$ vs. ϕ curves of different shapes, expressing different forms of damage buildup with dose, for presumably "identical" devices. This was already discussed in Section 2.2.3. Still another use of these figures comes from the fact that the curves shown are representative of 10, 20, or 30 devices which belonged to one, two, or three batches and exhibited very similar curves. The implication of the similar behavior within a transistor batch or date code will be further discussed in the Statistical Analysis Section (2.4).

ii) $\Delta 1/h_{FE}$ vs. I_C plots for a family of Φ values (Figures 47-52).

Six figures are included (both here and in iii)) to represent the Fairchild passive PNP, passive and active NPN, and the Raytheon passive NPN, passive and active PNP devices. These plots clearly express how the non-linear gain degradation depends on the measuring current. Actually the functional relation between $\Delta 1/h_{FE}$ and I_C, subject to certain assumptions. was already derived in Section 2.2.1.3 and is approximately given by

$$\Delta 1/h_{FE} = \text{const. } I_C^{(1/n)-1} \qquad (13)$$

This relation on a log-log plot, as shown in the figures, should result in straight lines, which in general they did at least below about 3 ma. The slopes of the lines furnish the "n" values which can identify the spatial origin of the dominant base current components at different fluences. This method of analysis was also discussed in Section 2.2.1.3. In order to get the "n" values for the devices prior to irradiation, $1/h^{\circ}_{FE}$ vs. I_C lines were also included in the figures. These are the lines with the very small slopes intersecting several other lines.

iii) $\Delta h_{FE}/h^{\circ}_{FE}$ vs. I_C plots for a family of Φ values (Figures 53-58).

These plots are complementary to the ones discussed previously under ii). Instead of $\Delta 1/h_{FE}$ we plot $\Delta h_{FE}/h^{\circ}_{FE}$ against I_C since the relative gain degradation is of more interest to a circuit design engineer. Then of course the knowledge of $\Delta h_{FE}/h^{\circ}_{FE}$ at different measuring current levels is also important. The figures express the fact, emphasized throughout the report, that nonlinear gain degradation is usually most severe at low current levels nevertheless can be significant even at higher current values.

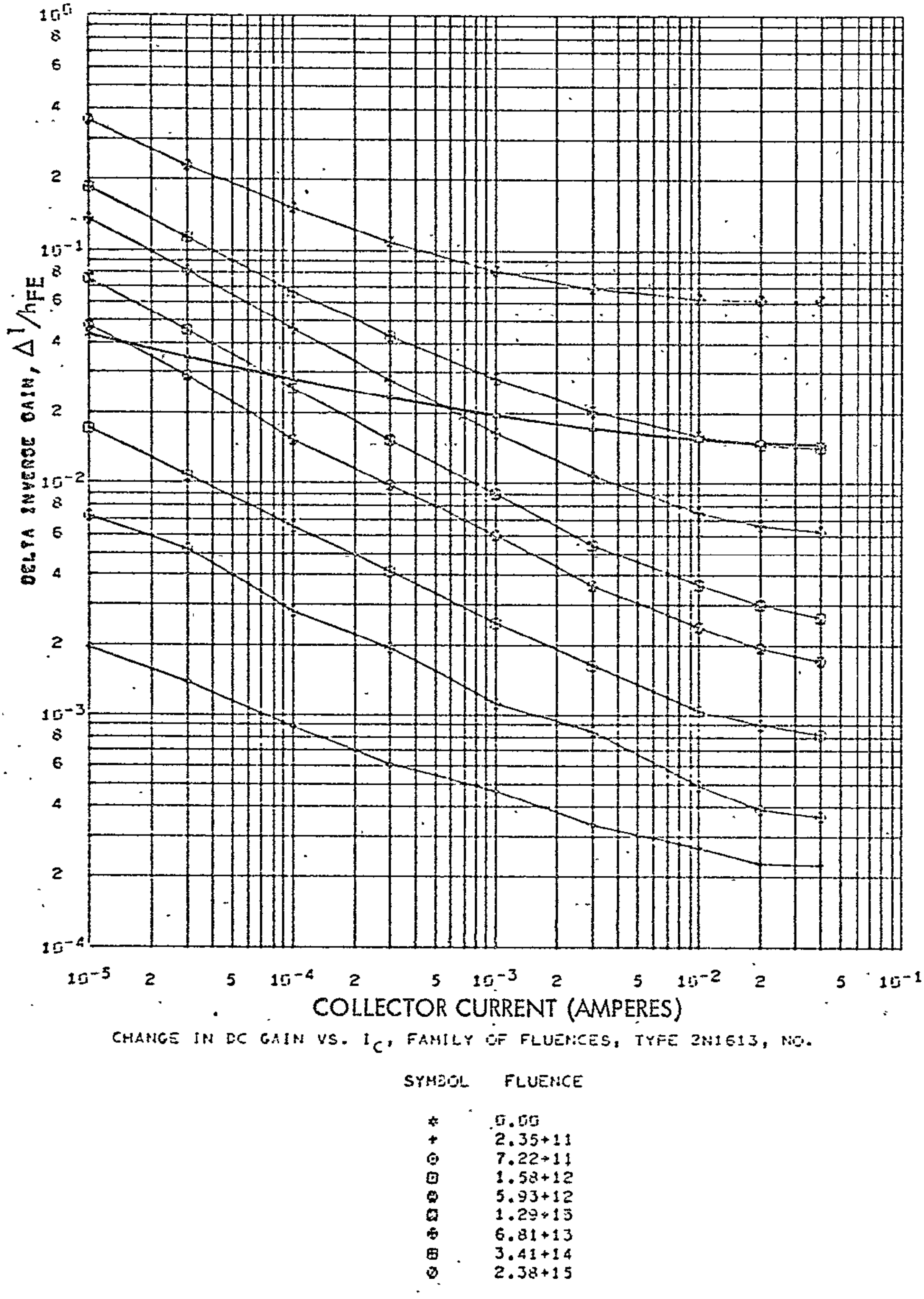

Figure 47: DEPENDENCE OF NONLINEAR DAMAGE ON THE INJECTION LEVEL DURING MEASUREMENTS (FAIRCHILD 2N1613 - PASSIVE)

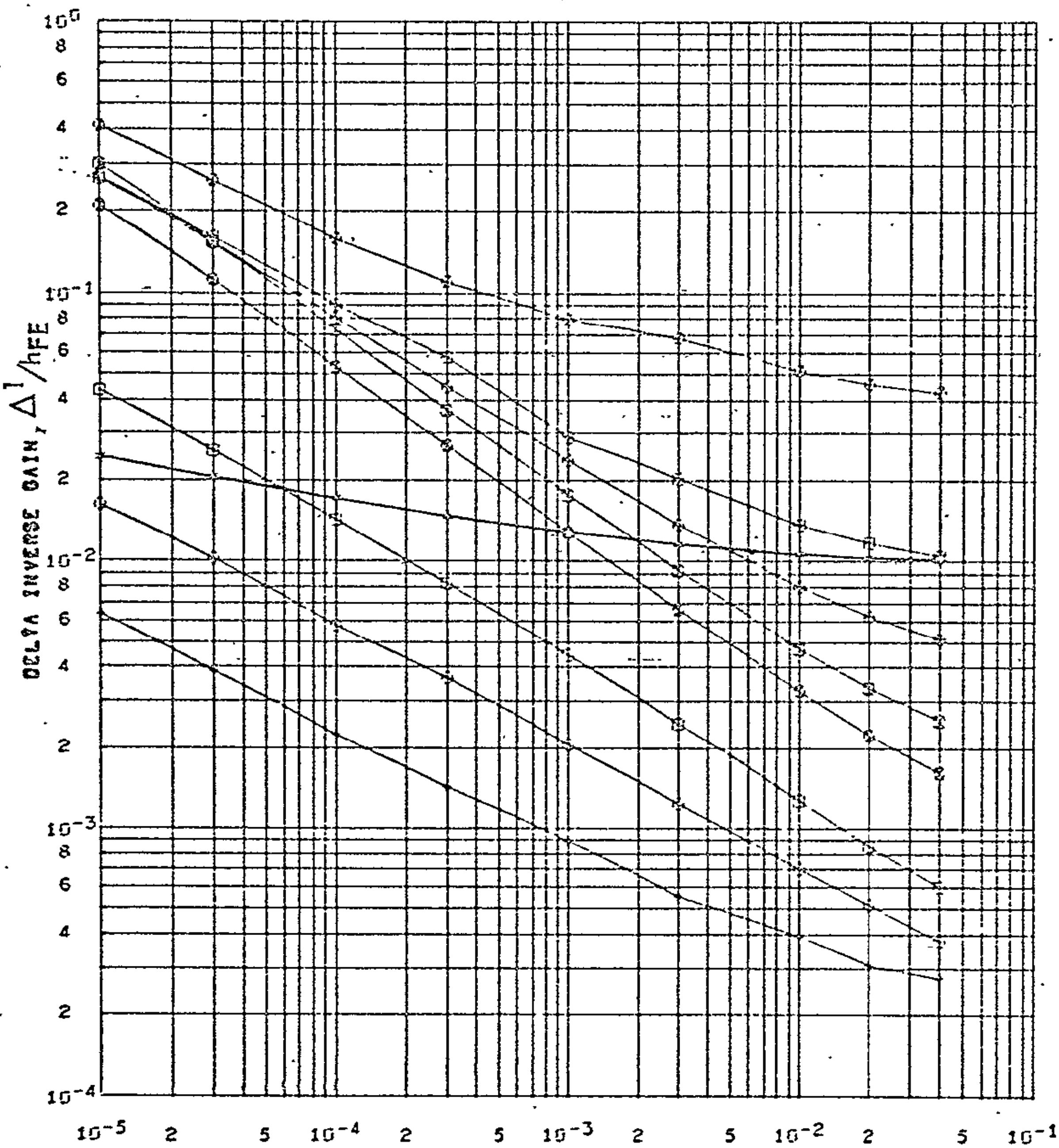

CHANGE IN DC GAIN VS. I_C, FAMILY OF FLUENCES, TYPE 2N1613, NO. 57

SYMBOL	FLUENCE
✲	0.00
⟡	3.24+11
⊙	9.97+11
⊡	2.18+12
⊗	8.19+12
⊡	1.77+13
⊕	9.40+13
⊟	4.70+14
⊘	3.29+15

Figure 48: DEPENDENCE OF NONLINEAR DAMAGE ON THE INJECTION LEVEL DURING MEASUREMENTS (FAIRCHILD 2N1613 - ACTIVE)

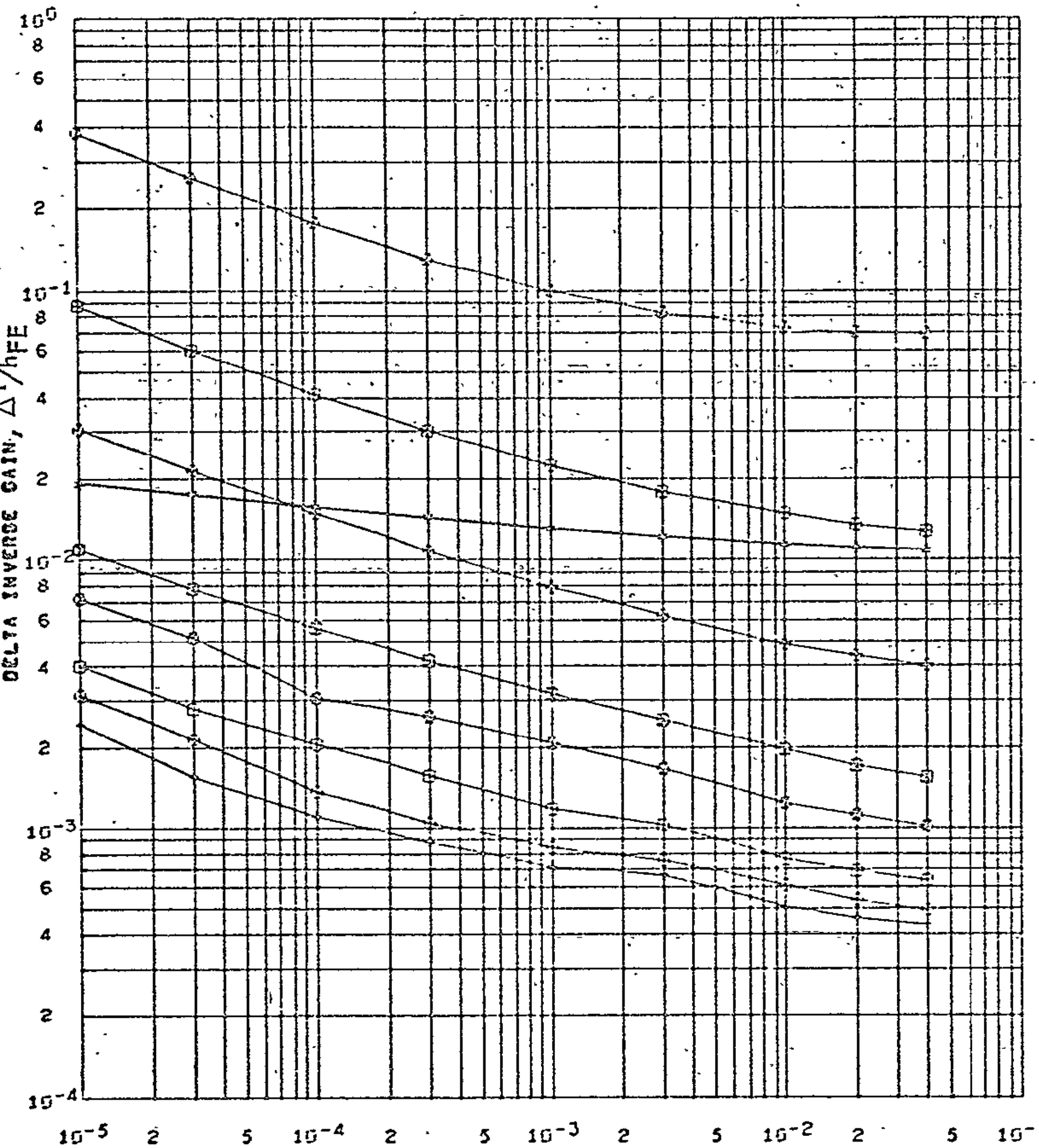

CHANGE IN DC GAIN VS. I_C, FAMILY OF FLUENCES, TYPE 2N1613, NO. 82

SYMBOL	FLUENCE
✲	0.00
+	2.64+11
⊙	8.13+11
⊡	1.78+12
⊛	6.67+12
⊠	1.45+13
⊕	7.66+13
⊞	3.84+14
∅	2.68+15

Figure 49: DEPENDENCE OF NONLINEAR DAMAGE ON THE INJECTION LEVEL DURING MEASUREMENTS (RAYTHEON 2N1613 - PASSIVE)

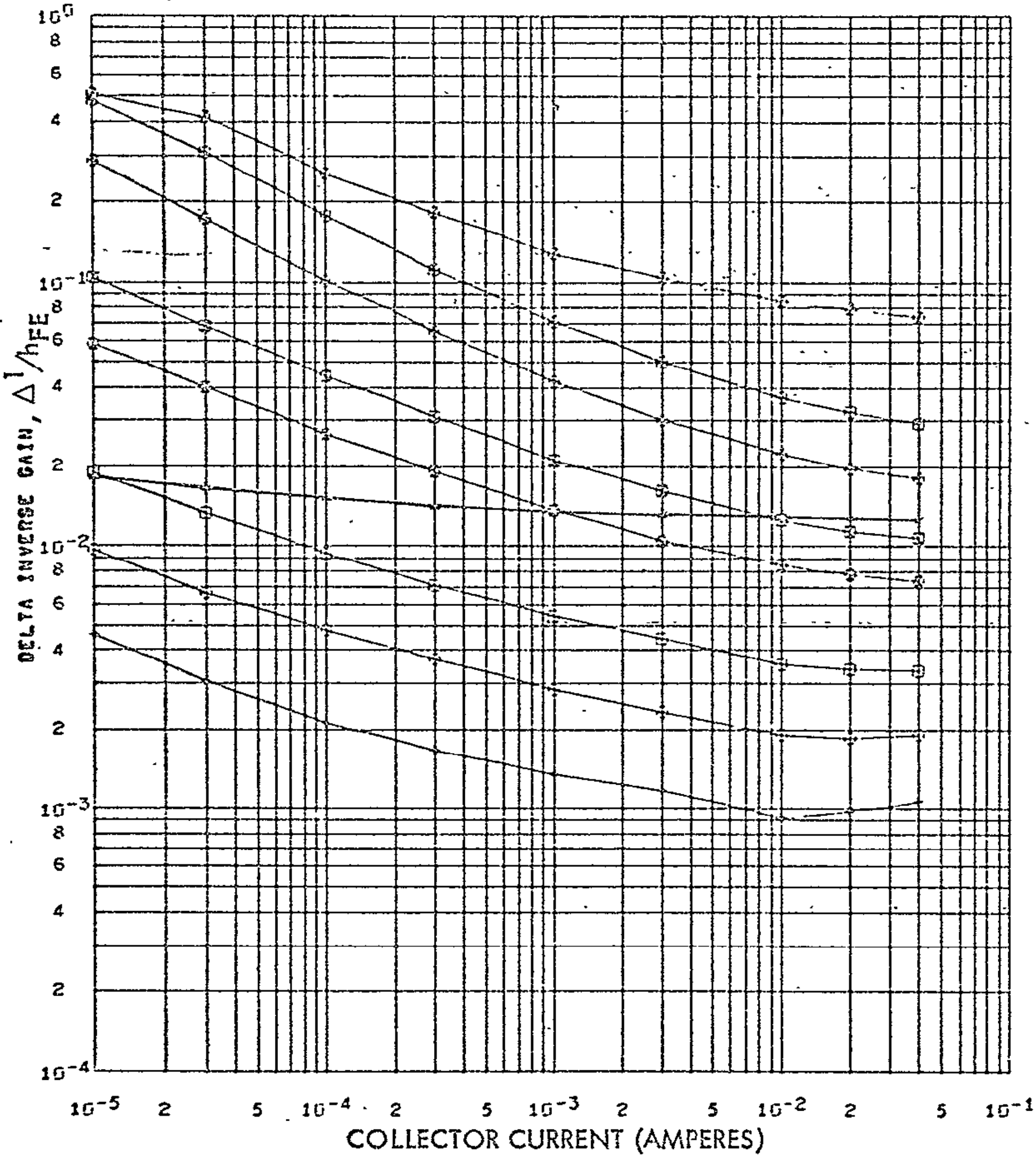

CHANGE IN DC GAIN VS. I_C, FAMILY OF FLUENCES, TYPE 2N1132, NO. 146

SYMBOL	FLUENCE
✲	0.00
+	2.64+11
⊙	8.13+11
⊡	1.78+12
⊕	6.67+12
⊘	1.45+13
✧	7.66+13
⊞	3.84+14
∅	2.68+15

Figure 50: DEPENDENCE OF NONLINEAR DAMAGE ON THE INJECTION LEVEL DURING MEASUREMENTS (RAYTHEON 2N1132 - PASSIVE)

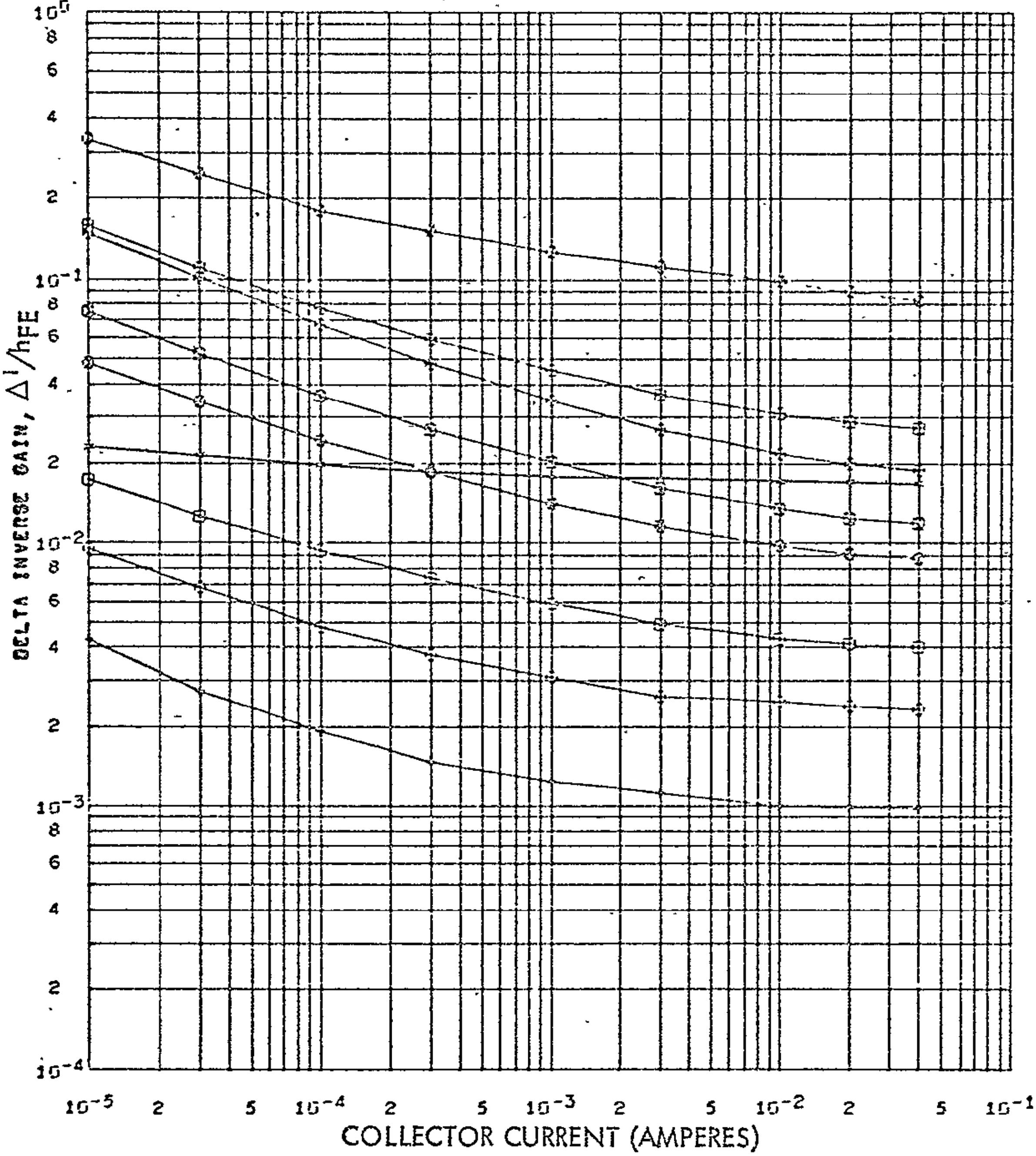

. CHANGE IN DC GAIN VS. I_C, FAMILY OF FLUENCES, TYPE 2N1132, NO. 153

SYMBOL	FLUENCE
✡	0.00
+	3.64+11
⊙	1.12+12
⊡	2.46+12
⊖	9.21+12
⊠	2.00+13
⊕	1.06+14
⊞	5.30+14
⌀	3.70+15

Figure 51: DEPENDENCE OF NONLINEAR DAMAGE ON THE INJECTION LEVEL DURING MEASUREMENTS (RAYTHEON 2N1132 - ACTIVE)

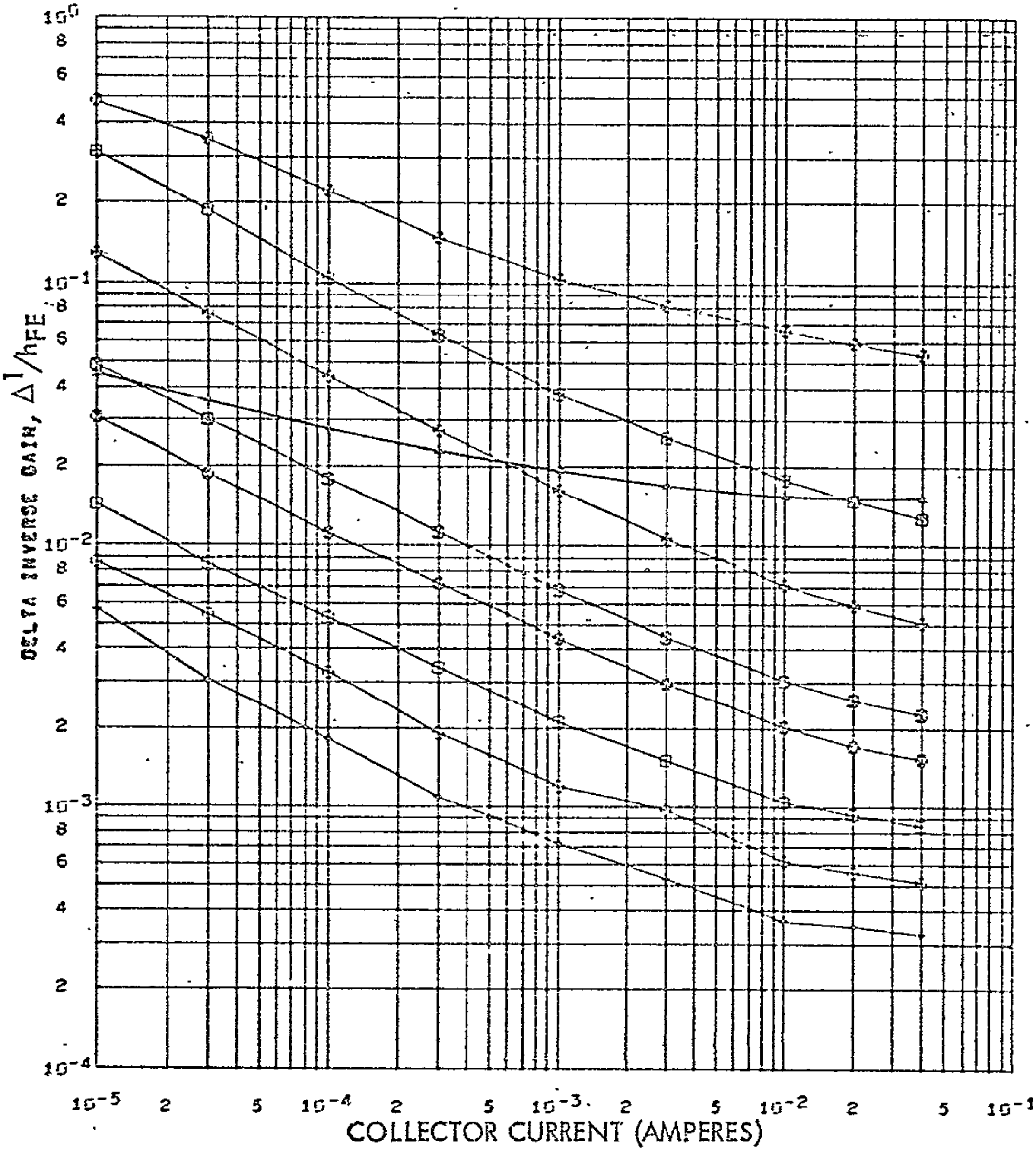

CHANGE IN DC GAIN VS. I_C, FAMILY OF FLUENCES, TYPE 2N1132, NO. 198

SYMBOL	FLUENCE
⊕	0.00
+	2.35+11
⊙	7.22+11
⊡	1.58+12
⊘	5.93+12
⊟	1.29+13
✣	6.81+13
⊞	3.41+14
⌀	2.38+15

Figure 52: DEPENDENCE OF NONLINEAR DAMAGE ON THE INJECTION LEVEL DURING MEASUREMENTS (FAIRCHILD 2N1132 - PASSIVE)

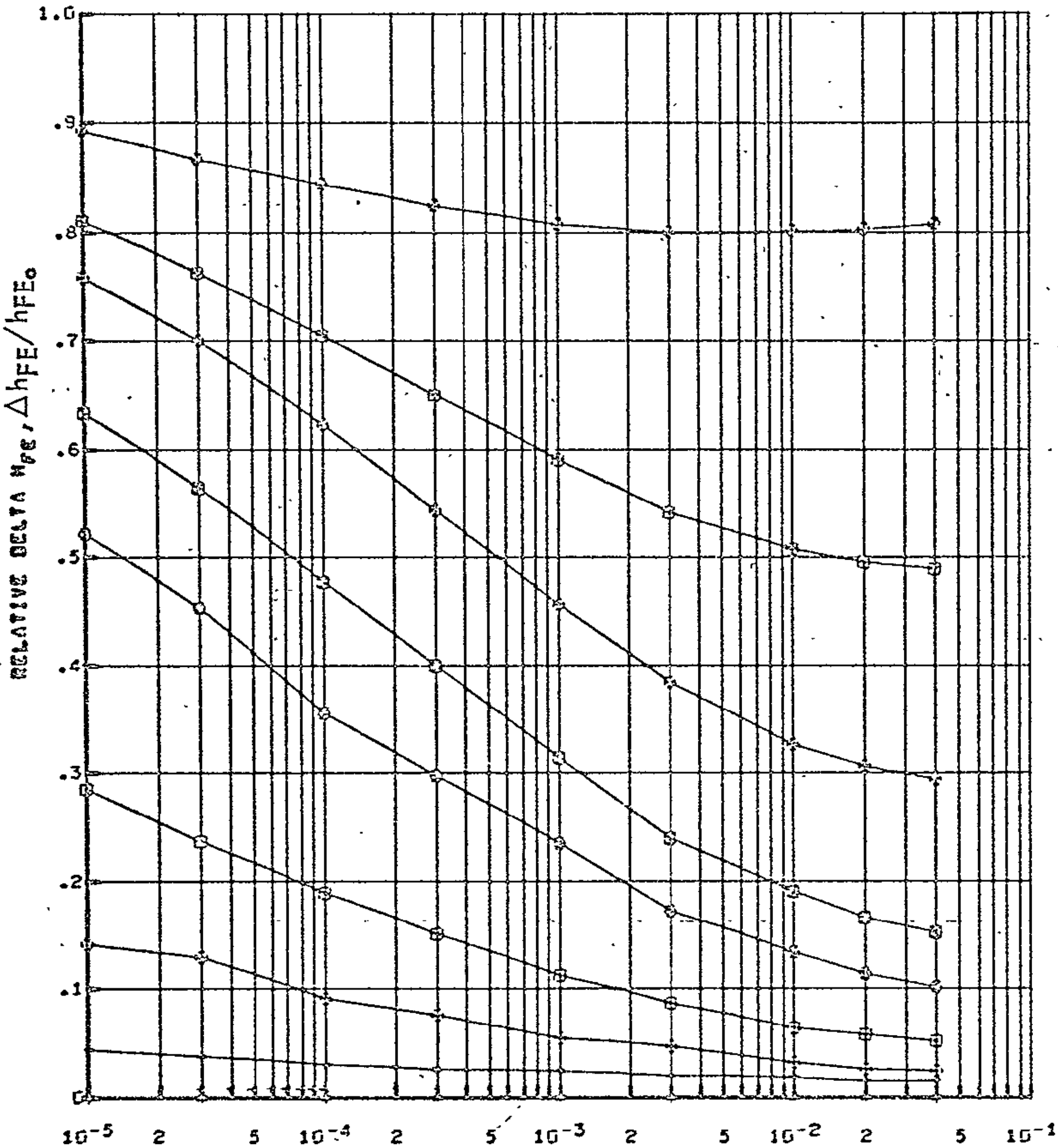

COLLECTOR CURRENT (AMPERES)

CHANGE IN DC GAIN VS. I_C, FAMILY OF FLUENCES, TYPE 2N1613, NO. 2

SYMBOL	FLUENCE
☆	0.00
+	2.35+11
⊙	7.22+11
⊡	1.58+12
⊕	5.93+12
⊠	1.29+13
⊖	6.81+13
⊟	3.41+14
⌀	2.38+15

Figure 53: DEPENDENCE OF THE RELATIVE GAIN LOSS ON THE INJECTION LEVEL DURING MEASUREMENTS (FAIRCHILD 2N1613 - PASSIVE)

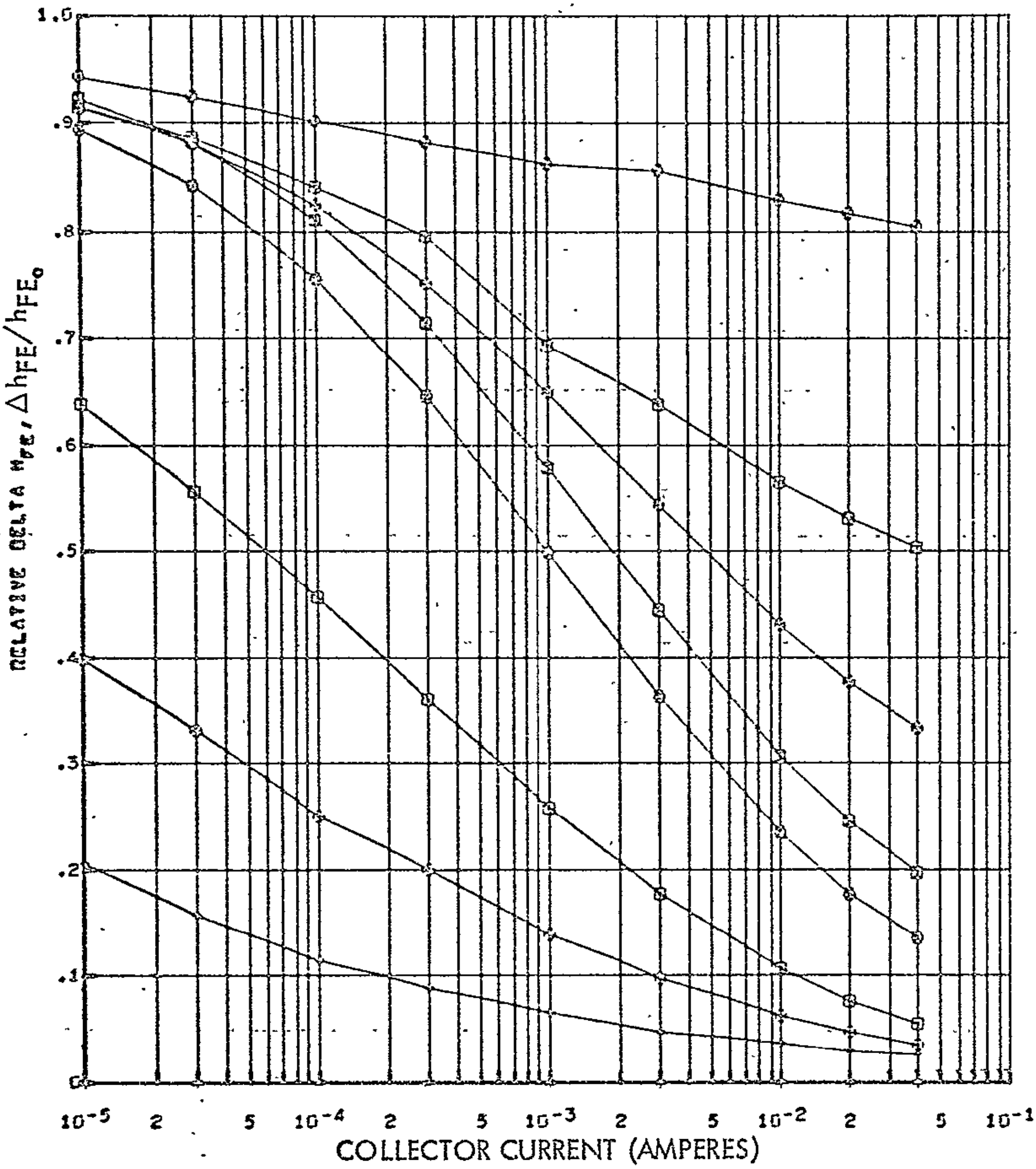

CHANGE IN DC GAIN VS. I_C, FAMILY OF FLUENCES, TYPE 2N1613, NO. 57

SYMBOL	FLUENCE
☆	0.00
+	3.24+11
⊙	9.97+11
⊡	2.18+12
@	8.19+12
⊠	1.77+13
⊕	9.40+13
⊞	4.70+14
⊘	3.29+15

Figure 54: DEPENDENCE OF THE RELATIVE GAIN LOSS ON THE INJECTION LEVEL DURING MEASUREMENTS (FAIRCHILD 2N1613 – ACTIVE)

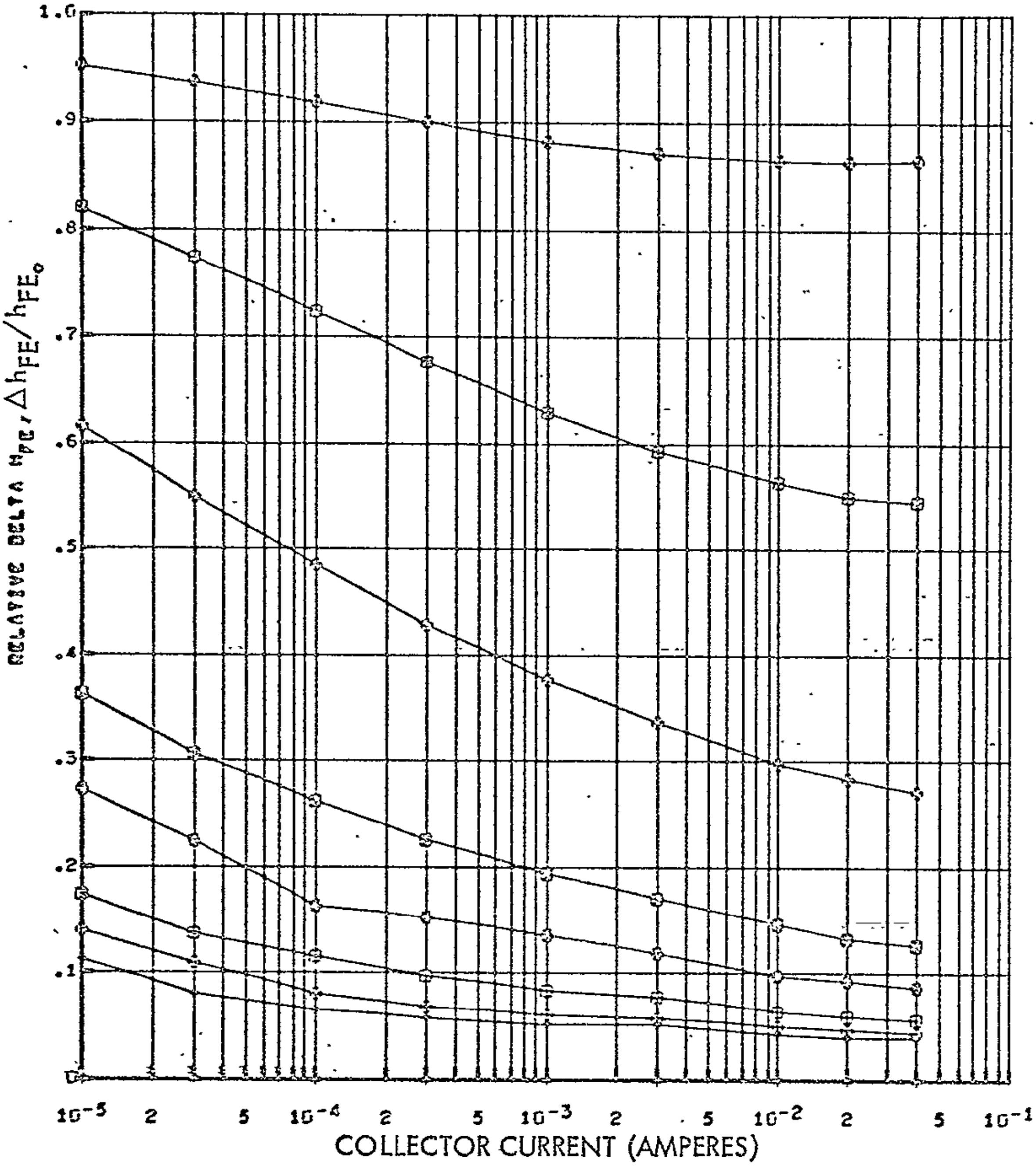

CHANGE IN DC GAIN VS. I_C, FAMILY OF FLUENCES, TYPE 2N1613, NO. 82

SYMBOL	FLUENCE
✲	0.00
+	2.64+11
⊕	8.13+11
⊡	1.78+12
⊖	6.67+12
⊞	1.49+13
◈	7.66+13
⊠	3.84+14
∅	2.68+15

Figure 55: DEPENDENCE OF THE RELATIVE GAIN LOSS ON THE INJECTION LEVEL DURING MEASUREMENTS (RAYTHEON 2N1613 – PASSIVE)

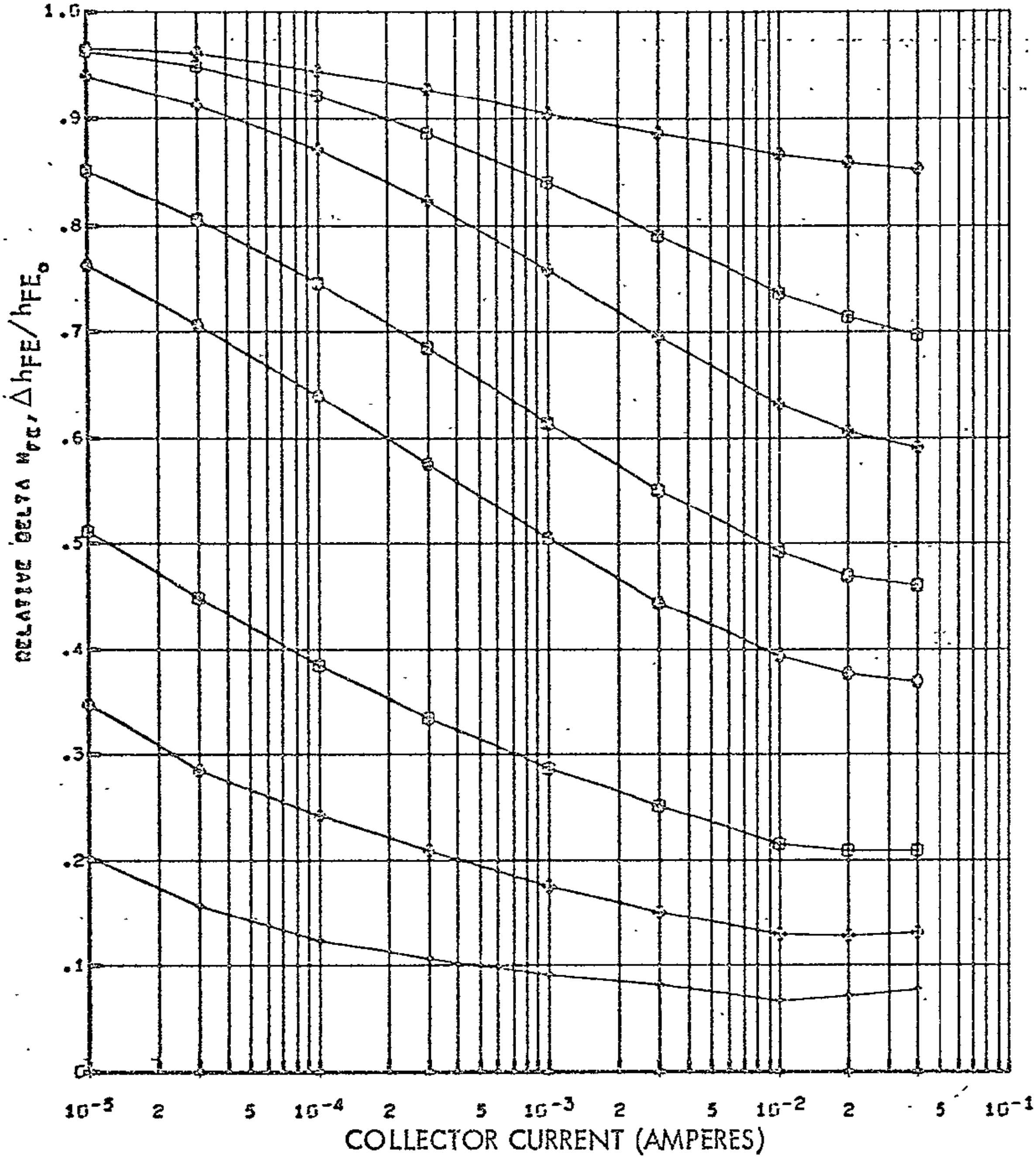

CHANGE IN DC GAIN VS. I_C, FAMILY OF FLUENCES, TYPE 2N1132, NO. 146

SYMBOL	FLUENCE
*	0.00
+	2.64+11
⊖	8.13+11
⊡	1.78+12
⊜	6.67+12
▨	1.45+13
⌂	7.66+13
⊠	3.84+14
Ø	2.68+15

Figure 56: DEPENDENCE OF THE RELATIVE GAIN LOSS ON THE INJECTION LEVEL DURING MEASUREMENTS (RAYTHEON 2N1132 - PASSIVE)

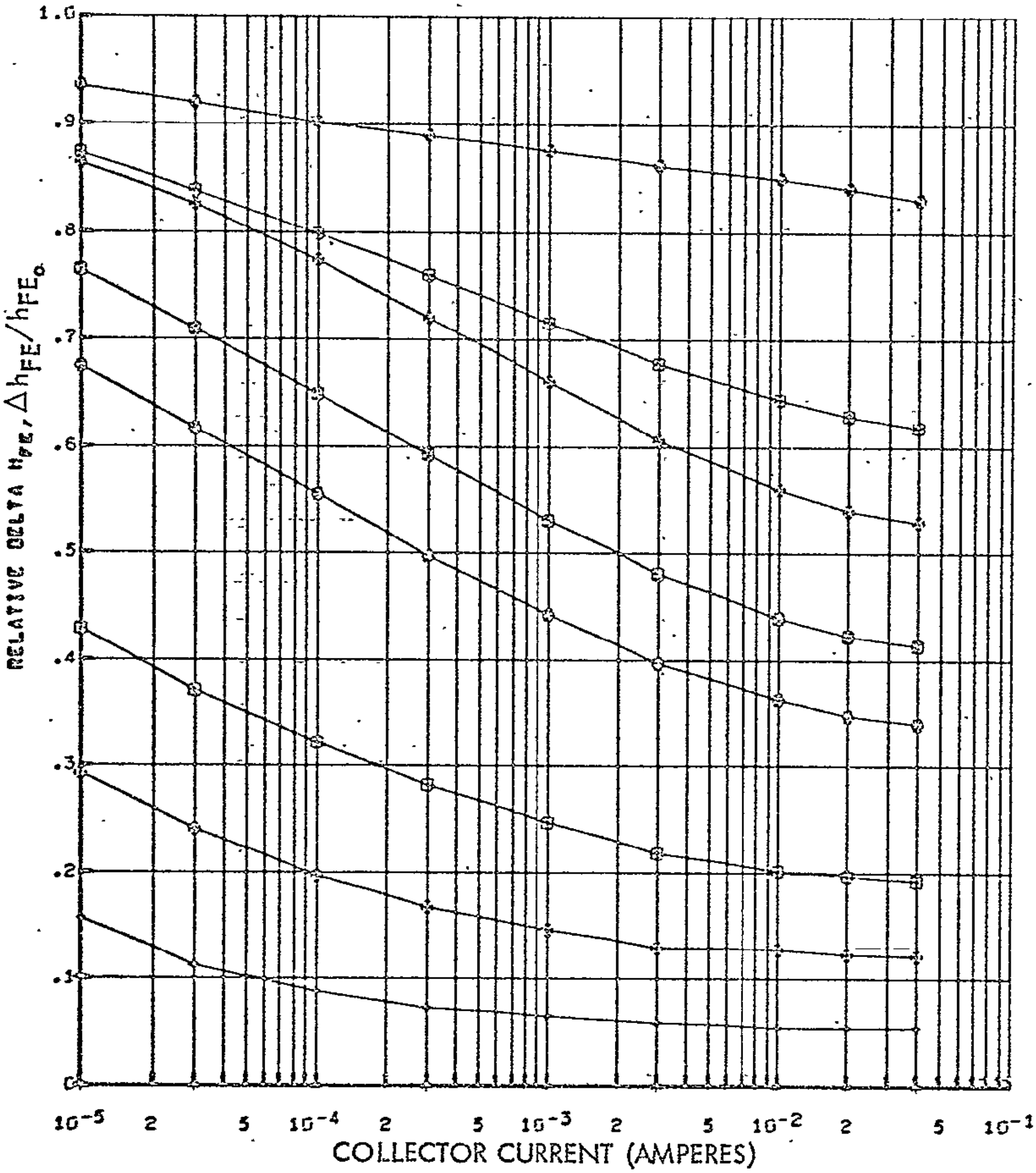

CHANGE IN DC GAIN VS. I_C, FAMILY OF FLUENCES, TYPE 2N1132, NO. 153

SYMBOL	FLUENCE
✡	0.00
+	3.64+11
⊙	1.12+12
⊡	2.46+12
⊙	9.21+12
⊡	2.00+13
⊙	1.06+14
⊡	5.30+14
Ø	3.70+15

Figure 57: DEPENDENCE OF THE RELATIVE GAIN LOSS ON THE INJECTION LEVEL DURING MEASUREMENTS (RAYTHEON 2N1132 - ACTIVE)

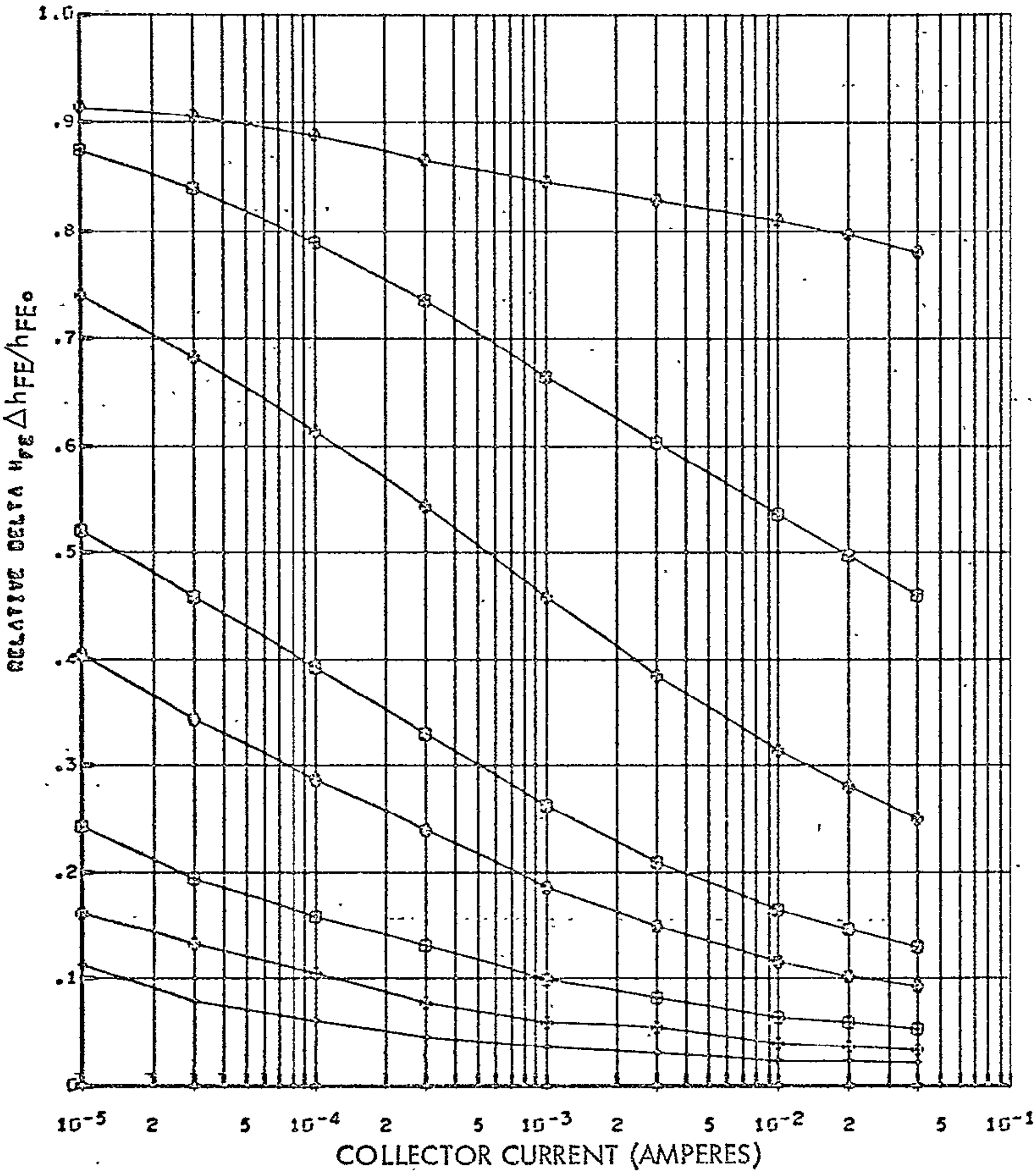

CHANGE IN DC GAIN VS. I_C, FAMILY OF FLUENCES, TYPE 2N1132, NO. 198

SYMBOL	FLUENCE
✲	0.00
✦	2.35+11
⊖	7.22+11
⊡	1.98+12
⊘	5.93+12
⊟	1.29+13
⊕	6.81+13
⊠	3.41+14
⊘	2.38+15

Figure 58: DEPENDENCE OF THE RELATIVE GAIN LOSS ON THE INJECTION LEVEL DURING MEASUREMENTS (FAIRCHILD 2N1132 – PASSIVE)

2.4 STATISTICAL ANALYSIS (TASK A2)

In trying to predict transistor gain degradation due to ionizing irradiation of the surface, one should have some idea about the statistical spread in device response among the presumably "identical" devices during identical exposure conditions. Certain spread in gain degradation is clearly expected among transistors, the question is how much. It is well known that the initial surface conditions are extremely critical for controlling certain transistor parameters as well as for influencing the degradation of those parameters during surface ionization effects. More specifically, the oxidation conditions and surface cleaning techniques will determine not only the low current gain values but also the degradation of this gain with exposure. Although the silicon chips are presumably subjected to "identical" fabrication conditions, it is not possible in practice to avoid some subtle differences in the fabrication procedures (e.g. due to small differences in surface cleaning steps done by different operators during assembly) consequently the surface conditions of the finished transistors can differ slightly.

In order to determine the size of the spread in device response during identical exposure, a statistical study was carried out on passive transistors. 30 Fairchild 2N1613, 30 Raytheon 2N1613, 30 Fairchild 2N1132 and 30 Raytheon 2N1132 transistors were procured, actually each group of 30 came from three different batches of 10 devices each. With such a selection of transistors we were able to observe differences among devices within one given batch, among batches and between manufacturers. By batch number as we said earlier, we mean the date code (year and week) stamped on the transistor can. The actual batch numbers or date codes of the devices used in our statistical study are listed in Table 4.

The results of the study are expressed in three different ways in Figures (59) through (70). Namely, the different device groups are compared in terms of the h_{FE} vs. ϕ, $\Delta\beta/\beta_o$ vs. ϕ and $\Delta 1/h_{FE}$ vs. ϕ. (For typographical reasons we write $\Delta\beta/\beta_o$ for $\Delta h_{FE}/h^{\circ}_{FE}$, i.e., $h_{FE} \equiv \beta$.) All gain values shown here refer to measurements at 10 μa. In each figure we find three curves superimposed where each curve represents the mean value of the particular parameter taken for a given batch (10 devices). The vertical bars across the curves represent the standard deviations (σ), i.e., express the size of the statistical spread in the values of the given parameters among the 10 devices. The curve for batch #1 is left in its original position the other two are shifted horizontally for clarity in order to avoid overlap of the σ bars.

The h_{FE} vs. ϕ data illustrate the initial gain distributions within the batches as well as the changes of these distributions with fluence. The $\Delta\beta/\beta_0$ vs. ϕ data, since they are "normalized," as discussed in Section 2.2.4, are well suited to show up some inherent differences in surface conditions among the batches. Without such differences the curves should overlap. The $\Delta 1/h_{FE}$ vs. ϕ data show the differences among the batches by using still another type of normalization as discussed in 2.2.4.

The following conclusions can be drawn from the figures:

i) Devices within a given batch:

Devices, as a general rule, tended to behave very similarly within a given batch, at least as far as their gain degradation was concerned, e.g., in terms of the $\Delta 1/h_{FE}$ vs. ϕ curves. Although the actual values of $\Delta 1/h_{FE}$ at given ϕ were somewhat different for different devices, as the size of the σ bars testifies in Figures (63), (64), and (69), (70), the shape of the curves for the individual devices were very similar. A given shape could almost serve as a marker for all the transistors within a batch. This was already emphasized in Section 2.3 in selecting Figures (35) - (46) ($\Delta 1/h_{FE}$ vs. ϕ for a family of I_C) where it was pointed out that the devices shown represented one or more batches because of the close similarity of the curves within one batch.

The reason for the similar behavior during exposure is presumably that the devices bearing the same date code went through the different fabrication processes together as a group, i.e., conditions were pretty much the same for all of them. Although this is probably true it is not necessarily the case as discussions during a visit to the manufacturers revealed. E.g. depending upon the number of devices produced within a particular week, the devices having the same date code may or may not come from the same "lot". (A group of wafers exposed to identical diffusion and oxidation conditions at the same time.) If only a relatively small number of transistors were produced then they are likely to originate from the same lot.

Of course it is still true that devices with the same date code although coming from different lots could, nevertheless, experience pretty much identical diffusion, oxidation and surface cleaning procedures within a week or so even though not exactly at the same time. To the contrary, devices having widely different date codes (by a year or more), probably experience slightly different fabrication conditions due to continuous improvement and changes in techniques, (surface cleaning!) equipment and operators during that time.

ii) Devices from different batches of the same manufacturer:

On the basis of what we said earlier in i) we do expect some differences in device response during irradiation among devices from different batches especially if the date codes are far apart. Experimentally, this is indeed the case. By checking the date codes in Table 4 and comparing the curves representing separate batches in Figures (59) - (70) we see the following:

a) NPN - Fairchild: The mean h_{FE} curves representing F2 and F3 are close while F1 is apart in Figure (59) as expected on the basis of the date codes. However, when the nonlinear damage is plotted in terms of $\Delta\beta/\beta_o$, then the curves of all batches superimpose as shown in Figure (61). Quite surprisingly, the superposition of the curves in terms of the $\Delta 1/h_{FE}$ data in Figure (63) is not nearly as good.

b) PNP - Fairchild: The initial portion of the mean h_{FE} curves representing F1P and F2P are far apart while F3P is close to F2P which is unexpected on the basis of the date codes. The superposition of the curves in terms of $\Delta\beta/\beta_o$ or $\Delta 1/h_{FE}$ is good for F1P and F2P but F3P is way off, indicating some small but significant differences between the exact surface conditions of transistors (F1P, F2P) and F3P.

c) NPN - Raytheon: Initial gain values of R1, R2, and R3 are very close in spite of the very different date codes. But their irradiation responses are widely different both in terms of $\Delta\beta/\beta_o$ (Figure 62), and of $\Delta 1/h_{FE}$ (Figure 64). Interestingly though, R1 and R2 remain quite close in the mean h_{FE} curves (Figure 60). R3 is way off even there and surprisingly suffers the worst damage in spite of its most recent date code.

d) PNP - Raytheon: R2P and R3P curves of mean h_{FE} are far apart in Figure (66) whereas their date codes are quite close. R1P and R3P curves are close in the same figure though the date codes are quite different. R1P and R3P curves also remain close, as expected, when the nonlinear damage is normalized either in terms of $\Delta\beta/\beta_o$ or $\Delta 1/h_{FE}$ (Figures 68 and 70), whereas R2P curve remains split off in either case. This indicates that the surface conditions of the devices in batch R2P are significantly different in some way with respect to the other two batches.

iii) Devices with identical designations from different manufacturers (Fairchild vs. Raytheon):

Differences in device response during exposure among devices coming from two manufacturers are certainly expected. There are constructional differences between the devices and the surface treatments can be entirely different (usually proprietary information) in spite of the fact that the devices are produced for the same functions in electrical circuits. These factors of course have a large influence on the radiation hardness of the devices. Then in order to be able to select the best possible transistors for ionizing radiation environment it is important to determine what and how large are the differences in radiation response among devices from different manufacturers during exposure. As proposed in Section 2.2.4 the quantity $\Delta\beta/\beta_o$ will be used primarily for comparing the devices of separate manufacturers in order to normalize against differences in the emitter-base junction perimeters.

The following conclusions can be drawn from the figures:

<u>2N1613 - NPN</u>

Radiation resistance: R1 and R2 are better than F1, F2, F3 whereas R3 is worse. (See the $\Delta\beta/\beta_o$ curves in Figures (61) and (62).) R2 was especially good.

Statistical spread: The different Fairchild batches were much closer in behavior than the Raytheon ones. This was especially true in the $\Delta\beta/\beta_o$ curves which is equivalent to saying that there was a good correlation between gain loss and initial gain for the Fairchild devices whereas absent for the Raytheon ones. Consequently the <u>prediction</u> of the gain loss, $\Delta\beta$, or the relative gain loss, $\Delta\beta/\beta_0$, was possible for the Fairchild devices but not for the Raytheon transistors. Also the statistical spread among devices within a given batch is much wider for the Raytheon devices than for the Fairchild as seen from the size of the σ bars.

2N1132 - PNP

Radiation resistance: Fairchild batches are somewhat better than the Raytheon ones. (See Figures (67) and (68).)

Statistical spread: Raytheon batches are slightly closer than the Fairchild ones, although the former batches cover over 1½ year period whereas the latter ones cover about a year. The error bars are approximately of the same size for both manufacturers. The correlation of the gain loss to the initial gain or equivalently the predictability of the relative gain loss, $\Delta\beta/\beta_0$, was approximately of the same degree for each manufacturer. (See Figures (67) and (68) or the Rank Coefficients of Correlation in Table 2.)

In summary of this section we can say that in order to select transistors (given type and manufacturer) with the least expected spread in radiation response one should specify not only that the devices carry the same date code but also that they come from the same lot of Si wafers. As a compromise one may settle for the same date code only, although a somewhat higher statistical spread is then expected.

Of course, selecting the particular manufacturer is also a very important problem since the statistical spread even among different batches can be smaller for one manufacturer than that within one batch from another manufacturer. This is a statistical consideration only. It says nothing about the average radiation hardness (i.e., the radiation sensitivity) of the devices coming from different manufacturers which can be significantly different.

We wish to re-emphasize that the previous statistical study was carried out on passive transistors only. Since in actual space applications the devices are often active during exposure, a similar statistical study carried out on biased devices would be highly desirable. On the basis of such a study, a much better prediction of the expected nonlinear gain degradation would be possible.

Table 4. Summary of Batch Number or Date Code Designations

Passive Devices

2N1613 - NPN			2N1132 - PNP		
Batch Number Designation	Actual Date Code	Device Number	Batch Number Designation	Actual Date Code	Device Number
F1	701	1 thru 10	R1P	6523	111-120
F2	552	31- 40	R2P	6710	141-150
F3	615	61- 70	R3P	6649	161-168
R1	446	81- 90	F1P	721	189-198
R2	6545	91-100	F2P	736	199-207
R3	6625	101-110	F3P	621	208-218

Active Devices

2N1613 - NPN Fairchild			2N1132 Raytheon		
Batch Number Designation	Actual Date Code	Device Number	Batch Number Designation	Actual Date Code	Device Number
No Number Assigned	Mixed Codes Were Used for These Tests	11-30 41-60 71-80	No Number Assigned	Mixed Codes Were Used for These Tests	121-140 151-160 169-188

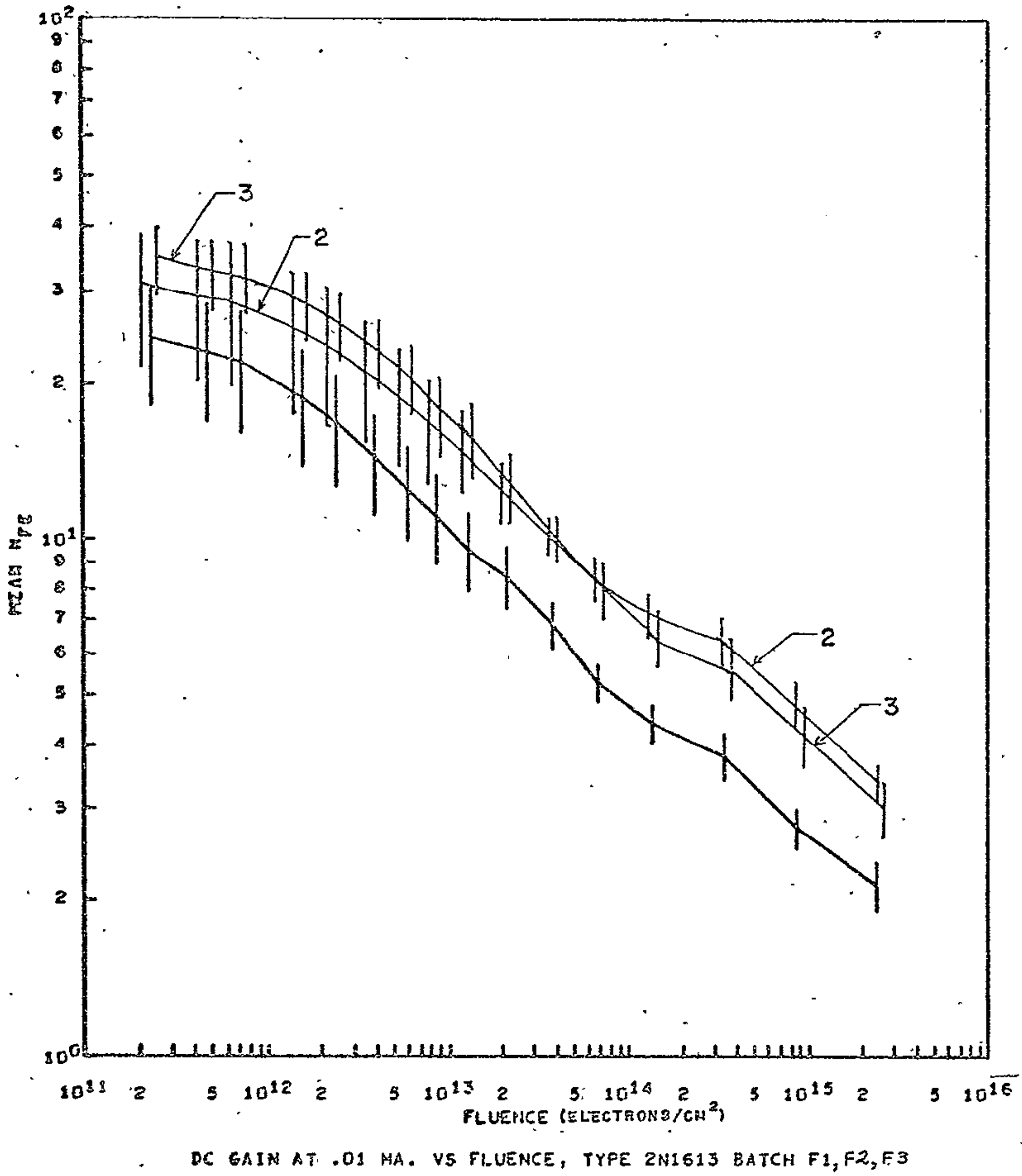

Figure 59: MEAN h_{FE} OF A GIVEN BATCH VERSUS FLUENCE (FAIRCHILD 2N1613 - PASSIVE, THREE BATCHES; THE VERTICAL BARS INDICATE STANDARD DEVIATIONS)

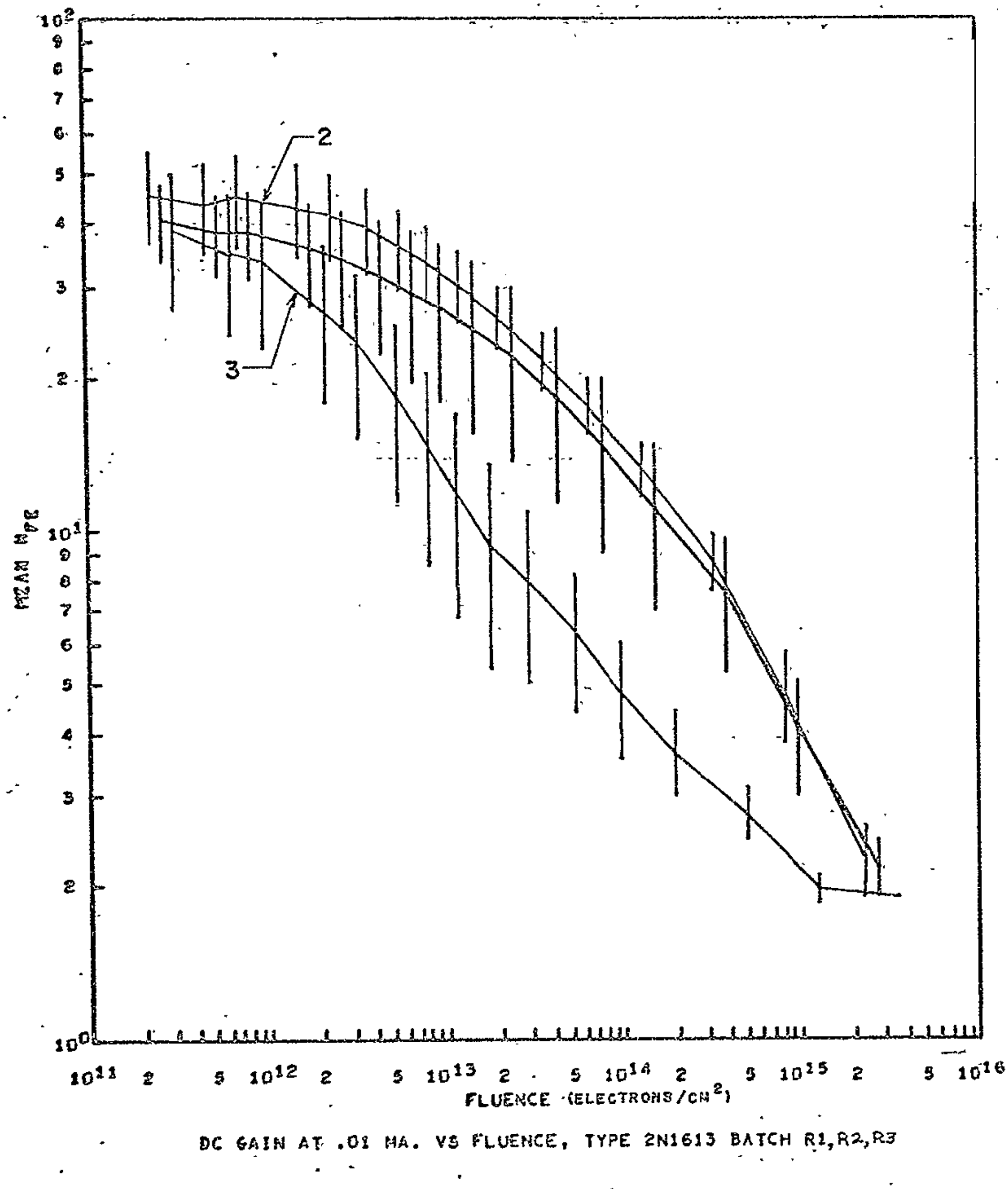

igure 60: MEAN h_{FE} OF A GIVEN BATCH VERSUS FLUENCE (RAYTHEON 2N1613 - PASSIVE, THREE BATCHES; THE VERTICAL BAR INDICATE STANDARD DEVIATIONS)

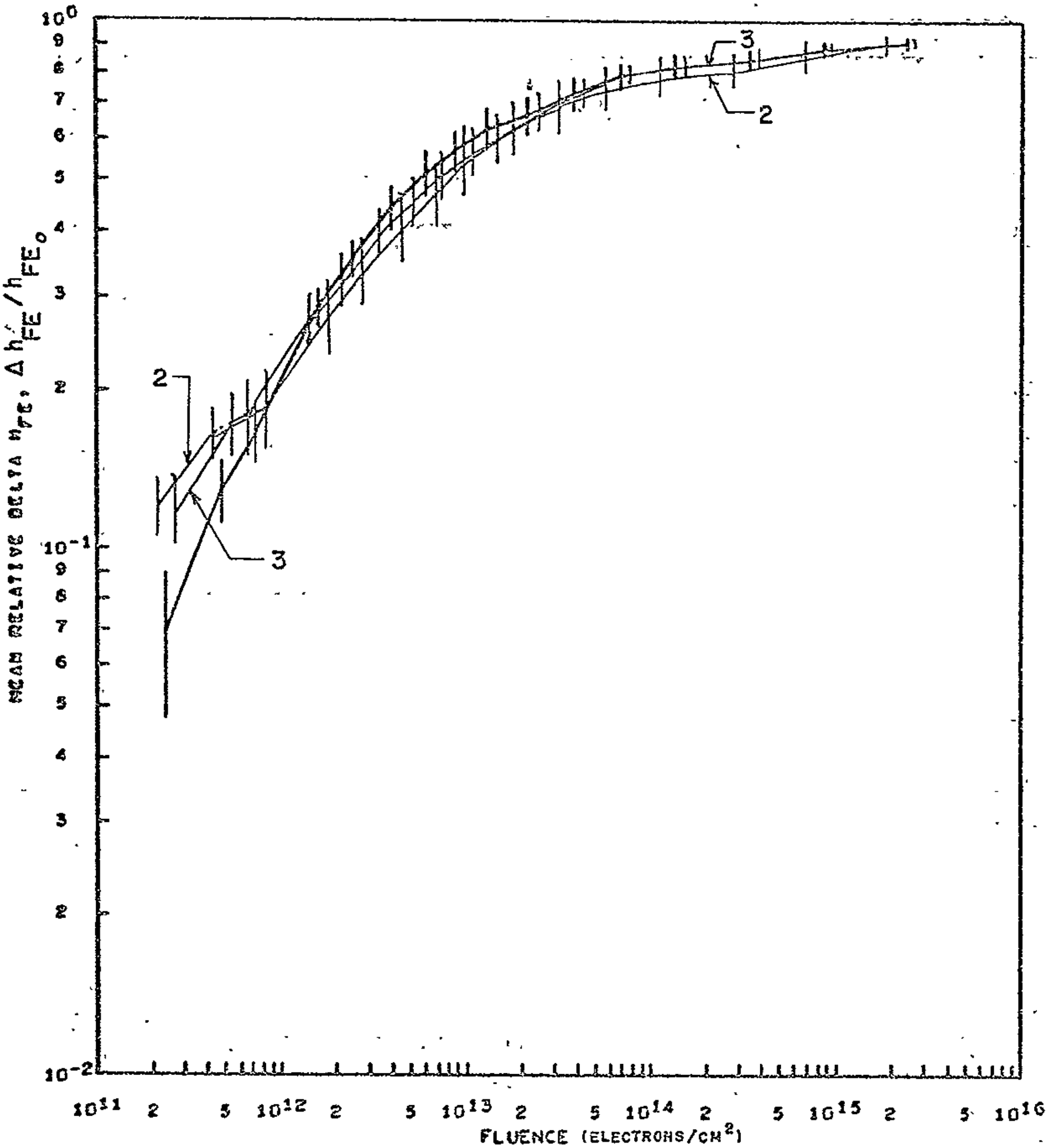

CHANGE IN DC GAIN AT .01 MA. VS. FLUENCE, TYPE 2N1613 BATCH F1, F2, F3

Figure 61: MEAN RELATIVE GAIN LOSS OF A GIVEN BATCH VERSUS FLUENCE (FAIRCHILD 2N1613 - PASSIVE, THREE BATCHES; THE VERTICAL BARS INDICATE STANDARD DEVIATIONS)

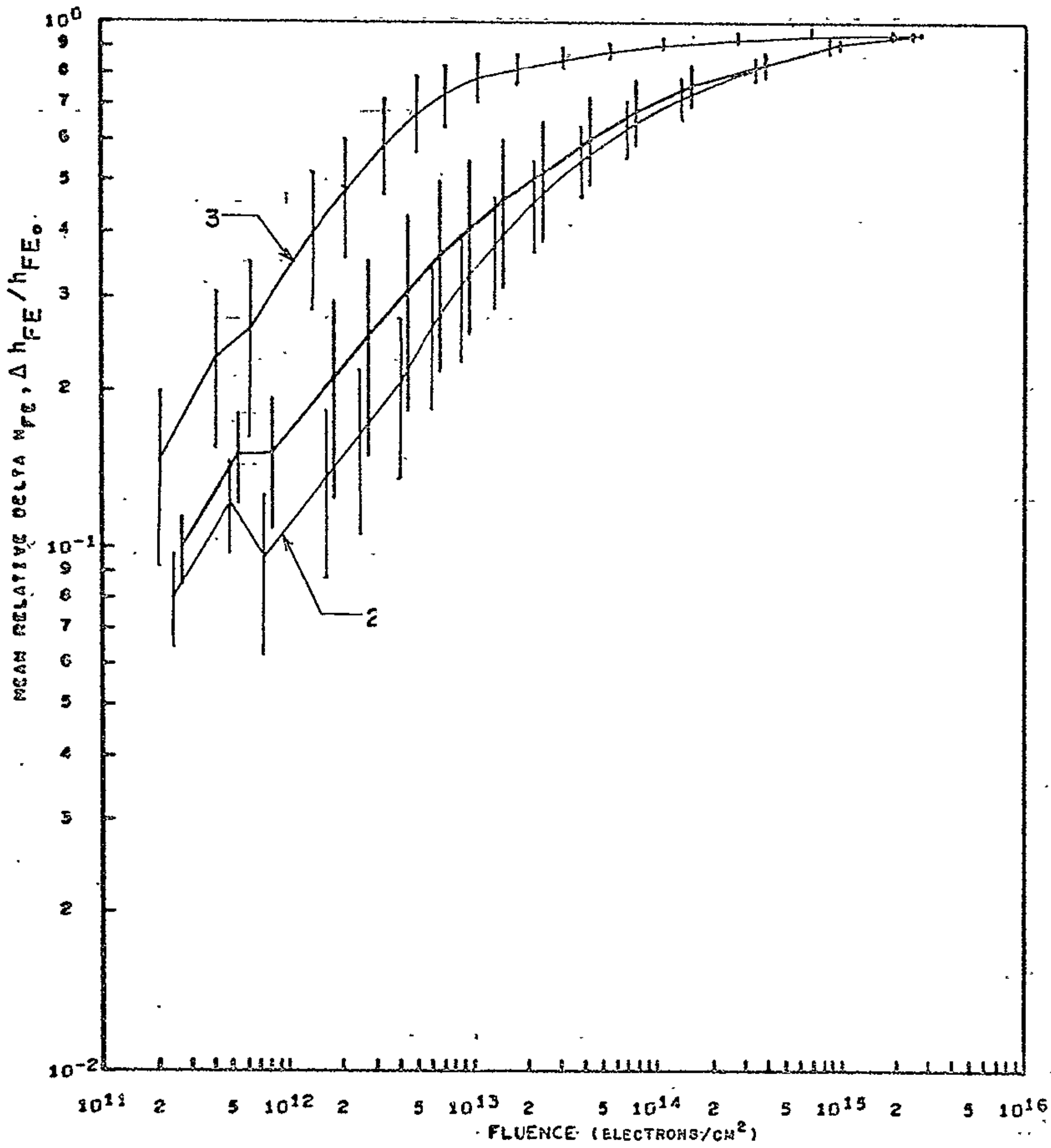

Figure 62: MEAN RELATIVE GAIN LOSS OF A GIVEN BATCH VERSUS FLUENCE (RAYTHEON 2N1613 - PASSIVE, THREE BATCHES; THE VERTICAL BARS INDICATE STANDARD DEVIATIONS)

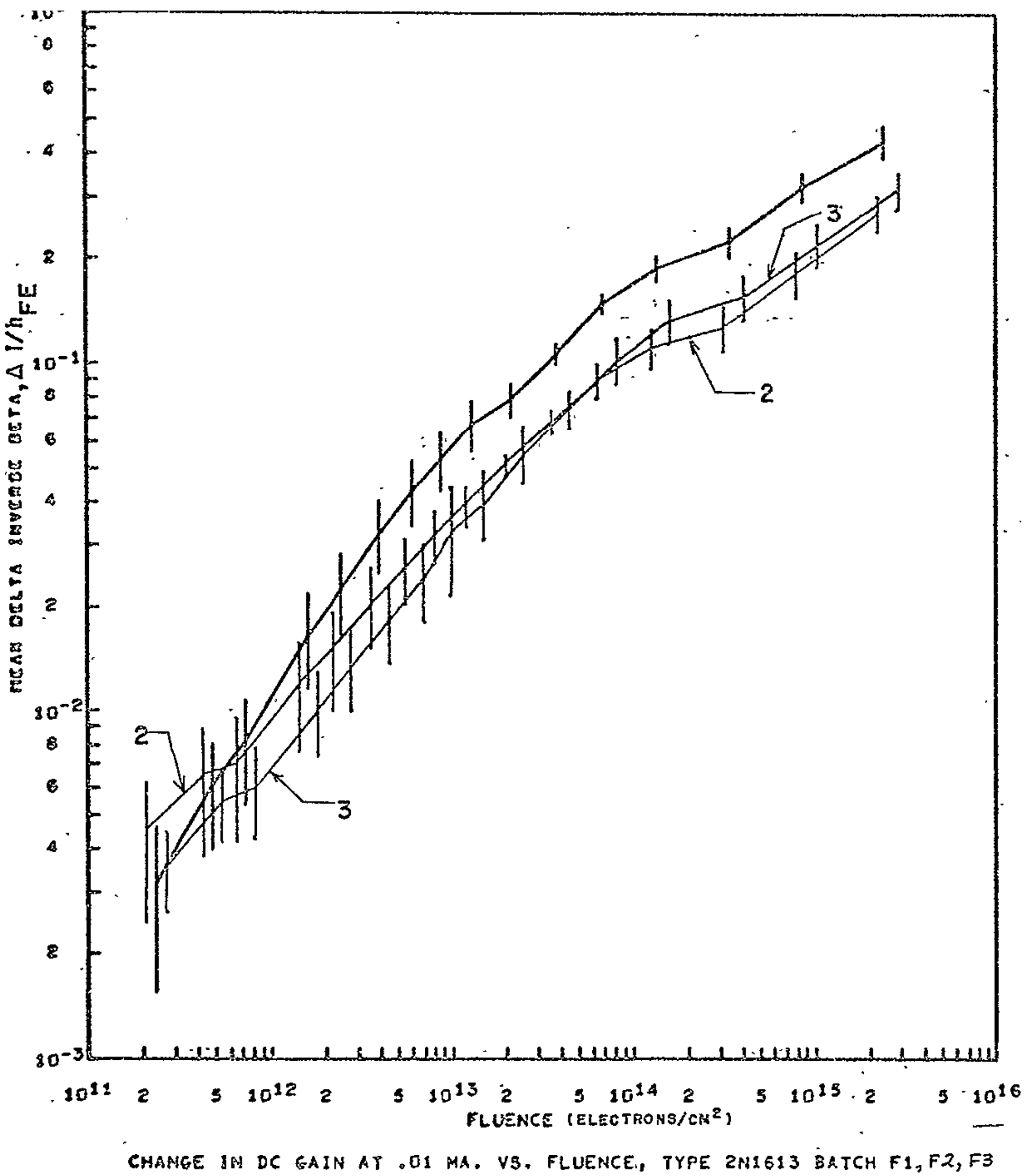

gure 63: MEAN Δ^1/h_{FE} OF A GIVEN BATCH VERSUS FLUENCE (FAIRCHILD 2N1613 - PASSIVE, THREE BATCHES; THE VERTICAL BARS INDICATE STANDARD DEVIATIONS)

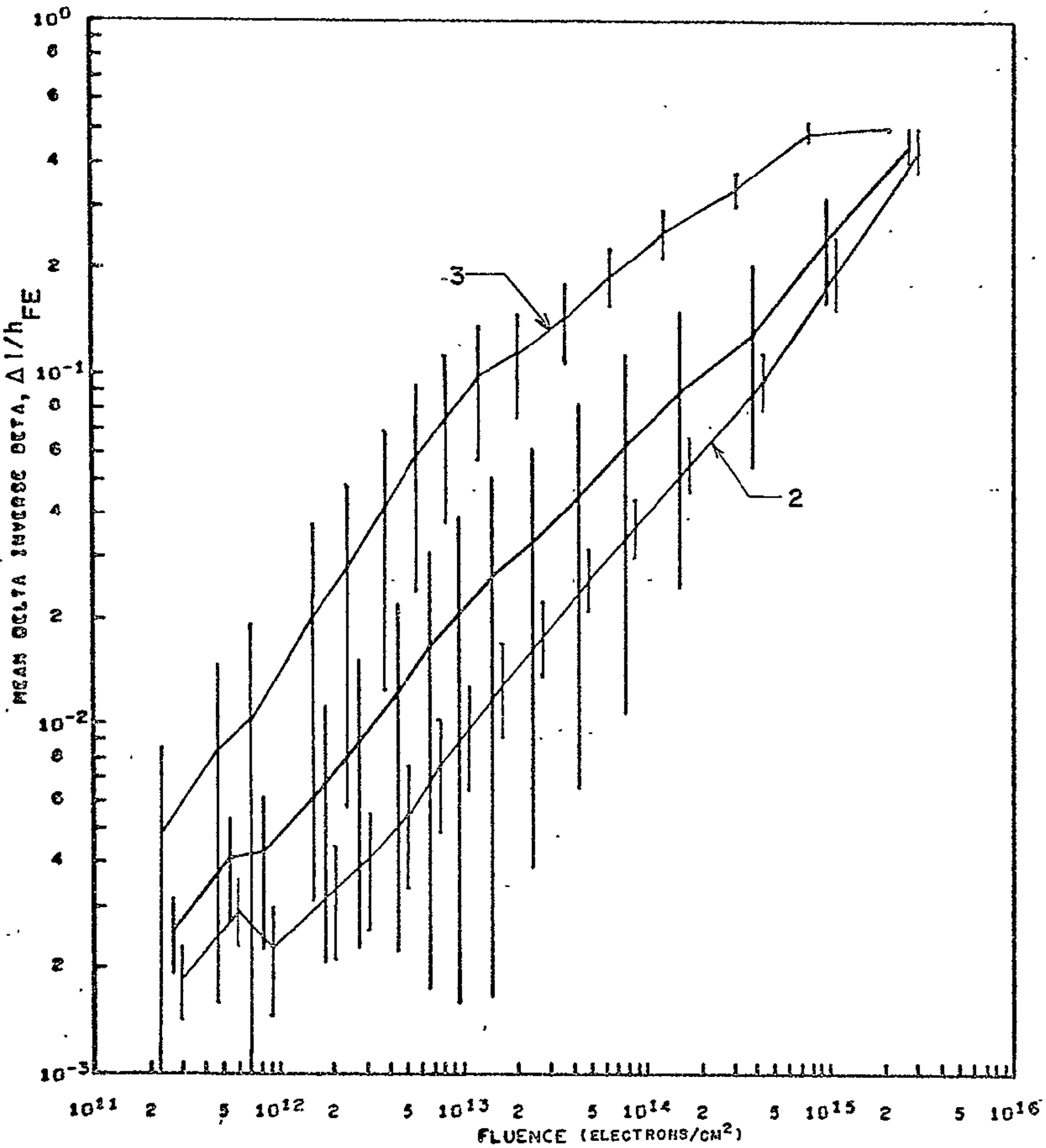

CHANGE IN DC GAIN AT .01 MA. VS. FLUENCE, TYPE 2N1613 BATCH R1,R2,R3

Figure 64: MEAN Δ^1/h_{FE} OF A GIVEN BATCH VERSUS FLUENCE (RAYTHEON 2N1613 - PASSIVE, THREE BATCHES; THE VERTICAL BARS INDICATE STANDARD DEVIATIONS)

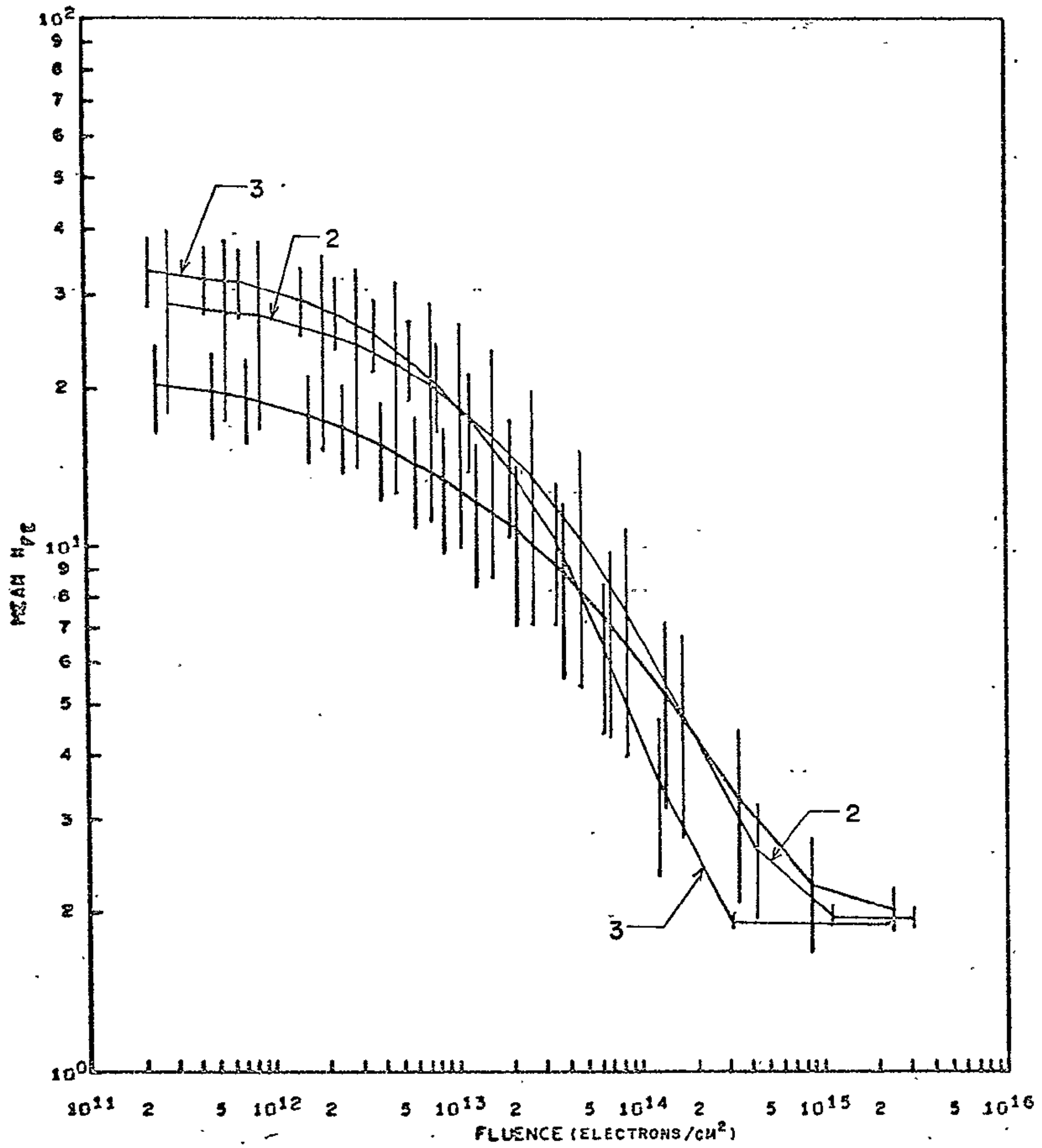

Figure 65: MEAN h_{FE} OF A GIVEN BATCH VERSUS FLUENCE (FAIRCHILD 2N1132 - PASSIVE, THREE BATCHES; THE VERTICAL BARS INDICATE STANDARD DEVIATIONS

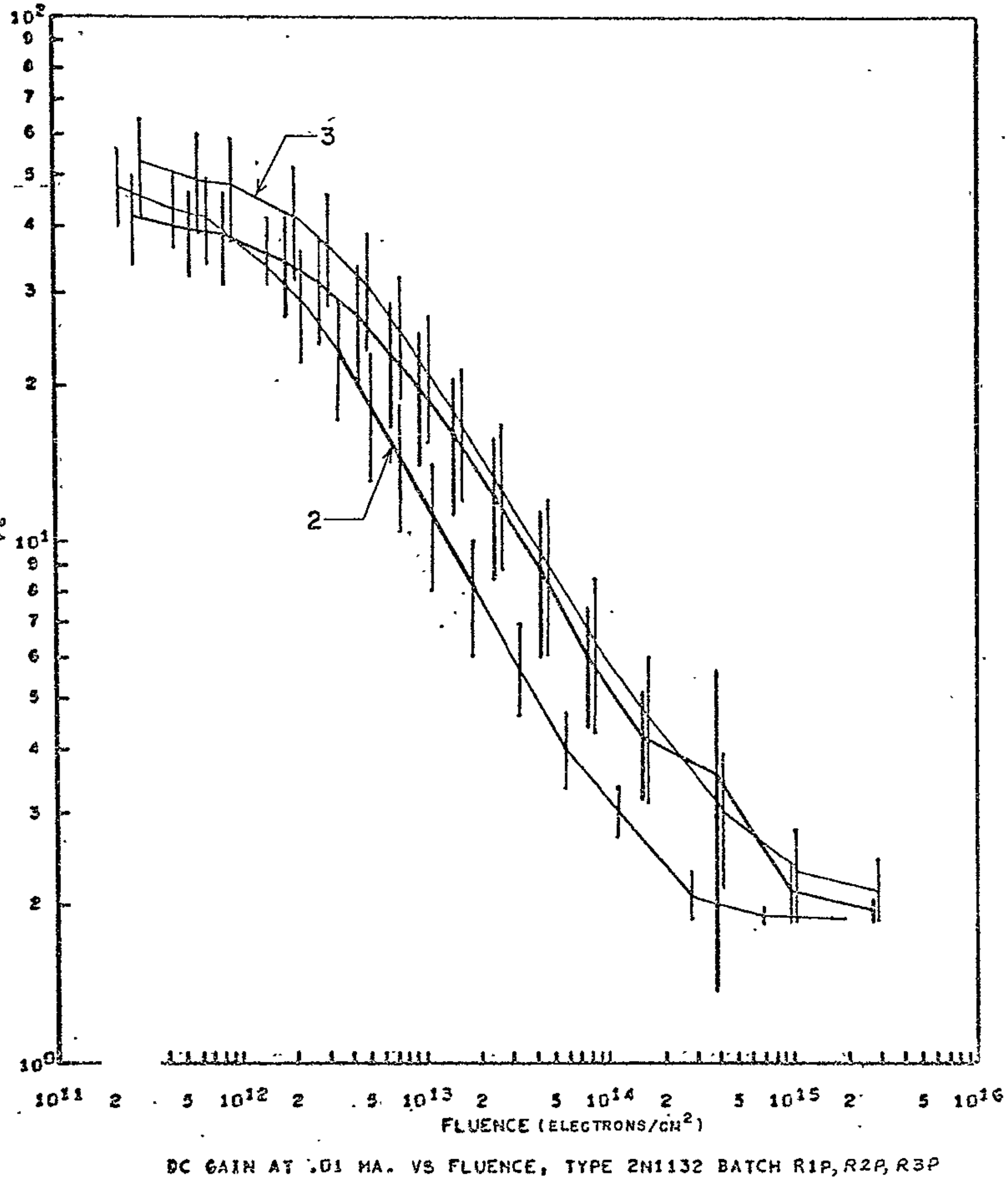

Figure 66: MEAN h_{FE} OF A GIVEN BATCH VERSUS FLUENCE (RAYTHEON 2N1132 PASSIVE, THREE BATCHES; THE VERTICAL BARS INDICATE STANDARD DEVIATIONS)

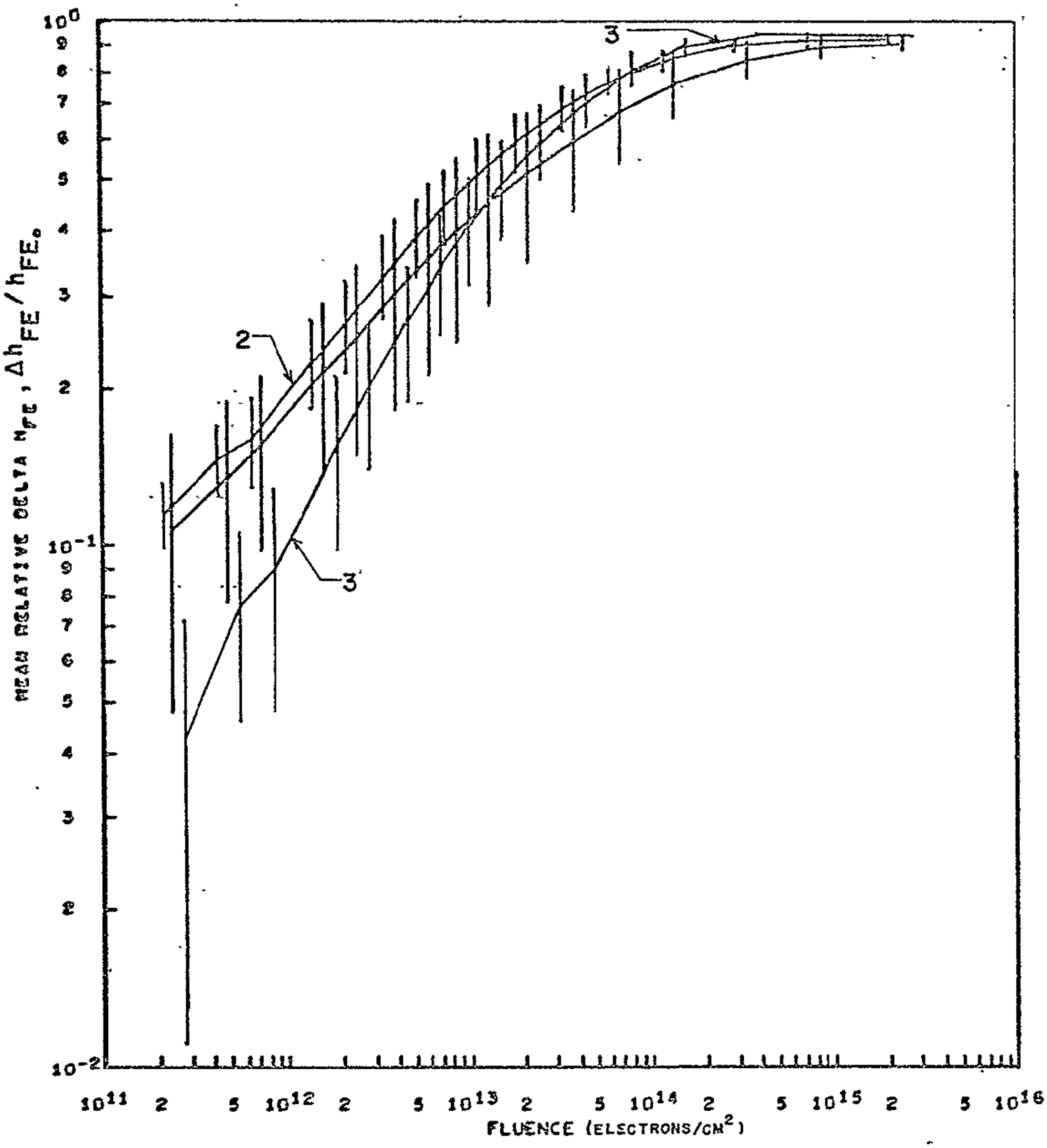

CHANGE IN DC GAIN AT .01 MA. VS. FLUENCE, TYPE 2N1132 BATCH F1P, F2P, F3P

Figure 67: MEAN RELATIVE GAIN LESS OF A GIVEN BATCH VERSUS FLUENCE (FAIRCHILD 2N1132 - PASSIVE, THREE BATCHES; THE VERTICAL BARS INDICATE STANDARD DEVIATIONS)

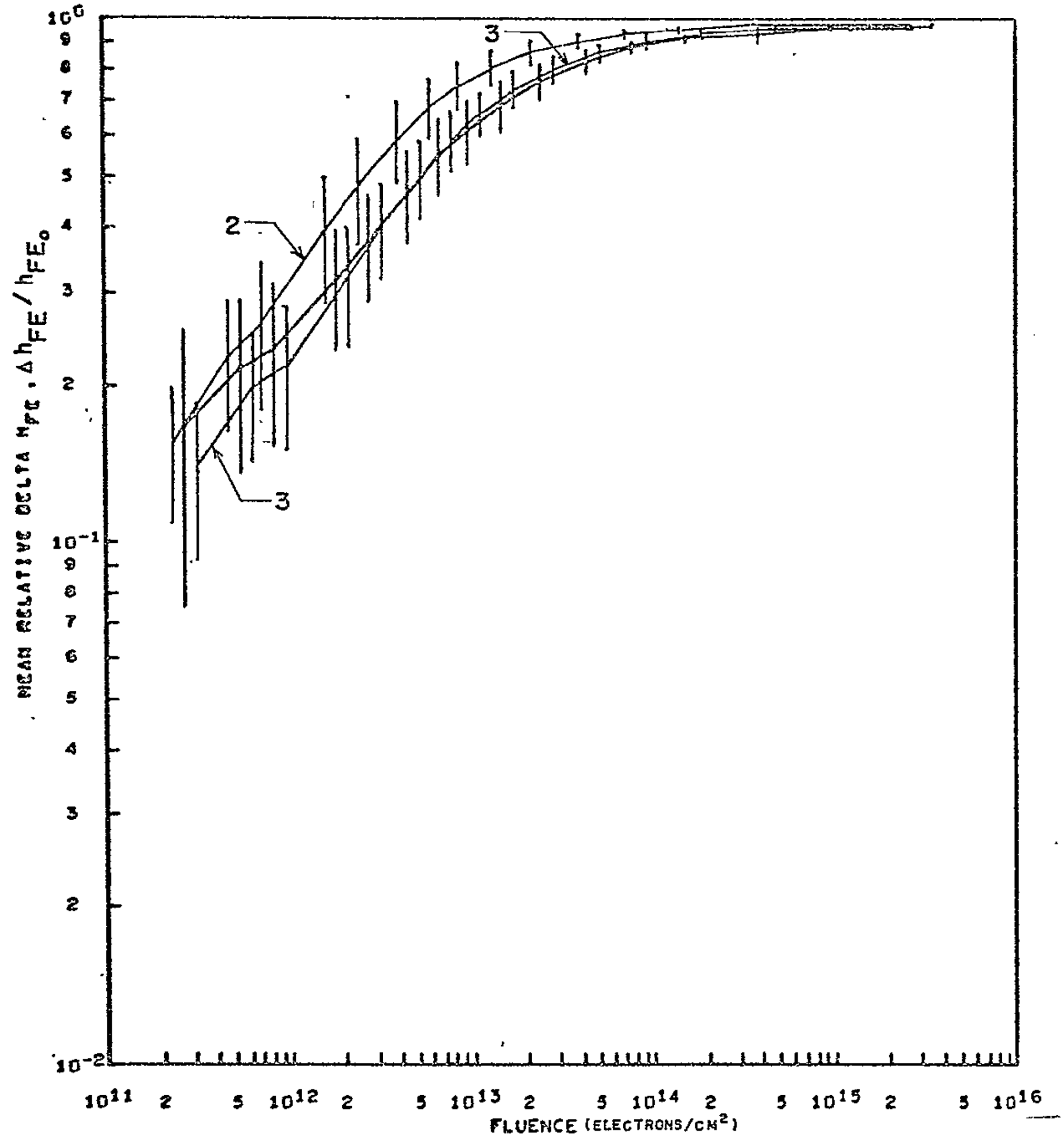

CHANGE IN DC GAIN AT .01 MA. VS. FLUENCE, TYPE 2N1132 BATCH R1P, R2P, R3P

Figure 68: MEAN RELATIVE GAIN LOSS OF A GIVEN BATCH VERSUS FLUENCE (RAYTHEON 2N1132 - PASSIVE, THREE BATCHES; THE VERTICAL BARS INDICATE STANDARD DEVIATIONS)

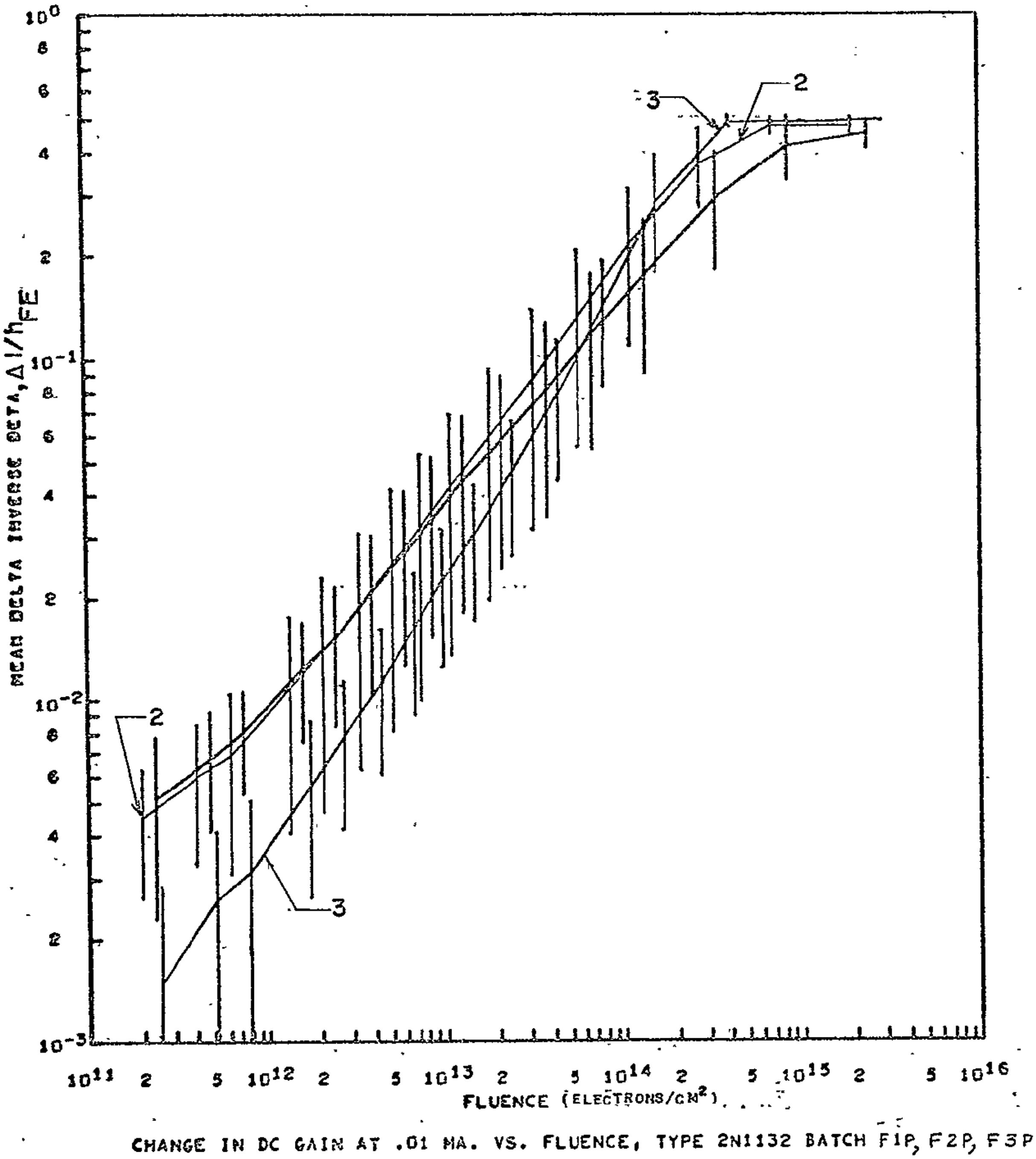

Figure 69: MEAN Δ^1/h_{FE} OF A GIVEN BATCH VERSUS FLUENCE (FAIRCHILD 2N1132 – PASSIVE, THREE BATCHES; THE VERTICAL BARS INDICATE STANDARD DEVIATIONS)

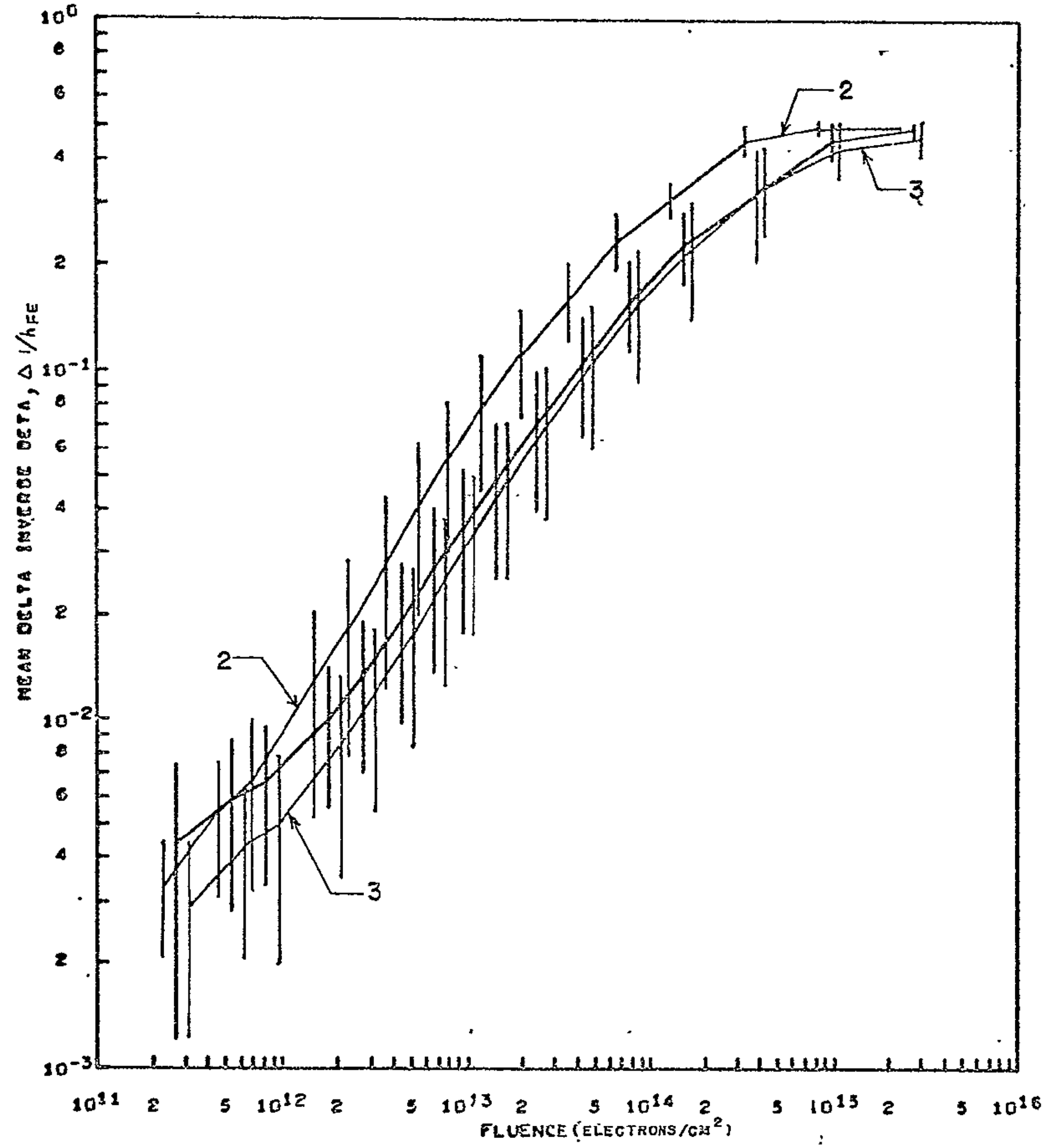

CHANGE IN DC GAIN AT .01 MA. VS. FLUENCE, TYPE 2N1132 BATCH R1P, R2, R3

Figure 70: MEAN Δ^{1}/h_{FE} OF A GIVEN BATCH VERSUS FLUENCE (RAYTHEON 2N1132 - PASSIVE, THREE BATCHES; THE VERTICAL BARS INDICATE STANDARD DEVIATIONS)

3.0 PROGRAM SCHEDULE

The program schedule is shown in Figure (71). 1 MeV electron tests were performed as scheduled. Preparations are completed for 15-MeV proton testing and combined testing. Those actual tests are behind schedule, but once they are underway they should be finished without need for a contract extension.

Figure 71. Program Schedule

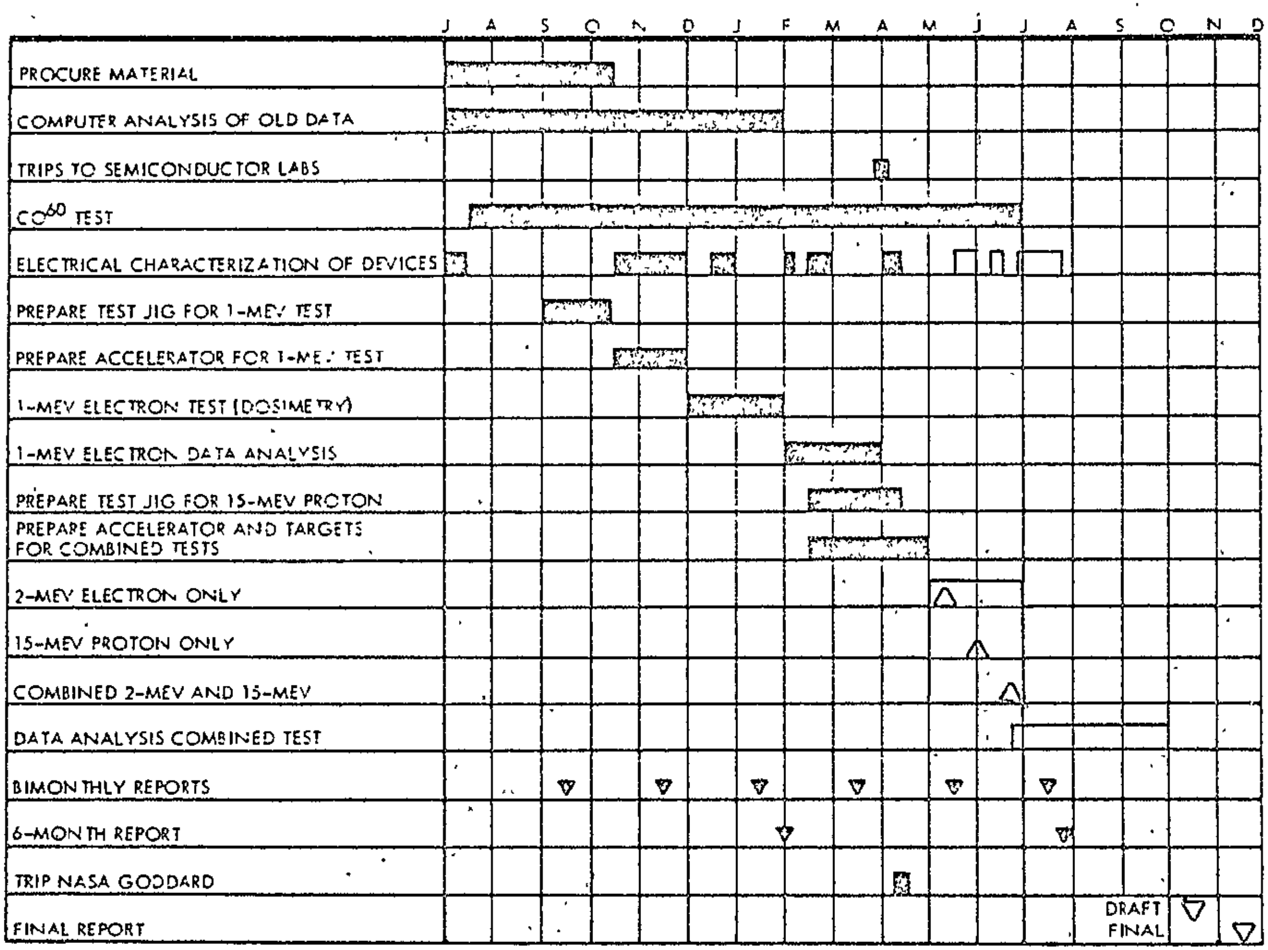

4.0 NEW TECHNOLOGY

The research work performed on this contract has been reviewed. To the best of our knowledge there is now new technology to report.

5.0 PROGRAM FOR NEXT REPORTING INTERVAL

The next major report will be the draft final due in October. By then computer analysis of all new test data should be complete.

6.0 REFERENCES

1. For good reviews, see e.g. J. P. Mitchell and D. K. Wilson, "Surface Effects of Radiation on Semiconductor Devices," Bell Syst. Techn. J. 46, 1 (1967), and A. G. Revesz and K. H. Zaininger, "The Si-SiO_2 Solid-Solid Interface System," RCA Review, 29, 22 (1968).

2. J. P. Mitchell, "Radiation-Induced Space-Charge Buildup in MOS Structures," IEEE Trans. El. Dev., ED-14, 764 (1967).

3. E. Kooi, "Influence of Heat Treatments and Ionizing Irradiations on the Charge Distribution and the Number of Surface States in the Si-SiO_2 System," IEEE Trans. El. Dev., ED-12, 238 (1966). See also A. G. Revesz, et al., "Interface States and Interface Disorder in the Si-SiO_2 System," J. Phys. Chem. Solids, 28, 197 (1967).

4. A. Goetzberger, et al., "Surface States in Silicon from Charges in the Oxide Coating," Appl. Phys. Let., 12, 95 (1968).

5. E. H. Snow, et al., "Effects of Ionizing Radiation on Oxidized Si Surfaces and Planar Devices," IEEE, 55, 1168 (1967).

6. See e.g., A. S. Grove, Physics and Technology of Semiconductor Devices (J. Wiley, New York, 1967).

7. D. J. Fitzgerald and A. S. Grove, "Surface Recombination in Semiconductors," Surf. Sci., 9, 347 (1968).

8. See e.g., V. G. K. Reddi, "Influence of Surface Conditions on Silicon Planar Transistor Current Gain," Sol. State Electr., 10, 305 (1967).

9. A. S. Grove and D. J. Fitzgerald, "The Origin of Channel Currents Associated with P^+ Regions in Silicon," IEEE Trans. El. Dev., ED-12, 619 (1965).

10. G. J. Brucker, et al., "Ionization and Displacement Damage in Silicon Transistors," IEEE Trans. Nucl. Sci., NS-13, 188 (1966).

11. W. J. Poch and A. G. Holmes-Siedle, "A Prediction and Selection System for Radiation Effects in Planar Transistors," presented at the Nuclear and Space Radiation Effects Conference, Missoula, Montana, July 1968.